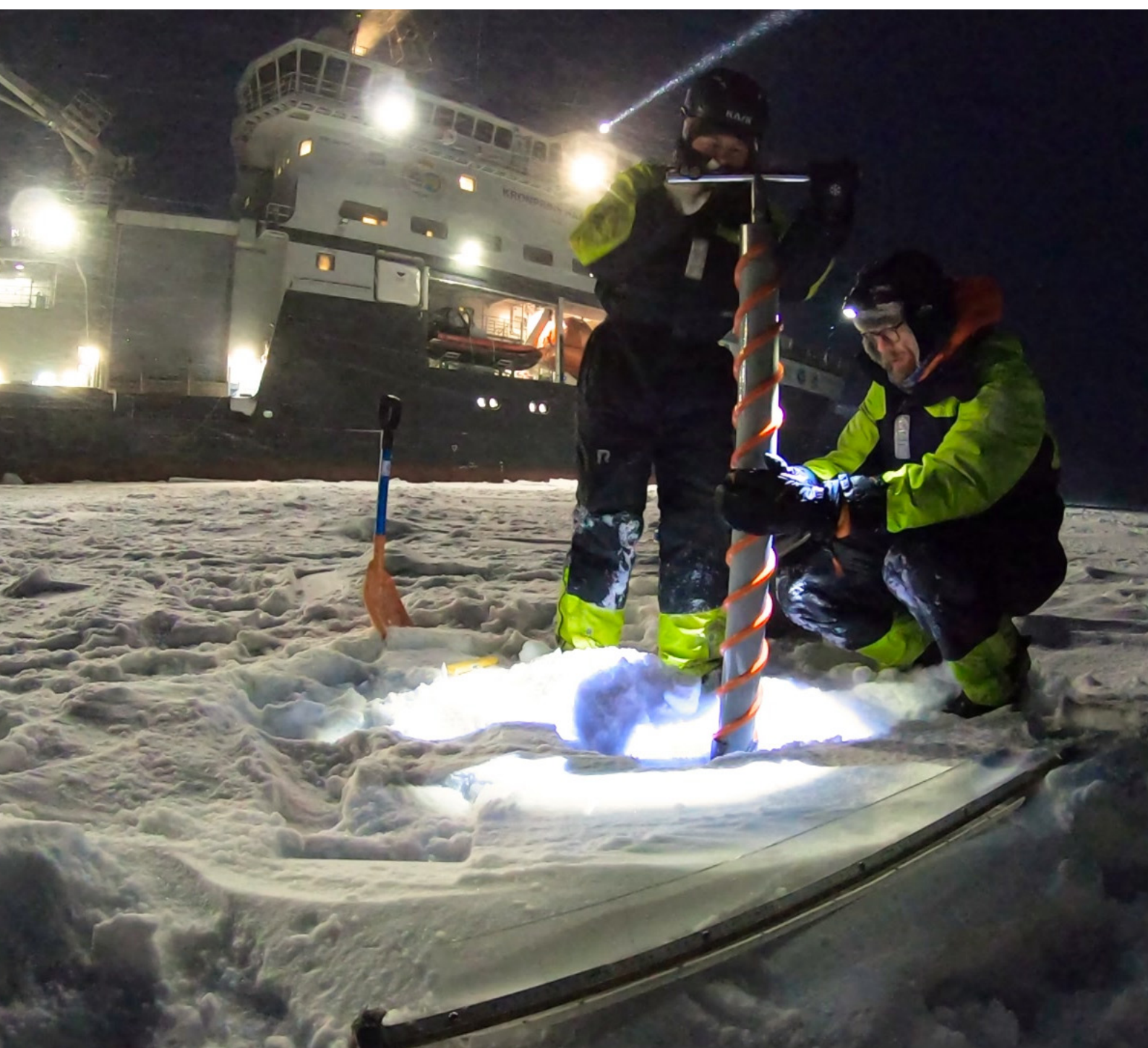


PC-2 Winter Process
Cruise (WPC)
Cruise Report



PC-2 Winter Process Cruise (WPC)

Cruise KH2021702

RV Kronprins Haakon

Longyearbyen-Tromsø

February 9 – March 1, 2021

Authors:

Frank Nilsen – cruise leader

Ilker Fer – cruise co-leader

Till M. Baumann

Øyvind Breivik

Ceslav Czyz

Lukas Frank

Kjersti Kalhagen

Zoe Koenig

Eivind H. Kolås

Stephan T. Kral

Bayoumy Mohamed A. Mabrouk

Tore Mo-Bjørkelund

Malte Muller

Jean Rabault

To be cited as: Frank Nilsen, Ilker Fer, Till M. Baumann, Øyvind Breivik, Ceslav Czyz, Lukas Frank, Kjersti Kalhagen, Zoe Koenig, Eivind H. Kolås, Stephan T. Kral, Bayoumy Mohamed A. Mabrouk, Tore Mo-Bjørkelund, Malte Muller, and Jean Rabault (2021). PC-2 Winter Process Cruise (WPC): Cruise Report. *Nansen Legacy Report Series* 26/2021. DOI: <https://doi.org/10.7557/nls.6324>

© The authors. This report is licensed under the [Creative Commons Attribution 4.0 International](#) license

ISSN 2703-7525

Publisher: Septentrio Academic Publishing, Tromsø, Norway

Summary

The Winter Process Cruise (WPC) aboard RV Kronprins Haakon (KH2021702) conducted observations on processes that control the position and variability of the polar front in the Northern Barents Sea and the distribution of Arctic and Atlantic water masses. Moreover, the WPC serviced 2 gateway moorings sites (M1 and M4) and collected complementary hydrographic, microstructure and current profiles to detect the winter circulation pattern and the layering structures between the two competing water masses. Meteorological measurements were also made. One mooring was retrieved from Kvitøyarena (M1b). Three moorings (M1, B1bioac and M1b) were deployed across the western slope of Kvitøyarena and one mooring (M4) close to Edgeøya on the ridge between Edgeøya and Hopen. Ocean stratification, current and microstructure measurements were made several times along two Polar Front sections (B, I) and along four water mass circulation sections (K, L, M, N) to follow the path of warm Atlantic water and cold Arctic water. Additional profiles were collected at two process stations (12-24 hours duration). Two Seagliders were recovered, in the West Spitsbergen Current and in the Polar Front. A Slocum glider equipped with microstructure sensors was deployed and recovered after 14 days. In total 89 CTD (conductivity temperature depth), 89 LADCP (lowered acoustic Doppler current profiler), 181 microstructure profiles and 20 days of SADCP (ship-mounted acoustic Doppler current profiler) data were collected. Approximately 20 km of undulating transects were made with an AUV (autonomous underwater vehicle). In total, 20 days of radiation data from ship-mounted radiometer, and 16 days of wave data from bow-mounted wave sensor were collected. 9 short flights with remotely piloted aircraft were made. 15 wave sensors and 19 surface drifters were deployed on ice floes from the southern ice edge into pack ice and various places in the northwestern Barents Sea.

1	Background	6
2	Survey area	7
3	Activity reports	9
3.1	<i>Hydrography – CTD measurements</i>	10
	Conductivity correction from salinity bottle samples.....	12
3.2	<i>Underway measurements.....</i>	13
	Weather Station.....	13
	Thermosalinograph.....	14
3.3	<i>Current Profiling</i>	15
	Lowered-ADCP (LADCP).....	15
	Shipboard-ADCP (SADCP).....	16
3.4	<i>Microstructure Profiling.....</i>	17
	The MSS.....	17
3.4.1.1	Profiling from the ship	18
3.4.1.2	Profiling during the ice station.....	19
3.4.1.3	Data processing.....	20
	uVMP on sea ice.....	21
3.5	<i>Mooring recoveries and deployments</i>	22
	Deployment of NLEG M1, M1 BioAc and M1b	22
	Deployment of NLEG M4.....	23
3.6	<i>Gliders.....</i>	23
	Seagliders.....	24
	Slocum glider.....	24
3.7	<i>Autonomous Underwater Vehicle - LAUV Harald</i>	25
	First attempt at the polar front.....	25
	Second attempt at the polar front.....	26
3.8	<i>ROV operations – Blueye.....</i>	26
3.9	<i>Meteorology.....</i>	27
	Radiative Flux Measurements	27
	SUMO – UAV	28
	Ship-based remote sensing.....	30
	Radiosonde measurements	32
	Weather Station on sea ice	32
3.10	<i>Surface Drifters.....</i>	32
3.11	<i>Measurements of waves in sea ice and open water.....</i>	36

4	Presentation of data.....	37
4.1	<i>Hydrography</i>	37
4.2	<i>Current Profiling</i>	39
	Lowered-ADCP (LADCP).....	39
	Shipboard-ADCP (SADCP).....	40
4.3	<i>Microstructure Profiling.....</i>	42
4.4	<i>Gliders (Eivind).....</i>	46
	Seagliders.....	47
	Slocum glider.....	48
4.5	<i>Autonomous Underwater Vehicle - LAUV Harald</i>	48
4.6	<i>Meteorology.....</i>	49
	Radiative Flux Measurements	49
	SUMO – UAV	50
	Ship-based remote sensing.....	52
	Radiosonde measurements	54
	Weather Station on sea ice	55
4.7	<i>Surface Drifters.....</i>	58
	Waves in ice instruments 'v1'	58
	Waves in ice instruments 'v2'	61
4.8	<i>Measurements of waves in sea ice and open water.....</i>	63
5	References	64
Appendix I. Cruise timeline, station tables, and participant list.....		65
Appendix III. Outreach.....		80

1 Background

The Winter Process Cruise (WPC) aboard RV Kronprins Haakon (KH2021702) conducted dedicated observations on processes that control the position and variability of the polar front in the Northern Barents Sea and the distribution of Arctic and Atlantic water masses. Moreover, the WPC serviced 2 gateway moorings sites (M1 and M4) and collected complementary hydrographic- and current cross-sections to detect the winter circulation pattern and the layering structures between the two competing water masses. Historically, the Northern Barents Sea have been difficult to access in winter, but it is during this time of the year that important atmosphere-ocean-processes are taking place and the heat fluxes between the sea and the atmosphere are greatest. These processes are important for the Barents Sea for the rest of the year through affecting, among others, the extent and variability of the sea-ice cover, the distribution of water masses and circulation patterns, and the availability of nutrients for plankton before sunlight returns.

KH2021702 is primarily a physical oceanography cruise with objectives to conduct wintertime hydrographic- and current profiling surveys, and ocean mixing and water transformation process studies within the northwestern Barents Sea region and in the gateways to the northwestern Barents Sea, both using the ship and a drifting sea ice floe as platforms. Meteorological measurements were also made. Activities included: recovery and deployment of oceanographic moorings and ocean gliders, an autonomous underwater vehicle, a remotely piloted unmanned aircraft and weather balloons; collecting underway measurements from ship-mounted ocean current profilers, wind profilers, radiometer and wave sensors; and collecting ocean stratification, currents, and microstructure profiles along selected transects across the Atlantic water pathways in the northwestern Barents Sea. Additionally, wave sensors were deployed on ice floes from the ice edge into pack ice.

At this time of year, important inflows of warm water masses from the Atlantic Ocean take place in the northwestern Barents Sea, and the vertical mixing throughout the water column is most effective. This cruise focuses on the physical processes in the sea, the sea ice, and the atmosphere, as well as the interactions between them. In the Nansen LEGACY structure, the cruise contributes to task T1-1 on the Atlantic Water inflow to the northern Barents Sea at key gateways, T1-2 on processes that control sea ice and stratification in the northern Barents Sea, TC-1 on environmental variables measurements from reliable and robust sensor carrying platforms for autonomous detection of important variables (RFs 1–3) in the Barents Sea and TC-2 on autonomous systems for measurement of key biogeochemical, physical and biological variables. More specifically, the cruise contributes to deliverables associated with subtasks:

T1-1.2 Ocean and sea ice fluxes into the northern Barents Sea

T1-2.1 Oceanic processes; fronts, upwelling, turbulent mixing and fluxes, upper ocean boundary layer exchanges

T1-2.3 Atmospheric processes

TC-1.1 In situ measurements and sampling

TC-2.2 Adaptive and collaborative vehicle behavior for mission management

TC-2.3 Instrumentation.

This report provides an overview of the methods employed and the data collected.

2 Survey area

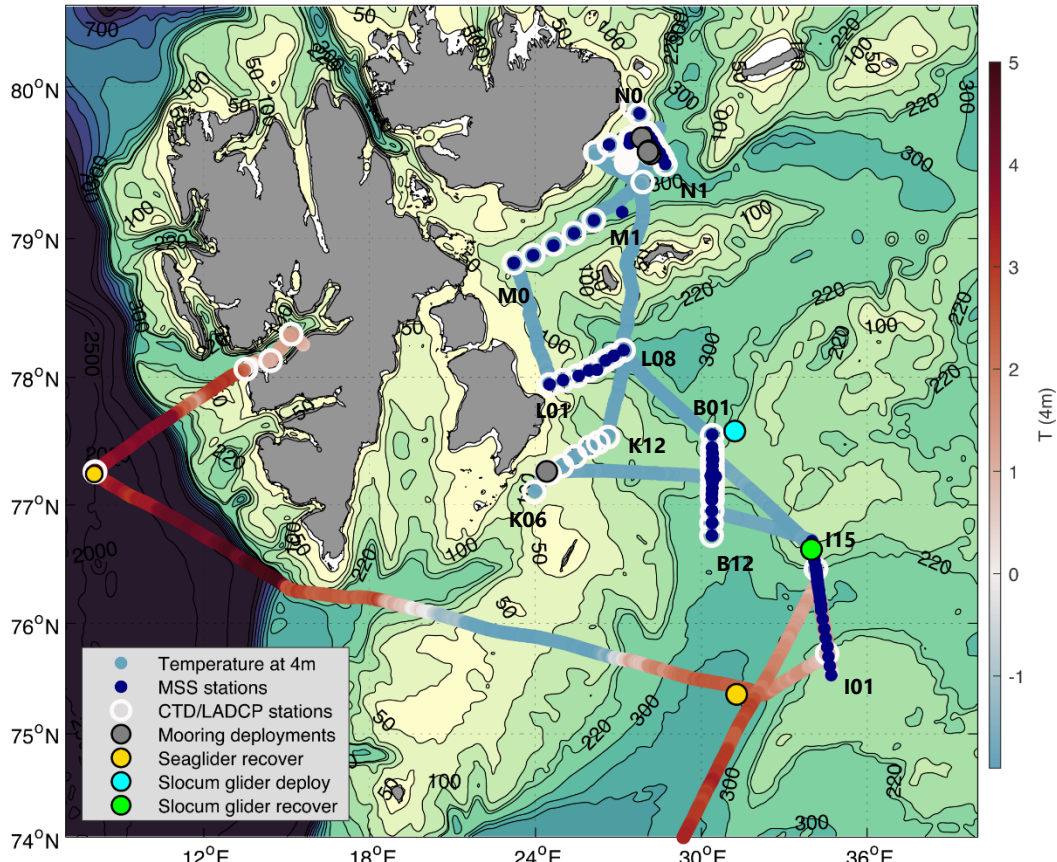


Figure 1: Map of cruise track, MSS stations, CTD/LADCP stations, mooring and ocean glider operations. The different transect names and station numbers are indicated in the beginning and end of the transect. The cruise track also shows the in situ sea water temperature at 4 meter depth.

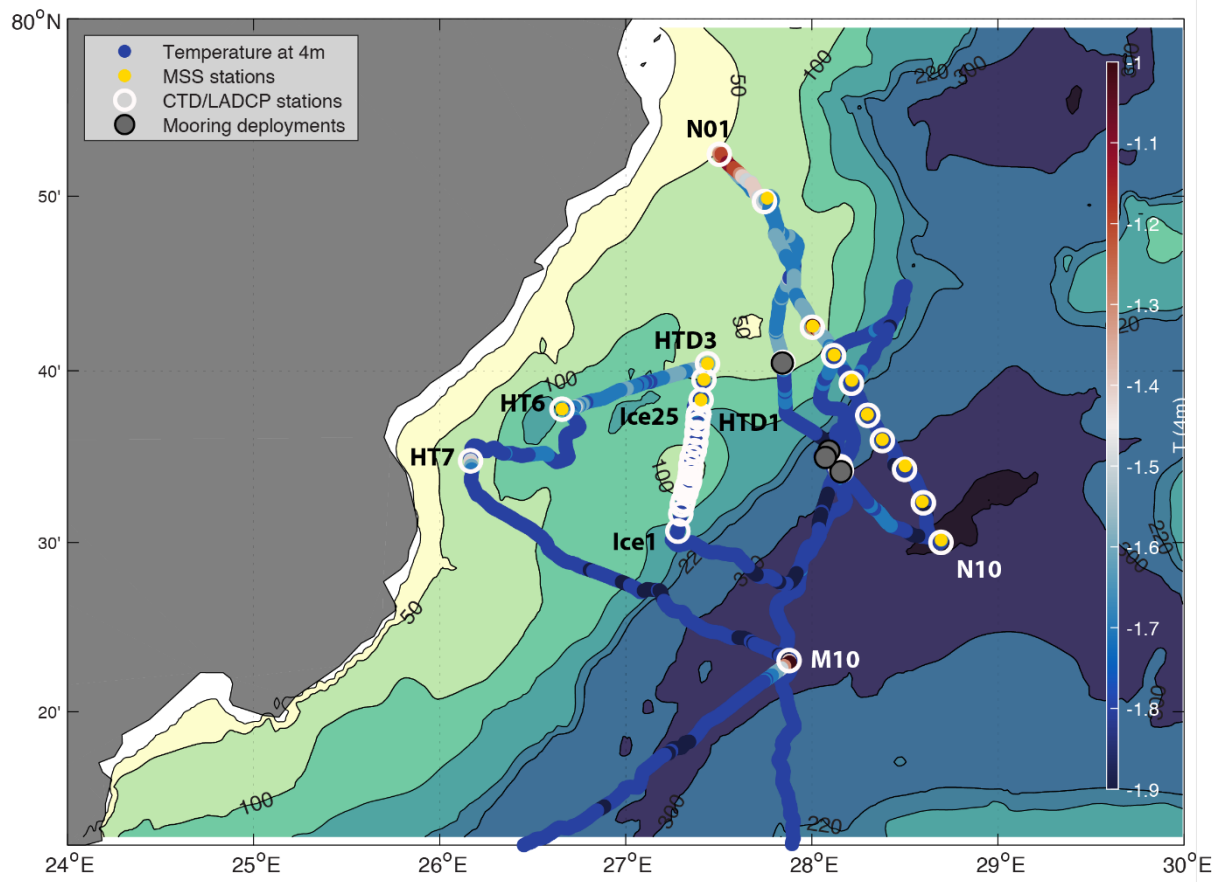


Figure 2: A close-up of the cruise track near Nordaustlandet, in Hartogbukta, where we established a sea ice drift camp. MSS stations, CTD/LADCP stations, and mooring operations positions are also indicated. The cruise track shows the in situ sea water temperature at 4 meter depth.

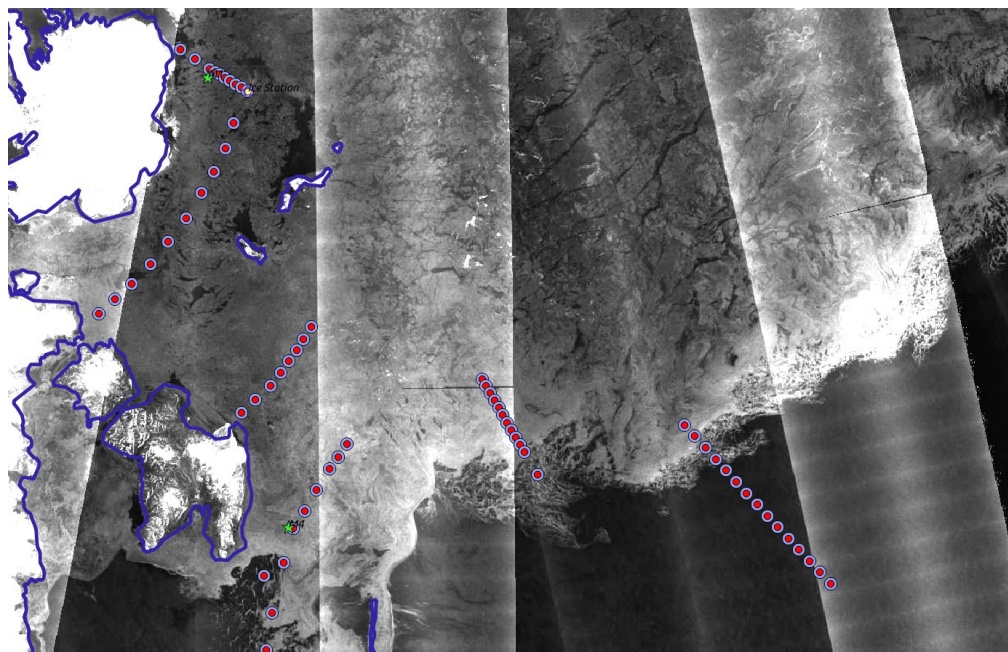


Figure 3: Mooring locations (green) and CTD/MSS stations (red). Background sea-ice conditions 2021-02-20 from Sentinel-1 provided by the Norwegian Ice Service.

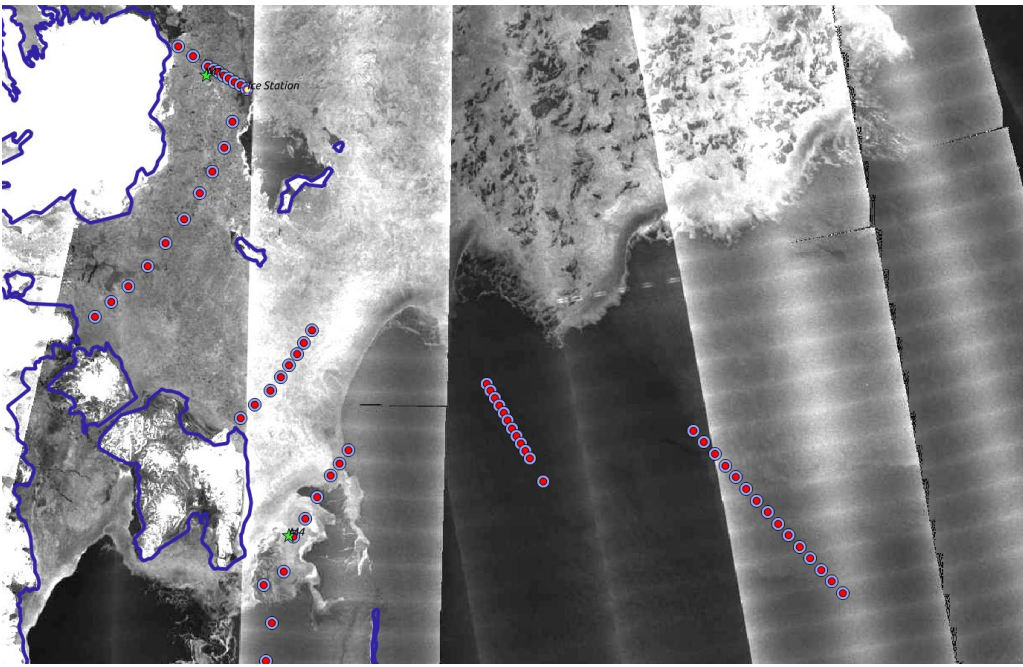


Figure 4: Mooring locations (green) and CTD/MSS stations (red). Background sea-ice conditions 2021-02-25 from Sentinel-1 provided by the Norwegian Ice Service.

3 Activity reports

After months of scientific preparations, risk analysis and home quarantine, 16 researchers from University of Bergen, Norwegian Polar Institute, NTNU, Meteorological Institute of Norway and UNIS sailed out from Longyearbyen on 9 February and arrived in Tromsø on 1 March. KH2021702 is an air-ice-ocean interaction cruise with concurrent measurements in the ocean, the atmosphere and in sea ice. However, it is primarily a physical oceanography cruise with objectives to collect hydrographic data and current sections in strategic transects, service and redeploy accessible gateway moorings, recover and deploy underwater gliders (cruise duration as well as concluding 4 months missions west and east of Svalbard) and conduct ocean mixing and water transformation process studies in the Barents Sea polar front region east of Svalbard. Further, the cruise was used to develop advanced robot technology and self-propelled crafts in both ocean and atmosphere in order study the polar front and air-ice-ocean interaction in more detail. Beside the polar front, we studied Kvitøyarena, a deep trench between Nordaustlandet and Kvitøya, through which warm Atlantic water penetrates the Barents Sea. Here, we also established a sea ice camp and drifted for 36 hours while collecting data in the atmosphere, in the sea ice and in the water column under the sea ice.

One mooring was retrieved from Kvitøyarena (M1b). Three moorings (M1, B1bioac and M1b) were deployed across the western slope of Kvitøyarena and one mooring (M4) close to Edgeøya on the ridge between Edgeøya and Hopen. Ocean stratification, current and microstructure measurements were made several times along two Polar Front sections (B, I) and along four water mass circulation sections (K, L, M, N) to follow the path of warm Atlantic water and cold Arctic water. Additional profiles were

collected at two process stations (12-24 hours duration). Two Seagliders were recovered, in the West Spitsbergen Current and in the Polar Front. A Slocum glider equipped with microstructure sensors was deployed and recovered after 14 days. In total 89 CTD (conductivity temperature depth), 89 LADCP (lowered acoustic Doppler current profiler), 181 microstructure profiles and 20 days of SADCP (ship-mounted acoustic Doppler current profiler) data were collected. Approximately 20 km of undulating transects were made with an AUV (autonomous underwater vehicle). In total, 20 days of radiation data from ship-mounted radiometer, and 16 days of wave data from bow-mounted wave sensor were collected. 9 short flights with remotely piloted aircraft were made. 15 wave sensors and 19 surface drifters were deployed on ice floes from the southern ice edge into pack ice and in selected locations in the northwestern Barents Sea.

3.1 Hydrography – CTD measurements

The hydrographic work was carried out using a CTD-water sampling package from SeaBird Inc., acquiring data during both down and upcast. The package consisted of a SBE 911plus CTD (underwater unit SBE9plus SN 141612, deck unit SBE11 SN 1121) with sensors listed below. The Benthos altimeter (200 kHz) allowed profiling close to the bottom. The CTD was equipped with a 24 position SBE 32 Caroussel (SN 1222). The rosette was fitted with 3 10-litre bottles for collecting water samples for salinity calibration at all stations. On the first 4 CTD stations the CTD was deployed over the side. On all following stations, the CTD package was lowered through the moonpool and the upper 15 meters of data cannot be trusted. In total 89 CTD-stations were taken, recorded in files sta0025 to sta0113. At all stations, water samples for salinity calibration were collected at the deepest sampling level. The CTD rosette, together with LADCPs, is shown in Figure 4. Their locations are listed in Appendix II. Station positions are shown in Figure 2 and Figure 3. During a CTD cast, the CTD package was lowered into the water for a 1-minute soak before lowering to the bottom. All CTD sensors worked well throughout the cruise. Offset between primary and secondary T and S sensors were in acceptable range.

Table 1. Sensor details installed on the CTD rosette.

Sensor	SN	Calibration/Service date
Temperature	4535	20.02.2020
Conductivity	4386	28.02.2020
Pressure	141612	19.12.2017
Temperature, 2	4306	28.01.2020
Conductivity, 2	2799	28.01.2020
Oxygen, SBE 43	3649	28.02.2020
Altimeter, Benthos PSA-916	73084	24.12.2017
Fluorometer, Wet Labs ECO-AFL	6506	18.09.2020
Transmissiometer, Wet Labs C-Star	2003 DR	01.10.2019
Fluorometer, Wet Labs ECO CDOM	4885	15.08.2019
PAR/Irradiance, Biospherical/Licor	70736	29.10.2018
SPAR, Biospherical/Licor	20568	27.11.2017

RDI WH300 LADCP, downward

24474

RDI WH300 LADCP, upward

24472

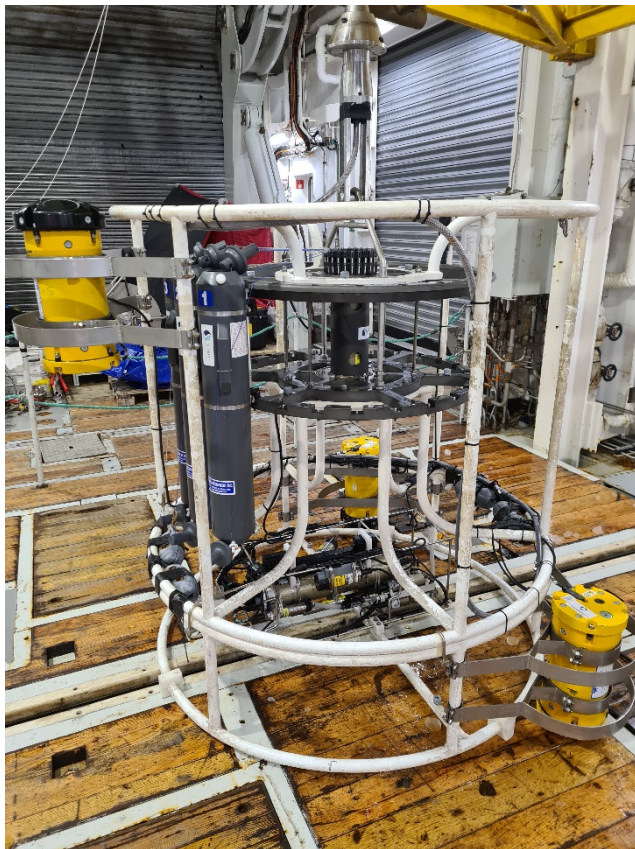


Figure 5: Picture of the CTD rosette with the LADCPs installed. The upper left (yellow pressure case) is the "slave", the outer at the back is the "master" instrument, and the lower on the right is the battery canister.

Data processing - SBEDataProcessing-Win32, standard Seabird Electronics software for Windows (version 7.26.7.114), is used for post-processing of the CTD data. Only data from downcasts are used to avoid turbulence caused by rosette package on the upcast. Raw data (pressure, temperature and conductivity from dual sensors) are converted to physical units using calibration files modified for air pressure and conductivity slope factor (DATCNV). Outliers, differing more than 2 and 20 standard deviations for the first and second pass, respectively, from the mean of 100 scan windows are flagged and excluded from analysis (WILDEDIT). WILDEDIT flags only the bad data point of each parameter, and does not flag the entire scan. The thermal mass effects in the conductivity cell are corrected for (CELLTM, with parameters alpha = 0.03 and 1/beta = 7.0). Pressure is low-pass filtered with a time constant of 0.15 s. Following the SBE recommendation, the conductivity or temperature signals were low-pass filtered. Auxiliary sensors (oxygen, CDOM, fIC, Trans) were filtered using a time constant of 0.03 s. Scans when the CTD package moved less than the set minimum fall rate of 0.25 m s^{-1} are flagged to remove pressure reversals due to ship heave (LOOPEDIT). Data are then averaged (BINAvg) into 1-dbar vertical bins and 1-s temporal bins (the latter is for the

LADCP data processing). In the final (converted and bin-averaged) data files, temperature is saved using the ITS-90 scale, and salinity on the practical salinity scale (PSS-78). Pressure, temperature, and salinity data are accurate to ± 0.5 dbar, $\pm 2 \times 10^{-3}$ °C, and $\pm 3 \times 10^{-3}$, respectively.

Conductivity correction from salinity bottle samples

A total of 89 salinity bottle samples are analyzed at IMR with a Guildline Portasal 8410 salinometer. Salinity and conductivity values from each bottle are merged with the corresponding CTD data. Bottle conductivity is calculated from bottle salinity and CTD temperature and pressure. Following the procedure recommended by UNESCO [1988], only data within the 95% confidence interval are used to correct the calibration of the CTD conductivity. After inspection of the conductivity difference $\Delta C = C_{CTD} - C_{Bot}$, obvious wrong measurements (outliers) were removed (station 25, 84, 72, 106 and 110) before ΔC values outside the 95% confidence interval were filtered out. The latter procedure were repeated twice and the final ensemble (74 data points) of calibration data is shown in Figure 6. Histogram of $\Delta C = C_{CTD} - C_{Bot}$, difference of conductivity measured by CTD and inferred from bottle salinity, is approximately normally distributed but skewed towards positive differences. The skewness might be linked to CTD profiles being collected in both open water and sea ice covered ocean. Following the recommendations given by Seabird Electronics, the conductivity values are corrected by the formula, $C_{new} = m C_{old}$, where m is the slope calculated by

$$m = \frac{\sum_{i=1}^n a_i \times b_i}{\sum_{i=1}^n a_i \times a_i}$$

Here a_i and b_i are the CTD conductivity and the bottle conductivity, respectively and $n=74$ is the total number of bottles. The results from all samples are shown in the Figure 6.

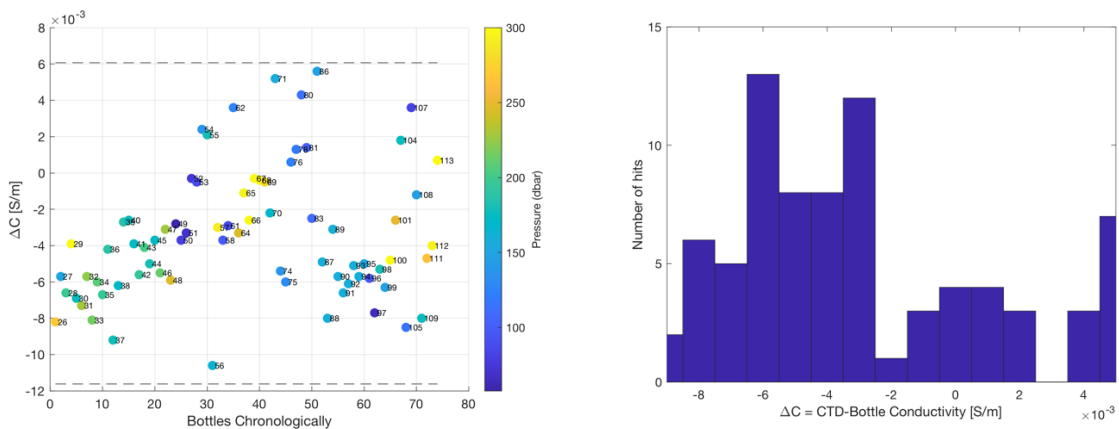


Figure 6: (Left) $\Delta C = C_{CTD} - C_{Bot}$ in chronological order ($n=74$) after outliers and data outside the 95% confidence intervals have been removed. (Right) Histogram of CTD-derived and bottle conductivity difference.

A slope correction of 1.0001 is obtained, which reduced the RMS salinity difference from 0.0055 to 0.0036 showing that the CTD conductivity sensor performed well with a marginally smaller value than the bottle sample. An alternative correction is a constant salinity offset with -0.0035 practical units, which also reduced the RMS salinity difference to 0.0036.

3.2 Underway measurements

Weather Station

Meteorological conditions (wind speed, directions, air pressure, humidity, air, and water temperature) were highly variable during the cruise period, as the cruise covered a wide latitudinal range in the Barents Sea. Figure 7 shows these datasets from the ship's log that have been averaged in 10-minute bins. Sections I and B were worked during the spring tides, as shown in Figure 8.

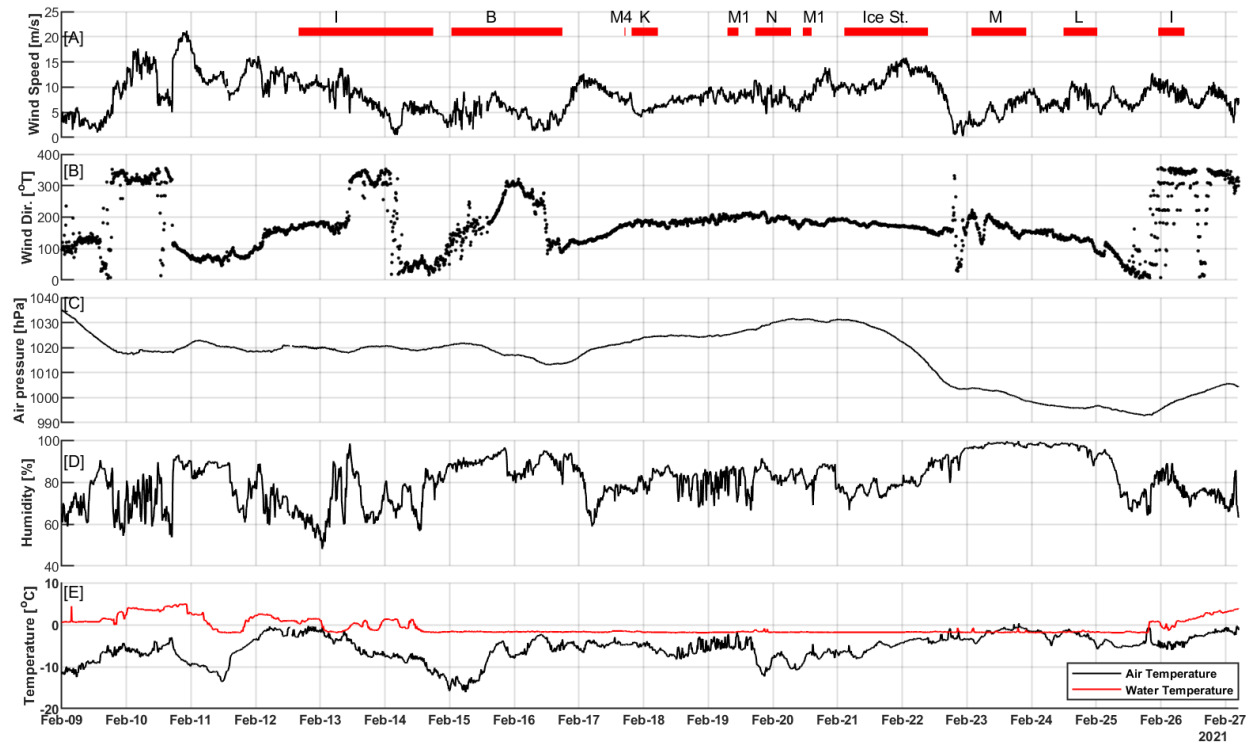


Figure 7: 10-minute averaged data from the ship's log: A) wind speed, B) direction, C) atmospheric pressure, D) relative humidity measured at 15-m height, and E) near surface water and 15-m height air temperature. Duration of activities (sections and process stations) are indicated at the top.

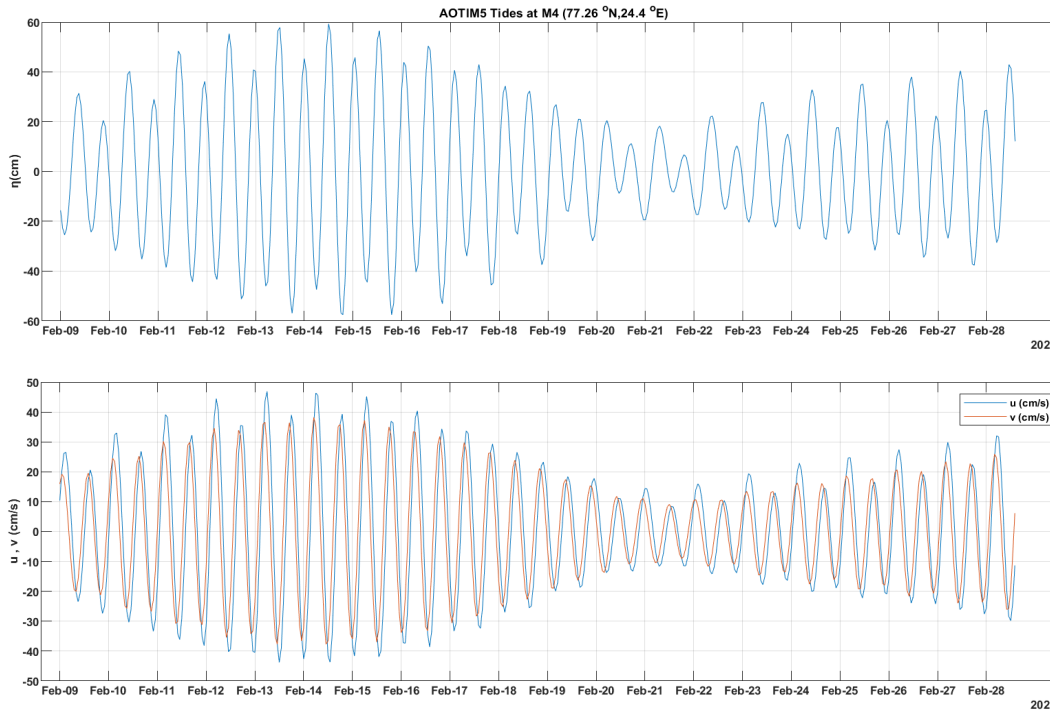


Figure 8: Tidal elevation and currents during a spring-neap cycle covering the cruise period, inferred from the AOTIM5 model at station M4 (77.26°N and 24.4°E).

Thermosalinograph

The thermosalinograph was running continuously during the cruise and the temperature time series is shown as a track log in Figure 1. On 13th February, a transect was made using the thermosalinograph to detect a surface temperature-salinity front. Time series are collected at 4 m depth from the ship's seawater intake, and the SBE38 remote temperature sensor (t168c, SN3429) is used. The front was detected between stations I-9 and I-11 at 300 m depth. After that, subsection (from I-9 to I-11) was repeated several times to determine the exact position of the front. Figure 9 shows the time series of temperature and salinity during the period of repetition, recorded at 10 second intervals, which clarify the high variability between Atlantic (warm and high saline) and Arctic (cold and less saline) water, hence the polar front.

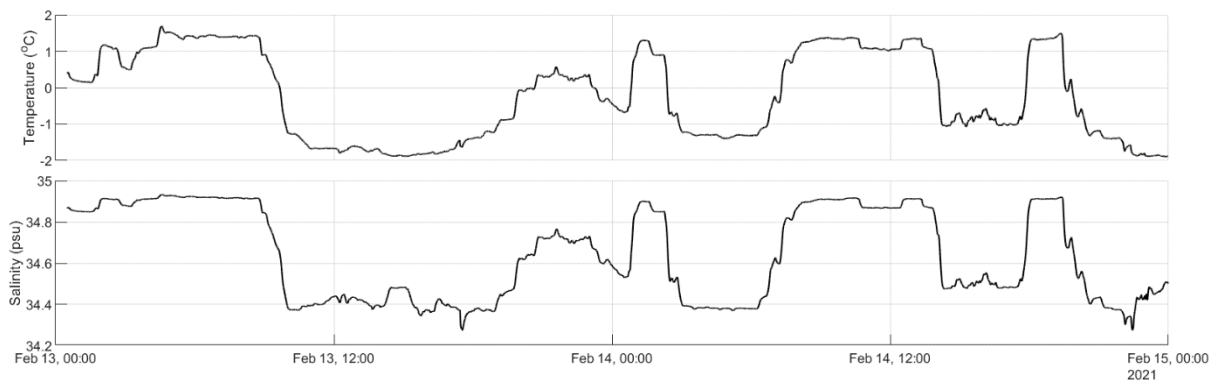


Figure 9: Time series of thermosalinograph temperature and salinity recorded at 10 second intervals from 4m depth during the repeating period of section (I) to detect the surface front.

3.3 Current Profiling

Lowered-ADCP (LADCP)

Two LADCPprofilers (RD Instruments) were mounted on the CTD rosette to obtain vertical profiles of horizontal currents. The ADCPs are 6000-m rated, 300 kHz Sentinel Workhorses. The units received power from an external battery canister with a housing identical to that of the instruments. All three units are installed on the rosette in a balanced distribution to ensure minimum tilt. Each ADCP has the L-ADCP option installed (firmware v16.3). The ADCPs were configured to sample in master and slave mode to ensure synchronization. The master ADCP pointed downward (SN 24474) and the slave ADCP pointed upward (SN 24472). The compass of each instrument was last calibrated in Tromsø, in their respective orientation in 2018. The resulting compass errors were less than 4°. Because the batteries are in an external canister, we expect the compass calibration to be valid.

In total 113 profiles of LADCP were taken. Communication with the instruments, start & stop of data acquisition and data download were done using the BBTalk software. PC time (UTC) was transferred to each instrument before each cast. The vertical bin size (and pulse length) was set to 8 m for each ADCP. Single ping data were recorded in narrow bandwidth (to increase range), in beam coordinates, with blank distance set to zero. The data from the first bin are discarded during post processing. To mitigate a possible influence of previous pinging, especially close to steep slopes, staggered pinging with alternating sampling intervals of 0.8 s and 1.2 s were used. The altimeter worked reliably and no sign of degradation of LADCP data quality was observed.

The LADCP data are processed using the LDEO software version IX-13 based on Visbeck (2002). For each master/slave profile data, synchronized time series of CTD and navigation is used. The NMEA GPS stream is automatically stored in the CTD *.hex files with each scan and are post-processed as 1-s bin averages, same as the ADCP ping rate. LADCP-relevant processing of the CTD data included the identical steps in the SBE-Data Processing software. Additionally, 2-minute time averaged profiles from the 150 kHz SADCP are included for constraint on the inversion of the LADCP data. The SADCP data are obtained from processing of single ping data using CODAS, but before a vigorous editing. The magnetic declination is obtained from <https://www.ngdc.noaa.gov/geomag/calculators/> magcalc.shtml, using the WMM (2019-2024) model, at the day and position of the profile.

The CTD rosette together with the CTD sensors, 10-liter Niskin bottles, a down and uplooker ADCP, and a benthos altimeter installed (Figure 5). The transducers of both ADCPs and the altimeter have a non-obstructed path. The third yellow pressure case is for the LADCP batteries. The position of the lead weights and the ADCPs are adjusted to have a negligible tilt of the entire system.

Shipboard-ADCP (SADCP)

Kronprins Haakon is equipped with two pairs of downward pointing RDI Ocean Surveyor Acoustic Current Doppler Profilers (ADCPs): 2 units with a transducer frequency of 150 kHz and 2 units with 38 kHz. One of each is mounted in the lowering keel, while the other pair is mounted flush with the hull of the ship. Due to our planned operations in the ice, the lowered keel could not be used, so all SADCP data collected during this cruise stems from the pair (1x38 kHz and 1x150 kHz) mounted in ca. 8 m depth flush in the hull. After some testing within the first 3 days during transit from Longyearbyen to the Barents Sea, the following settings were decided upon:

- 38 kHz: 16 m bins, 16 m blanking distance, broadband mode (optimized for accuracy)
- 150 kHz: 4 m bins, 4 m blanking distance, narrowband mode (optimized for range, yielding data until ~200 m depth which covers all or most of the water column in the Barents Sea)

The acquisition of raw data (single-ping data from the ADCPs as well as vessel navigational data) and primary processing (creating of short-term averages (120 s, STA) and long-term averages (300 s, LTA)) were carried out using the VmDAS software. Preliminary processing has been done using the CODAS package maintained at <https://currents.soest.hawaii.edu>. The typical processed horizontal velocity uncertainty is 2-3 cm s⁻¹.

Preliminary processed data revealed that during much of the heavy icebreaking, SADCP data return was very low (Figure 10). We suspect one or both of the following reasons to play a role in creating this issue:

- The shaking and strong vibrations experienced by the ship during icebreaking contaminates the echo returning to the transducers.
- Due to the box shape of the hull, large chunks of ice are continuously funneled along the underside of the ship, likely blocking the transducers for extended durations.

Moreover, due to side-lobe contaminations arising from beam reflections at a boundary (in this case, the sea floor), data from the bottom 10-15% of the water column is lost (Figure 10). This is an expected behavior of ADCPs and cannot be avoided.

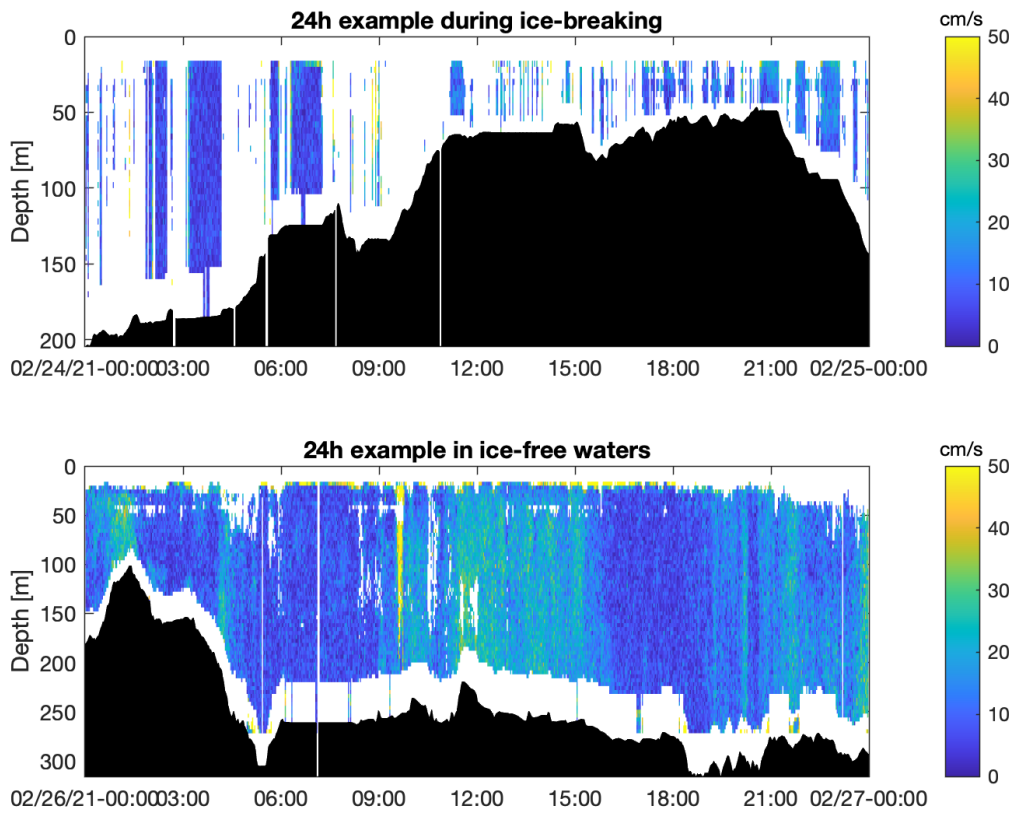


Figure 10: Example of bad data returns during icebreaking compared to data return in ice-free waters.

3.4 Microstructure Profiling

Microstructure profiling during the cruise was performed using an MSS (Microstructure Sensor Profiler, Sea&Sun Technology, Germany). Additionally, an uVMP (upriser Vertical Microstructure profiler, Rockland Scientific, Canada) was deployed on the ice station.

The MSS

Ocean microstructure measurements were made using the MSS90L profiler (SN 047), a loosely-tethered free-fall instrument equipped with two airfoil probes aligned parallel to each other, a fast-tip thermistor (FP07), an acceleration sensor and conventional CTD sensors for precision measurements. The shear probes used were SN067 (sensitivity 4.58e-04, SHE1) and SN068 (sensitivity 4.83e-4, SHE2). The same sensors were used throughout the cruise and the sensors point downward when the instrument profiles vertically, and all sample at 1024 Hz. The instrument is ballasted for a typical fall speed of 0.6-0.7 m s⁻¹ and is decoupled from operation induced tension by paying out cable at sufficient speed to keep it slack. Data are transmitted in real time to a ship-board data acquisition system. Until cast 5, the MSS was used with 7 ring weights, resulting in a fall speed of more than 0.8 m s⁻¹. We removed one weight after cast 4, and a

second one prior to cast 26. The remaining casts until the end of cruise were done using 5 ring weights.

In total 181 casts were attempted. 9 were aborted resulting in 172 profiles, down to about 5-15 m height above the seabed. The profiler is equipped with a sensor protection guard at the leading end, and occasionally the profiler landed at the bottom. A full list of MSS casts is given in Table 8. MSS data reported here are from the processing conducted during the cruise. Substantial editing and salinity offset correction were already performed in the version processed on board.

Two different setups of the MSS were implemented, depending on if it was operated from the ship or from the sea ice.

3.4.1.1 Profiling from the ship

The deployment of the MSS from the ship was done from the starboard side, from the "small" CTD room. A motor-driven winch was mounted on several pallets and an arm was used to extend the cable from the winch to outside. The profiler was lowered in the water and brought back on board by pulling on the data cable transmission by hand. One to two casts were performed at each station.

Because of the keel of the ship, the upper 12 m of each cast were excluded from dissipation estimates. During section B, we noticed that the salinity measurements in the upper 20 to 70 m suffered from the conductivity sensor adjusting to environment. After cast 67, we routinely sent the profiler to 10 m depth and waited up to two minutes until the measured salinity stabilized. Furthermore, we vertically placed the profiler in a container full of seawater (brought using the Niskin bottles) to hold the sensors in conditions similar to ambient during the transit from one station to the other one.

Occasionally, ship's extensive thruster action to remove the sea ice at the station affected the turbulence measurements in the upper 40-50 m. To mitigate this, starting from section N (cast 116), we waited for 5 min once the ship was in position for the MSS cast (drifting, and not using the thrusters) before starting the profile (in addition to holding 2 min at 10 m depth). In some stations, we collected a second profile if the ship did not have to relocate because of ice.

The connector to the profiler had to be terminated before cast 41.

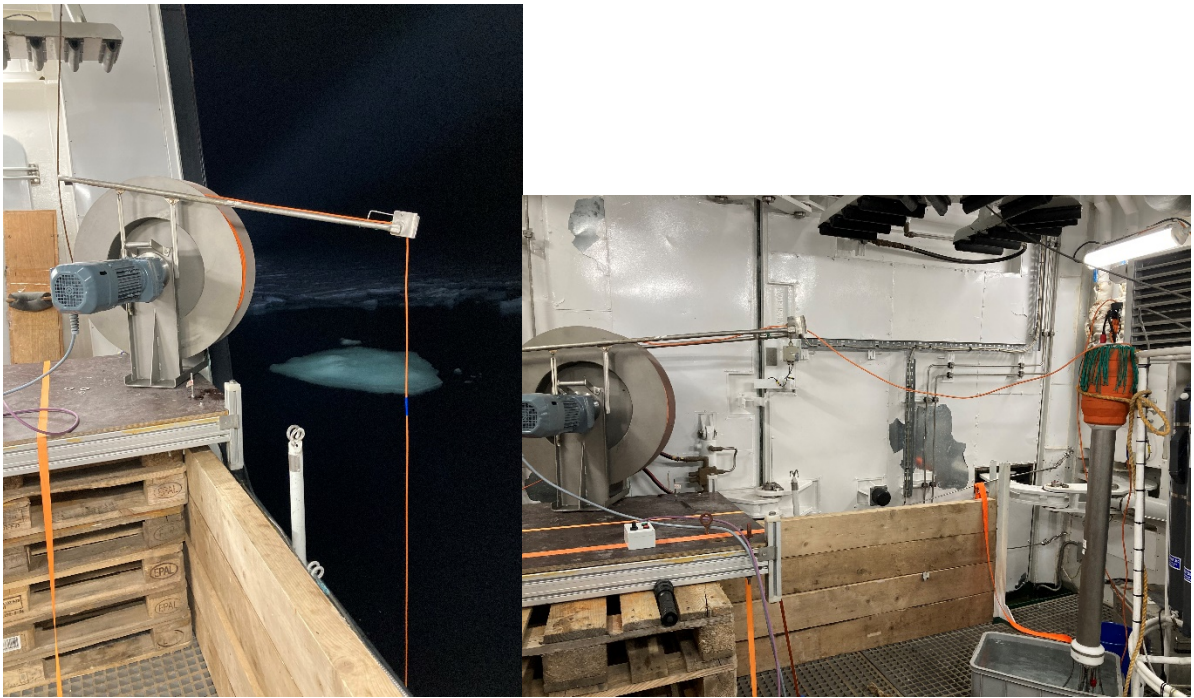


Figure 11: Set up of the MSS on board

3.4.1.2 Profiling during the ice station

The MSS was operated from the sea ice during an ice station. We deployed the MSS through a 1 m x 1 m hole in 60 cm thick sea ice. The hole was located approximately 150 m away from the ship, in the direction of the ice/ship drift, ensuring sampling of undisturbed waters. The winch was set up by the hole, and a pop-up tent was installed next to it to protect the electronics (data acquisition unit, a laptop and motor power supply). We collected a profile every 30 min. To avoid freezing of the sensors, the profiler was left in water, at about 10 m depth between the casts.

The MSS temperature and salinity data were compared against the thermosalinograph and the ship CTD data. We applied a constant salinity offset of -0.02 to all profiles.

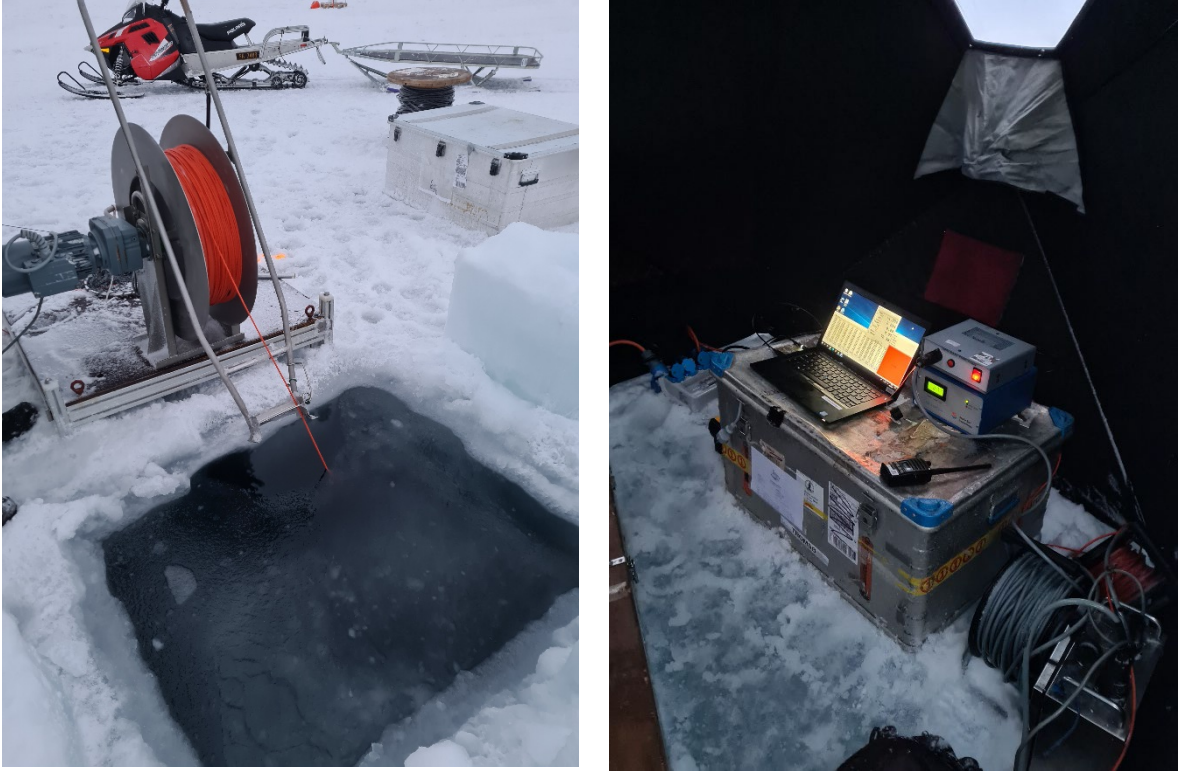


Figure 12: Setup of the MSS on ice. The motorized winch is located outside, next to the tent which is setup with a laptop computer, power unit for the motor and a data acquisition unit.

3.4.1.3 Data processing

Processing of the MSS data was performed using routines developed at the University of Bergen and reported in detail elsewhere. Full-scan (1024 Hz) data from all channels of the MSS profiler are edited for transmission errors and spikes, and then averaged to 256 Hz to reduce noise. Time series are converted into vertical wavenumber space using a smooth fall-speed profile. The fall speed is derived from the time derivative of the (2-Hz low passed) pressure record. The dissipation rate of turbulent kinetic energy per unit mass, ε , is estimated from the isotropic relation $\varepsilon = 7.5 v \langle u_z^2 \rangle$, where v is the viscosity of seawater (approximated as a function of temperature) u_z is the shear of the horizontal velocity resolved at cm-scales. Shear wavenumber spectra are calculated using half overlapping 256-point (about 0.7 m) Hanning windows. The shear variance is obtained by integrating the shear wavenumber spectrum between 2 cpm and an upper cutoff number depending on the Kolmogorov wavenumber. The upper cutoff is determined by iteration and is set to maximum 30 cpm (a limitation of the probe size) or 14 cpm when 2-14 cpm integrated $\varepsilon < 2 \times 10^{-8} \text{ W kg}^{-1}$. This range is not affected by the narrowband noise peaks. A small correction is applied for the unresolved variance assuming the Nasmyth's form. A further check is employed by comparing dissipation values from both probes, and anomalous data were discarded prior to averaging at 1 m resolution. The noise level measured in quiet regions is about $\sim 10^{-9} \text{ W kg}^{-1}$.

CTD data from the precision sensors are low-passed at 10 Hz. Conductivity and temperature records are aligned by advancing one record over the other in -100 to 100 scan range, with unit increments, and obtaining the best advance giving the minimum

salinity spiking (result is typically 35 to 50 scans). CTD data are then averaged at 10-cm intervals prior to calculate salinity. Finally, the 10-cm vertical averaged salinity and density profiles are despiked (detecting only large spikes).

uVMP on sea ice

The aim with using the uprising vertical microstructure profiler was to obtain dissipation rate estimates in the upper 50-80 m up to the ice-water interface and to resolve the under-ice boundary layer. The VMP upriser (uVMP) is a VMP250 (SN104) from Rockland Scientific, Canada. It is a VMP250 modified for upward profiling measurements. It is an internally logging instrument fitted with rechargeable batteries. It is equipped with two shear probes and a fast response temperature sensor (and a pressure, tilt and vibration sensors). Turbulence channels are sampled at a rate of 512 Hz, and the slow channels at 64 Hz. Up to 4 brushes at the rear end provide a drag. We profiled using 3 brushes, giving a rise speed of about 0.6 m s^{-1} . The uVMP was deployed from the sea ice through a 1 m x 1 m hole, and the sea ice was about 60 cm thick. The hole was located 30 m away, and parallel to the MSS hole (150 m away from the ship, updrift). The uVMP was deployed only on 22 February.

During each deployment, we lowered the instrument to about 80 m depth using a weight (about 10 kg) connected to the surface via an electric cable sending a release signal. The uVMP is also attached to a rope that is used to bring the profiler back to the sea ice hole. We waited 4 minutes after lowering the uVMP before releasing, to avoid measuring the turbulence created by the lowering of the instrument. Upon release, the instrument rises freely (but there is drag on the rope paid out). A free-rise to the surface takes approximately 2 minutes. After the release, we waited 3 minutes (and the profiler is then at the underside of ice), and sent a weight of about 6 kg along the rope attached to the VMP. This ensures the profiler is pulled deeper, away from the ice, and is not dragged under the ice while pulling it back to the hole. When the profiler is at the surface, we recover the release cable and the weight attached to the end of it. This is to make sure we do not sample the turbulence at the wake of the weight bar being pulled up. Both lines (the rope attached to the profiler and the electric cable attached to the releaser) were pulled up by using an electric line puller. The release weight was then re-attached, and the procedure repeated 3 to 4 times in total.

Occasionally, the two lines entangled while lowering the instrument, resulting in bad data. We collected 3 sets of 4 casts on 22 February. In total, 12 profiles were performed (4 between 09 and 10:15 UTC; 8 between 12-15:30 UTC), but 3 suffered from tension and drag on the rope in the entire profile.

Processing of the VMP data is performed using the routines provided by Rockland Scientific (ODAS v4.4) and described in detail in their technical notes. We did not remove the shear probe signal coherent with the vibrations, since this requires a long analysis segment length which compromises the aim of resolving the under-ice boundary layer. We used 1 s FFT length, and estimated dissipation using spectra over half-overlapping 2 s windows.

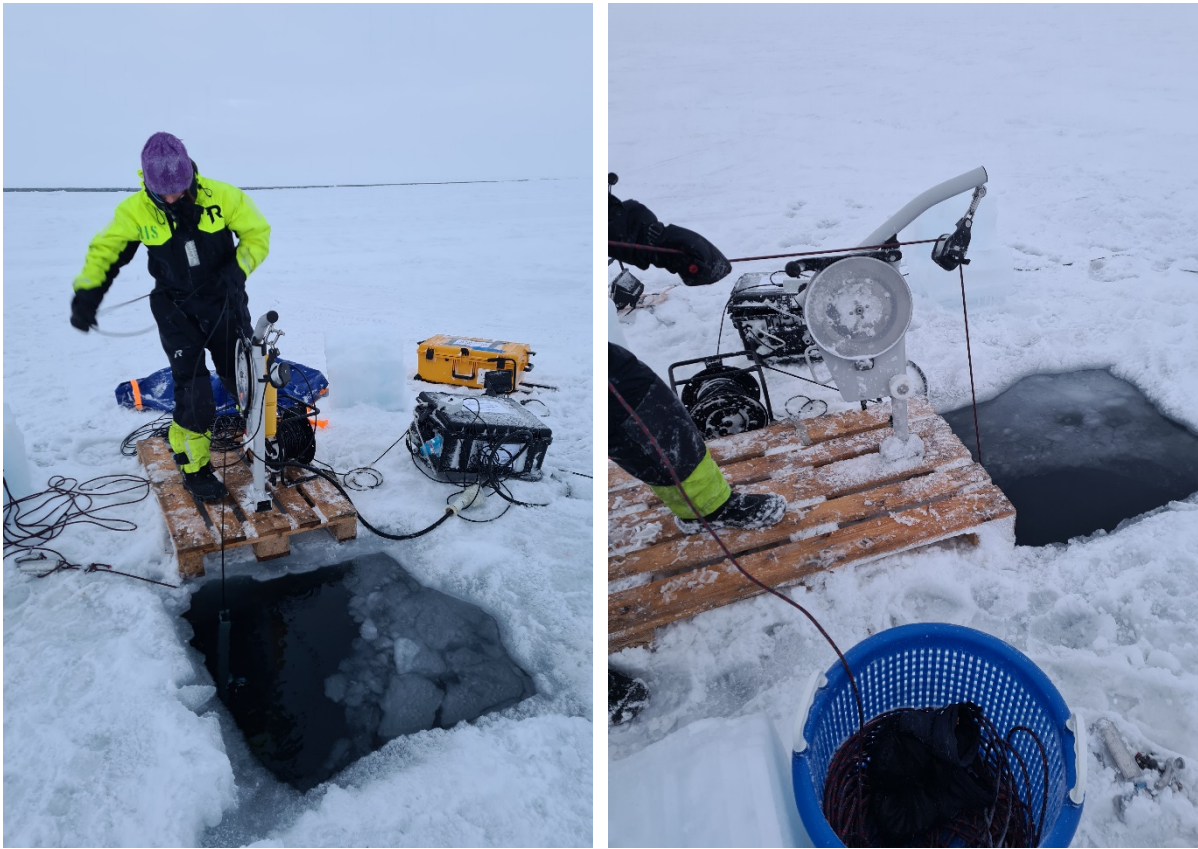


Figure 13: Setup of the VMP on ice. A motorized linepuller helped recover the robe (in the basket) and the electric release cable (black cable). The black case is the power unit connected to the ship's mains.

3.5 Mooring recoveries and deployments

Deployment of NLEG M1, M1 BioAc and M1b

Mooring NLEG M1 was deployed on 20.02.2021, 19:00 UTC at N 79 35.034, E28 03.937. Deployment depth is 265 meter, and the top of the mooring is 20 meter below sea surface. The mooring consists of two ADCP's, one deep and one shallow, Sea-Bird CO₂ and Ph sensors, sensor measuring scattering, CDOM and chlorophyll, 21-bottle sediment trap and temperature loggers and CTD's at various depths. Deployment time is 9 months and expected recovery time is November 2021. Detailed drawing of the mooring is in Appendix 1b.

Mooring M1 bioAC was deployed on 20.02.2021, 21:00 UTC at 79 35,325N, E 28 05.303. Deployment depth is 260 meters, and the top of the mooring is 12 meter above the seafloor. The mooring consists of Nortek Signature 100 ADCP/echosounder. Deployment time is 9 months, expected recovery time is November 2021. Drawing of the mooring is in Appendix 1b.

One mooring, M1b, was recovered and redeployed. Its twin M1a deployed 2019-11-16 at 100 m depth at 79.6742 °N, 27.8413 °E, was communicated with, but could not be recovered due to large sea ice concentration at the site. Instruments on M1b, deployed

at the same time as M1a, were still logging, so there is a chance of getting longer timeseries at M1a.

Deployment of NLEG M4

The bottom-frame mooring M4, deployed 2019-11-14 at 67 m depth at 77.2686 °N, 24.4067 °E, could not be recovered because it is upside-down (trapped under its anchor) and heavy sea ice drift hampered the rescue mission. Its successor M4 was deployed. The auxiliary hydrography mooring M4b, deployed 2019-11-14 at 70 m depth at 77.2699 °N, 24.4071 °E, was not found and is considered lost.

Table 2: Mooring recoveries

Mooring ID	Date	Time [UTC]	Latitude	Longitude	Depth	Mooring info
M1b	2021-02-19	18:28	79.5746	28.1746	297.7	CTDs, T-loggers, bottom pressure recorder

Table 3: Mooring deployments

Mooring ID	Date	Time [UTC]	Latitude	Longitude	Depth	Mooring info
M4	2021-02-18	01:20	77.2708	24.4095	71.5	Bottom frame; ADCP, CTD
M1	2021-02-20	20:04	79.5840	28.0667	265.3	ADCP, CTD, BGC, OA, sediment trap
M1-BioAc	2021-02-20	20:44	79.5888	28.0898	263.5	Bio-acoustics ADCP
M1b	2021-02-20	22:47	79.5734	28.1537	298.8	CTDs, T-loggers, bottom pressure recorder

3.6 Gliders

Table 4: Glider metadata

	Odin (775)	SG560	SG562
Deployment date	12-Feb-2021	22-Oct-2020	7-Oct-2020
Retrieval date		10-Feb-2021	12-Feb-2021
Deployment duration	13 days	113 days	126 days
Deployment location	77°N 35.30', 31°E 12.52'	75°N 35.9', 33°E 22.0'	76°N 58', 11°E 51'
Retrieval location	76°N 38', 33°E 59'	75°N 21.9', 32°E 16.6'	77°N 15', 8°E 2'
Number of profiles		1267	625

Distance covered		1484 km	
Mission	uib01amr.mi		
Payload	CTD41CP, SN:9545 MR-1000, SN:324		

Seagliders

Two Seagliders were recovered during the cruise. Sg562 was recovered on 10 February 2021 19:30 UTC in the West Spitsbergen Current ($77^{\circ}\text{N } 15'$, $8^{\circ}\text{E } 2'$), after 126 days in the water. The conditions were challenging, and after several failed attempts at picking it up with lasso, we deployed a net. The net was attached to a hexagonal frame, which we lowered under the glider. A CTD cast from the moonpool (sta029) was conducted upon recovery. Sg560 was recovered on 12 February 14:45 UTC in the Barents Sea ($75^{\circ}\text{N } 21.9'$, $32^{\circ}\text{E } 16.6'$), after 113 days in water. The battery on sg560 went below the 20% safety margin one week before recovery, and the glider had been drifting on the surface since. No CTD cast was made upon recovery.

The Seagliders were equipped with Paine strain-gauge pressure sensors, SBE CT Sail and Aanderaa dissolved oxygen sensors (see Table 4 for serial numbers) and operated between the surface and 1,000 m depth (or seabed when shallower than 1,000 m). CTD and oxygen were sampled on both dives and climbs. CTD was sampled approximately every 1 m in the upper 400 m while oxygen was sampled at approximately every 5 m. Below 400 m depth the sampling frequency was lower. The vertical velocity was about 10 cm s^{-1} . For each dive, a depth-averaged current (DAC) was estimated based on the deviation between expected surfacing location deduced from the flight model, and the actual surfacing location. The 5m vertically averaged data from sg562 and sg560 are shown in Figure 18 and Figure 19, respectively.

Slocum glider

One Teledyne Webb Research 1000m electric glider (Slocum G3) was deployed on 12 February 23:00 UTC, during the cruise. Before deployment, a free-wave antenna was set up on top of the bridge, and the free-wave modem was set up on the bridge and connected to a computer with the appropriate software (terminal and Matlab). During deployment, the antenna cable was fed through a window on the bridge and connected to the modem. Four test dives were conducted within the range of the free-wave, before giving the control to onshore pilot, Fiona Elliot, who piloted it throughout the mission.

The Slocum G3's are buoyancy-driven autonomous underwater vehicles that provide high-resolution surveys of the physical properties of the water column. Our Slocum G3, named Odin, (SN775) was equipped with a Seabird conductivity-temperature-depth sensor (CTD41CP, SN9545) and an integrated RSI MicroRider (MR-1000, SN324) with two shear probes (S1=M2031, S2=M2032) and two thermistors (T1=T1849, T2=T1851) for measuring turbulence microstructure. CTD was sampled during the dives and

climbs. Final profiles have an average horizontal along-track resolution of 0.5 km and vertical bins of 1 m.

The MicroRider was configured to sample on dive and climb. To minimise vibration noise in the vehicle and achieve the desired science goals the glider mission was configured as follows:

- “Fixed mode” battery position was used to control the trim of the glider, which prevented the pitch motor from running during the glide. The fixed position was determined from a test dive to 100 m.
- Auto ballast control determined pump volumes for diving and climbing to keep the profiles symmetrical while maintaining a minimum vehicle speed of 0.1 m/s.
- To capture the complete water column, particularly the top few meters, the glider carried out one dive-climb profile per segment. The “climb to” depth was set to 0 m to avoid noise contamination from the air bladder and ballast bump that automatically switch on when the glider reaches surface. We were aware that this could cause the glider to sit on the surface un-commanded if the pressure sensor were offset when it reached surface, and thus it was monitored throughout the mission.

Odin ran the transect along the I section three times, but on the first northward transect it turned southward early due to sea ice blocking the way (Figure 3). On 13 February, the MicroRider stopped working due to a depleted CR123 cell. The same happened during a mission in October 2020, but then the malfunction was attributed to a bad CR123 cell. With the same malfunction occurring on this mission, it is unlikely to be a bad cell, and further investigation is needed to conclude on what is causing the malfunction. After the MicroRider stopped working, the mission continued with only the CTD running.

The glider was retrieved on the morning of February 26 0415 UTC (76°N 38', 33°E 59'). Conditions allowed us to retrieve it using the small working boat. Figure 20 and Figure 21 show temperature and salinity data from the mission.

3.7 Autonomous Underwater Vehicle - LAUV Harald

First attempt at the polar front

LAUV-Harald was deployed from KPH at 22:00 on the 13th of February at 76N 15.849 34E 15.248. During the pre-mission check of diving capabilities and compass calibration, the vehicle dived unintentionally to the seabed and got stuck. 17 hours later, it surfaced, and was located from the bridge. The vehicle had experienced a leak of about 10 cc of water and some corrosion on the CTD bulkhead connector, otherwise the vehicle was fine. It was carrying a Microrider sensor, on which one thermistor probe was destroyed. The reason for the unintended dive was as follows: a command issued through the “quick commands” in Neptus (the software used to control the vehicle) will cause the vehicle to ignore errors. When the vehicle breached the maximum depth

limit of 70 m, it was ignored. The data from the seabed shows some variability in T and S (see Figure 22).

Second attempt at the polar front

LAUV-Harald was deployed from KPH at 07:30 on the 26th of February at 76N 24.94 34E 09.61. The mission was to find and measure the polar front with 5000 m horizontal North-South transects at five different depths: 10, 20, 30, 40 and 50 meters. The vehicle was carrying a Microrider sensor with two shear-probes and one thermistor, in addition to its sensor suite of CTD, fluorometer and oxygen optode. The initial front position was set to 76N 25.462 34E 13.396, and maximum fin rotation was set to 30 degrees to compensate for the Microrider. The vehicle aborted after two dives due to timeout from the Follow-Reference maneuver, caused by a minor bug. The vehicle was set to continue its mission. After the first dive of the continued mission (at 30m), the vehicle aborted again due to a more substantial error, where it lost contact to the Inertial Measurement Unit (IMU) and the GPS card within the vehicle. At this point the vehicle was recovered. Preliminary investigations of the data showed that the vehicle found and adapted to the front position, defined as the point in the transect with the largest temperature gradient. A bug was found in the CTD-driver of the system, rendering all negative temperature values positive (absolute value of temperature in degrees C).

3.8 ROV operations – Blueye

At 09:00 on the 21st of February the ice station at 79N 37.5 27E 23.58, the double Blueye was deployed in a hole in the sea ice. Power from the ship was used to power an acoustic modem and the computers logging the data. It was carrying an Underwater Hyperspectral Imager (UHI), an altimeter and a Multibeam Echosounder (MBES), all instruments facing the ice. Due to network issues, the MBES did not log data. Several transects were run, both at varying depth and at fixed depth. The measurements will be used as a benchmark for under ice operations with UHI in the future.



Figure 14: Deployment of the double Blueeye on February 21st during the sea ice drift station in the northern Barents Sea (Photo: Frank Nilsen).

3.9 Meteorology

Radiative Flux Measurements

A portable station has been used to study the temporal variations of surface radiative fluxes. The sensors are mounted on a 4-meter-long horizontal pole, reaching out at Deck 6, approximately 11.5 meter above the surface (Figure 11). The station includes a Kipp & Zonen CNR 4 surface net radiometer. It measures broadband electromagnetic radiation shortwave (0.3-3 micrometer) and longwave (4-50 micrometer) bands at the surface (incoming and outgoing). The shortwave measurements include visible light but excludes the most UV-radiation. The instrument has also an internal temperature sensor for internal correction of the longwave radiation. This is taken care of in the logger. The CNR4 is ventilated and heated when connected to an external power source. The surface skin temperature is measured using two IR radiometers (Apogee SI-411 SDI-12 and Campbell Scientific IR120 IR), mounted on a horizontal pole as shown. The main IR radiometer (CS IR120 IR) points downwards to the surface with an angle of about 35 degrees (relative to the vertical), for measuring the surface skin temperature. The second IR radiometer (Apogee SI-411) points directly upwards for measuring the sky temperature, which is used for atmospheric correction of the surface skin temperature measured by the main IR radiometer. Geographic position is measured by a Campbell Scientific GPS16X-HVS GPS sensor.



Figure 15: Horizontal pole with CNR 4 radiation, infrared, and GPS sensors. Picture from Deck 6, beside the bridge.

SUMO – UAV

Fixed-wing unmanned aircraft systems (UAS) have shown great capabilities for atmospheric research over the past decades. However, shipborne operations are still sparse and remain challenging, mostly due to the spatially limited and additionally moving landing area, and thus largely depend on the experience of the operators and in particular the RC pilot's skills. To reduce these challenges, a net landing system, designed by Lindenberg & Müller GmbH & Co. KG, has been used during the Nansen Legacy WPC1 cruise for the Small Unmanned Meteorological Observer (SUMO). The SUMO is a fixed-wing system with a wingspan of 80 cm and a takeoff weight of about 700g. This combination of SUMO and net-landing system has been used for the first time during the Nansen Legacy cruise in September 2018. Since this first test deployment the system has been improved by increasing the net dimensions from 4m x 4m to 6m x 4m. In addition, the deployment of two GNSS reference systems mounted to the port and starboard side of the ship's helicopter deck enabled the UAS crew to monitor the ship's movement, which aided orientation during operation and in particular the landing procedure.

The observation strategy for SUMO had two main components: a) sampling of vertical profiles of temperature, humidity, wind speed and direction; and b) surveying the surface temperature of sea ice and/or open water. For a), SUMO performed a helical flight track from a start altitude of about 20m to 40m and up to the maximum allowed altitude, resulting in a smooth profile, or alternatively a stepped profile where SUMO was kept at fixed level for a certain period before being sent to the next higher level. Temperature and humidity are measured directly during these profile flights, whereas wind speed and direction must be estimated from the GNSS ground speed of the SUMO, which relies on the assumption of a constant airspeed. For b), SUMO is operated along straight parallel flight tracks with an approximate distance of 100m at a fixed altitude of around 50m. The chosen flight altitude is a compromise between safety

considerations and the strength of the surface infrared (IR) signal and the footprint of the IR sensor. Under conditions with high humidity and strong near-surface temperature gradients, as often found over sea ice, the IR signal observed at a certain level has a strong dependency on the atmospheric column between the surface and the IR sensor, due to long-wave flux divergence.

During WPC all flights except flight #0 (see Table 5 for an overview of all SUMO flights) were carried out under the operation manual of the Andøya Space Center, which allows for visual line of sight (VLOS) operations up to an altitude of 300m above surface and within a horizontal radius of 1500m from the pilot in command. In accordance with these regulations our maximum altitude for vertical profiles was set to 290m and our surveys covered areas of up to roughly 2km x 1km. Limiting factors for our operations were the visibility, wave height or ship movement, wind strength, the coordination with other measurement operations (MSS), and the rest times for the RC pilot and GCS operator. The visibility and wind conditions were the main factors setting constraints on our operations. In total we carried out 8 measurement flights and one test flight (see Table 5), making use of two SUMO models.

In addition to the SUMO flights, with takeoff and landing from the helicopter deck, it was also planned to carry out fixed-wing and additional multicopter flights from the sea-ice during the sea ice station, however wind speeds exceeding the operational conditions of both UAS did not allow for any UAS operation during period of the sea ice station.

Table 5: Summary of all SUMO flights.

#	Date	Location	Aircraft ID	Start Time	Stop Time	Mission Type
0	2021-02-15	76.9502N 30.3784E	SUMO-1	10:08	10:17	test (62 m)
1	2021-02-15	77.1362N 30.4021E	SUMO-1	14:32	14:57	profile (278 m)
2	2021-02-16	77.0850N 30.3780E	SUMO-5	11:33	11:47	profile (289 m) survey
3	2021-02-16	76.8518N 30.3780E	SUMO-5	15:37	16:07	profile (283 m) survey
4	2021-02-17	77.2259N 30.3983E	SUMO-5	06:31	07:02	profile (286 m) survey
5	2021-02-17	77.2285N 30.3506E	SUMO-5	10:02	10:30	profile (284 m)
6	2021-02-20	79.6235N 28.3025E	SUMO-1	08:46	09:05	profile (277 m) survey
7	2021-02-23	79.3838N 27.8792E	SUMO-1	10:36	10:47	profile (119 m)
8	2021-02-25	78.2016N 27.1871E	SUMO-1	09:11	09:27	profile (285 m) survey

Ship-based remote sensing

To continuously monitor wind profiles within the atmospheric boundary layer throughout the entire cruise, the meteorological instrumentation included two Doppler wind lidars. Wind lidars are active remote sensing instruments, emitting infrared laser beams into the atmosphere. A small fraction of the emitted beams are backscattered by aerosols in the air. As these scattering targets drift with the local winds, the frequency of the backscattered signal is Doppler-shifted with respect to the emitted frequency. This allows to retrieve the radial wind speed along the beam axis. Height information is inferred from the time difference between the emitted and the received signal and the speed of light.

A Leosphere Windcube v2, a pulsed Doppler wind lidar, was used to measure winds at 12 heights between 40 and 290 m above instrument level. The Windcube sends out five beams: four into cardinal directions along a 28° (zenith) scanning cone and a fifth vertical one. Applying a basic coordinate transformation, orthogonal wind vector components are computed from the line-of-sight measurements. To extend the wind profiles and enhance the vertical resolution at lower levels, an additional Zephir ZX300 wind lidar was set up with a vertical measurement grid width of 10 m between 10 and 60 m above instrument level and five additional levels up to 200 m. For each height level, the Zephir scans along a full 360° scanning cone with an opening zenith angle of 30° using a rotating mirror. In contrast to the Windcube, the Zephir is a continuous wave lidar, focusing on specific height levels by adapting the focus of the receiving optics.

Both lidars were mounted next to each other at starboard on the helicopter deck (see Figure 12), which is located approximately 11 m above sea level. The measurements started on the 11.02.2021, 12.00 UTC and ended on the 27.02.2021, 12.15 UTC. Visual inspections and checks of the carrier-to-noise-ratio were performed at least twice a day in order to ensure continuous high-quality measurements. Additionally, automatic wipers, anti-freeze solution sprayers and manual cleaning on a regular basis were applied to keep the optical windows clear from salt, sea spray, snow and icing. The Windcube was initially set up with an additional shielding plate, which was, however, suspected to be slightly influencing the measurements and removed on the 16.02.2021, 17.30 UTC. The total mean data availability increased from 71.09 % before the removal of the plate to 87.34 % afterwards. The Windcube is additionally equipped with an internal IMU and two GPS antennas. This setup allows for compensation of the ship's motion. For the Zephir, an external IMU was installed on 17.02.2021 for experimental purpose, thus the resulting data is not included in the preliminary data presentation in Section 4 of this cruise report.



Figure 16: The lidars installed on starboard on the helicopter deck.

In addition to the wind lidars, a RPG HATPRO microwave radiometer was supposed to continuously monitor temperature and humidity profiles up to 10000 m altitude. Unfortunately, the radiometer suffered from heavy icing during the installation on the first day of the cruise (see Figure 13), as the instrument could not be powered and heated due to a missing power connector. The resulting icing most likely led to an electronic short circuit when finally powering up the heating/fan element on the following day. After the instrument was de-iced and inspected, it was decided to not power it again before a more sophisticated assessment of the damage by the manufacturer. Therefore, it was not possible to collect the planned continuous temperature and humidity profiles throughout the cruise.



Figure 17: Removal of the ice layer from the HATPRO microwave radiometer.

Radiosonde measurements

On behalf of the Deutscher Wetter Dienst, Vaisalla radiosondes were launched daily, to collect profiles of air temperature, wind speed, wind direction and air humidity. The sondes are launched from a specialized container at the vessel at about 1045 UTC. Additional radiosondes were launched in the period from 2021-02-19 – 2021-02-22, at 2245 UTC. The sondes rise quickly to about 20 000 – 30 000 masl before they explode. Although the vertical resolution is somewhat coarse, the radiosondes provide valuable data for meteorological model validation.

Weather Station on sea ice

During the 1-day long sea ice station we employed a 5.3-m micrometeorological mast on the sea ice in a distance of about 200 m from the ship. Due to the relatively short observation period this mast was set up in advance on board of RV KPH so that the final installation only comprised raising the mast and the mounting of sensitive instruments, such as, the eddy- covariance systems and the radiation sensors. Furthermore, the suit of sensors was rather limited and included only the most relevant systems (see Table 6 for details).

Table 6: Sensor specifications of micrometeorological mast.

Parameters	Sensor	Measurement Heights	Sampling Frequency
u, v, w, T_{sonic}	Campbell Sci. CSAT-3	2.0 m, 5.2 m	20 Hz
T	Campbell Sci. ASPTC (aspirated)	1.0 m, 2.0 m, 5.3 m	1 Hz
T	PT100 (aspirated)	1.0 m, 2.0 m, 5.3 m	1 Hz
RH	Rotronic HC2-S (aspirated)	1.0 m, 2.0 m, 5.3 m	1 Hz
$SW_{up}, LW_{up}, SW_{down}, LW_{down}$	Kipp and Zonen CNR1	1.7 m	1 Hz
H_2O, CO_2, p	LI-COR LI7500	2.0 m	20 Hz

The purpose of this station was to sample time series of; a) the surface energy balance (SEB) over sea ice; b) turbulence at different levels; and c) vertical gradients of wind, humidity and temperature. The conditions during the observation period were characterized by strong winds and mostly overcast.

3.10 Surface Drifters

Sea ice drift and waves in ice were monitored using 20 surface drifters and wave monitoring ice buoys. These were of 2 kinds, developed and produced in-house at the Meteorological Institute. More specifically, we deployed:

- 6 drifters and wave monitoring instruments of the "v1" model. These are built following the design described in Rabault et al. (2020). These are similar to the drifters and sea ice buoys that had been deployed during the NL cruise in September 2018. These instruments transmit GPS coordinates and complete wave information (significant wave height, peak period, wave spectra) around each 3 hours. The instruments are equipped with a large battery and a solar panel. Battery operation time is over 3 weeks. As soon as the daylight exceeds 8 hours a day, the solar panel are sufficient to cover all energy needs. These instruments are built around a cost-efficient Iridium modem, a GPS, and a high-accuracy inertial motion unit (IMU, for which we use the VN100 from Vectornav) that is used to measure wave motion. Processing is performed on-board using a Raspberry Pi microcomputer. The total bill of material for each instrument is around 2.5 kUSD, where the IMU alone is 1.3kUSD. All the waves in ice instruments v1 worked flawlessly from a technical point of view.



Figure 18 : waves in ice loggers 'v1' are contained in a single Pelican case (total weight around 5kg, dimensions around 30cm x 18cm x 16cm).

- 13 drifters and wave monitoring instruments "v2" model. These are an early prototype of the next generation of waves-in-ice instruments developed at the Meteorological Institute, and this cruise was the first time this design was assembled, tested, and deployed. Since these are early prototypes and still in the design / testing phase, higher failure rate was observed, and only 9 of these worked as expected. Several technical challenges were discovered and will be fixed and improved in the next iteration of these

buoys. Therefore, the cruise has been a very valuable occasion to full-test the designs. These new generation instruments are built around an updated Iridium modem, GPS receiver, and an IMU. A much less expensive IMU (BNO080 from Hillcrest Lab) was used. Not all of the prototypes were equipped with an IMU, i.e. some of these instruments operated as pure drifters. The processing is performed directly on the microcontroller, and no external microcomputer is used. This design is powered solely by batteries only, which we estimate are enough for at least over 4 months of operation. These instruments transmit GPS position each hour, as well as wave acceleration spectrum each 3 hours. The individual cost of each of these instruments is around 0.5 kUSD, which is around 10 to 20 times less expensive than the cheapest commercial alternatives, and 5 times less expensive than the instruments 'v1'. This allows large-scale deployments at a moderate cost.

When a large number of waves in ice instruments get deployed on the ice, this has implications on how efficient deployment should be so as to not delay other operations taking place during the cruise. This year, a novel method was used. Rather than using a smaller boat or the gangway to access the ice, the ice cage was used for deploying the instruments. Two people were present in the ice cage, to both check ice conditions, measure ice thickness, and deploy the instruments themselves. This allows to perform deployment of an instrument in less than 10 minutes, and to minimize the impact on the boat schedule. For even larger deployments, we will in the future consider using an even faster deployment method, such as using a long rod to directly put the instruments on the ice, without the need for anybody to physically get on the ice.



Figure 19: Deployment of the waves in ice instruments was performed using an ice cage, which allowed to perform deployments quickly and effectively.

A summary of the deployments, as well as local snow and sea ice conditions, is presented in Table 7 and shown in Figure 1. This is, to the best of our knowledge, the first medium-scale deployment of such types of instruments in this region of the Arctic.

Table 7: Surface drifter deployments.

	Date	Time	Lat	Lon	Sea-ice Thickness	Snow Depth	IMU	Kind of instrument
1	2021-02-16	18:30	77.26	29.83	0.6		X	V1
2	2021-02-16	21:00	77.55	30.14	0.5		X	V1
3	2021-02-16	23:00	77.68	29.75	0.5		X	V1
4	2021-02-22	19:00	79.63	27.39	0.5		X	V2
5	2021-02-23	16:00	79.15	26.16	1			V2
6	2021-02-23	22:00	78.97	24.76	0.7			V2
7	2021-02-24	06:00	78.85	23.39	0.7			V2
8	2021-02-24	12:00	78.55	23.71	1			V2
9	2021-02-24	22:00	77.96	24.77	0.8	0.1	X	V2
10	2021-02-25	01:20	78.02	25.58	0.7	0.15	X	V2
11	2021-02-25	05:00	78.10	26.28	0.6	0.15	X	V2
12	2021-02-25	10:00	78.20	27.18	0.75	0.1-0.15	X	V2
13	2021-02-25	11:00	78.17	27.30	0.65	0.1-0.15	X	V1
14	2021-02-25	11:35	78.13	27.46	0.5	0.1	X	V2
15	2021-02-25	12:00	78.09	27.61	0.7	0.1-0.15	X	V1
16	2021-02-25	12:00	78.09	27.61	0.7	0.1	X	V2
17	2021-02-25	12:50	78.05	27.94	0.8	0.1	X	V1
18	2021-02-25	13:40	78.01	27.92	0.5	0.1	X	V2
19	2021-02-25	14:15	77.96	26.92	0.5	0.1	X	V2

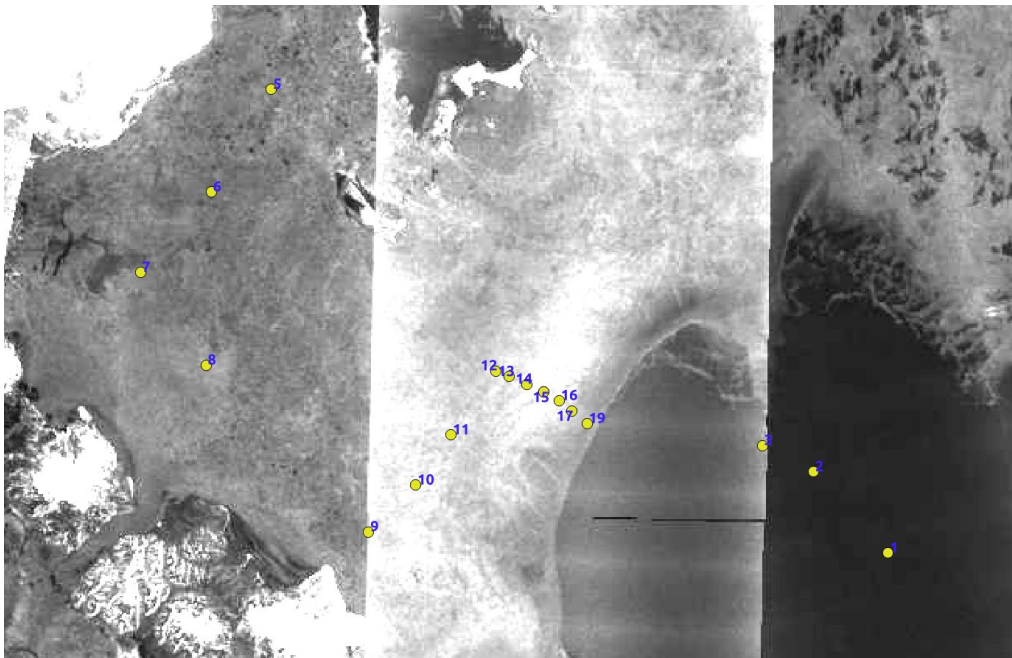


Figure 20: Positions of the deployment of the drifter / wave loggers. In the background the Sentinel-1 satellite sea ice picture for 2021-02-25 provided by the Norwegian Ice Service. Note that 3 instruments (1, 2, 3) appear to be deployed in the open water, but this is an artifact of the figure as they were deployed much earlier than the date of the satellite image, at a time when sea ice was present in the corresponding region.

3.11 Measurements of waves in sea ice and open water

Measurements of waves in both the open water and the sea ice were performed using a ship-born ultrasonic probe (Banner QT50ULBQ6) for measuring the distance from a pole mounted on the helicopter deck to the water, and an inertial motion unit (IMU, in our case, the VN100 from Vectornav) for compensating for the motion of the ship and calculating the wave elevation. This system is similar to the one used during the September 2018 NL cruise. Technical details about the system are available in Løken et al. (2020, 2021).

The system was operational during the entire cruise, with exception at the start of the cruise (first 5 days) as well as the end of the cruise (last 4 days). Both interruptions in data collection were due to icing on the ultrasonic wave probe. Icing had to be removed manually before re-installing the ultrasonic sensor. In addition, a known limitation of this system is the relatively limited dynamic range of the ultrasonic gauge used, which means that this system is mostly usable only for quite small waves (typically under or around 1m significant wave height). This is however fine to use in the sea ice. The Meteorological Institute will consider starting the design work for a new generation of such waves measurements, which would avoid these limitations of both range (by using a new sensor) and icing (by adding heating to the system), and could be mounted permanently on the boat if this is deemed relevant. The strength of such a system is to provide accurate waves in ice measurements for the full time of the boat presence in the MIZ and the drift ice, which is of great value for tuning operational parametrizations and models.

4 Presentation of data

4.1 Hydrography

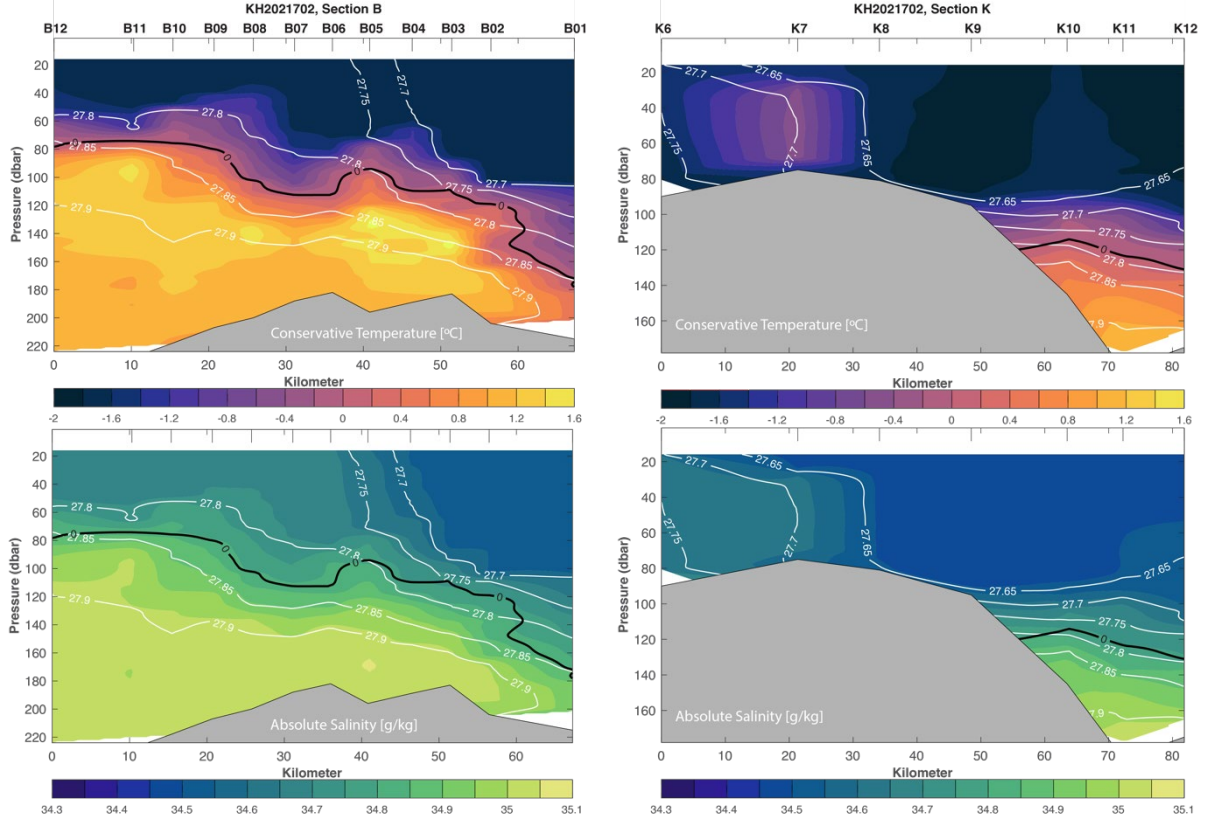


Figure 21: Selected CTD sections (in columns) obtained from the SBE sensors. Upper panels are for Conservative Temperature and lower panels are Absolute Salinity. White contours are σ_0 and the black contour are the 0 °C for reference. Ticks at the top of each figure mark stations locations with station names indicated. Note that the upper 15 meters are left out since the CTD was lowered through the moonpool.

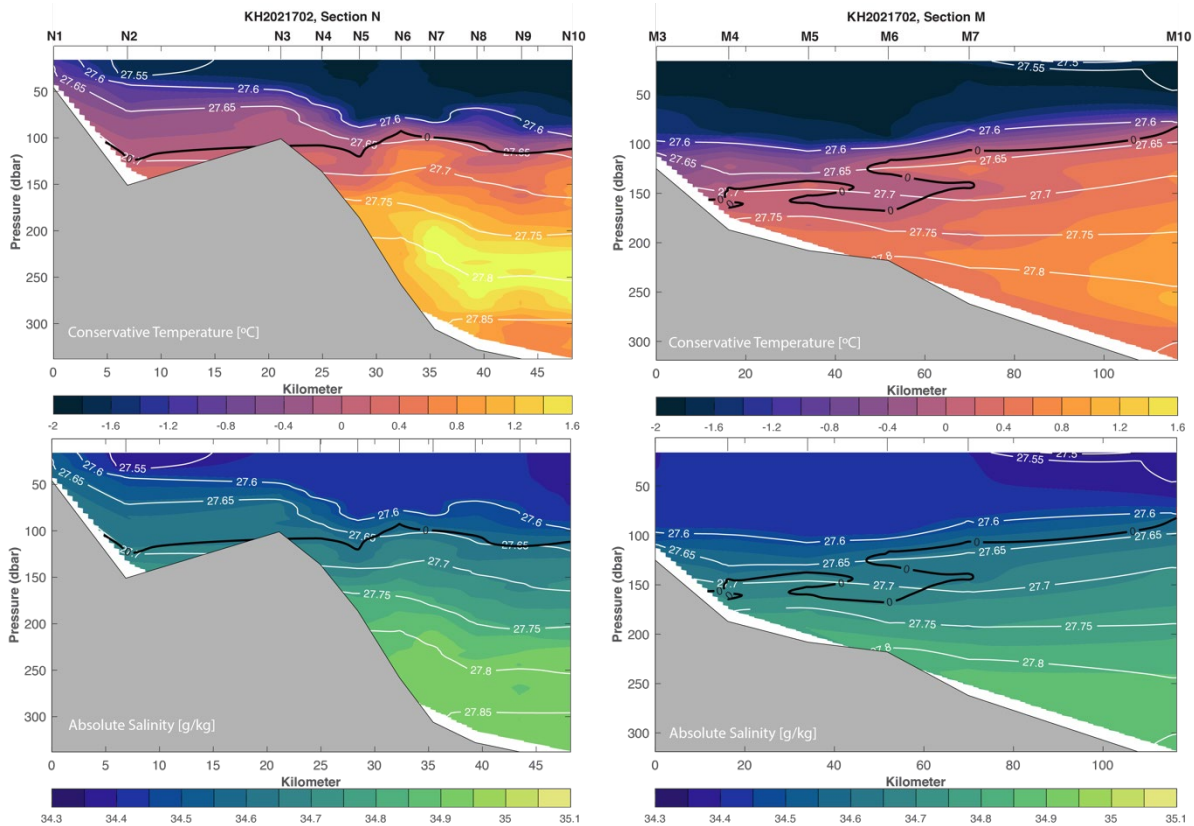


Figure 22: Continued.

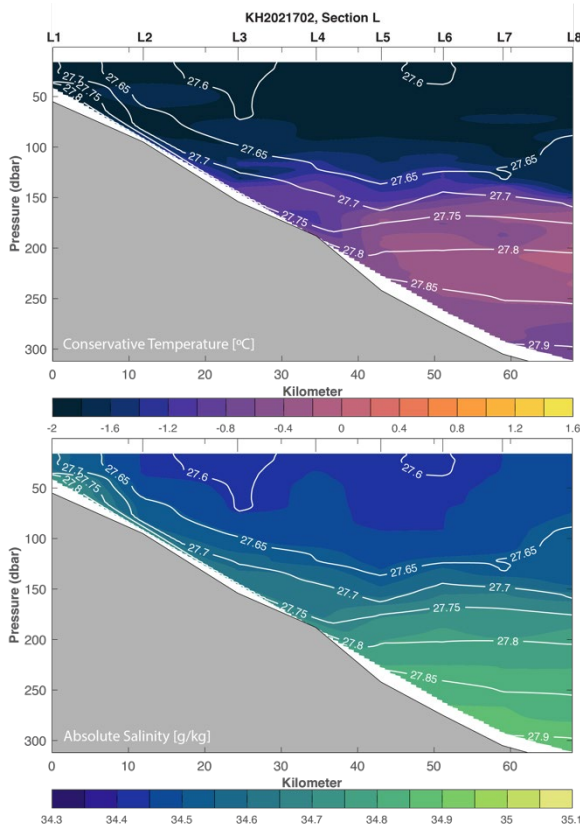


Figure 23: Continued.

4.2 Current Profiling

Lowered-ADCP (LADCP)

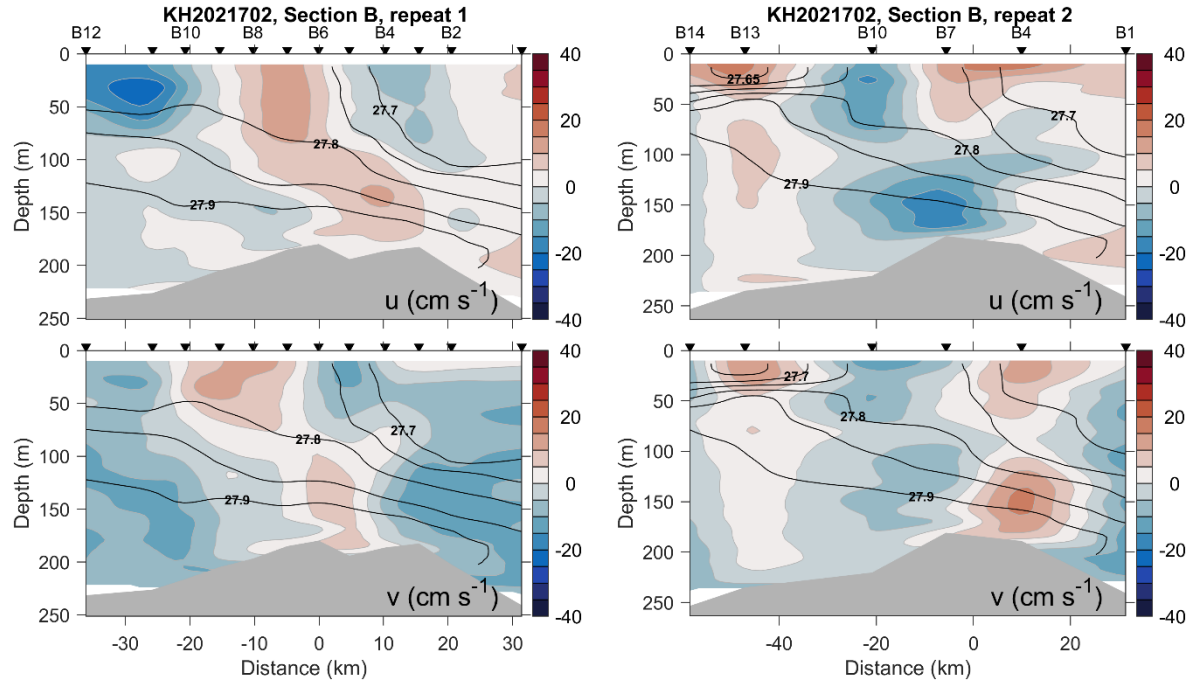


Figure 24: Distribution of the east (u) and north (v) components of velocity measured by the LADCP at two repeat occupations of Section B. Isopycnals are σ_0 at 0.05 kg m^{-3} intervals. Bottom topography (gray) is from the ship's echosounder at station locations (arrowheads and lettered numbers). Horizontal distance is referenced to B6, the approximate front location.

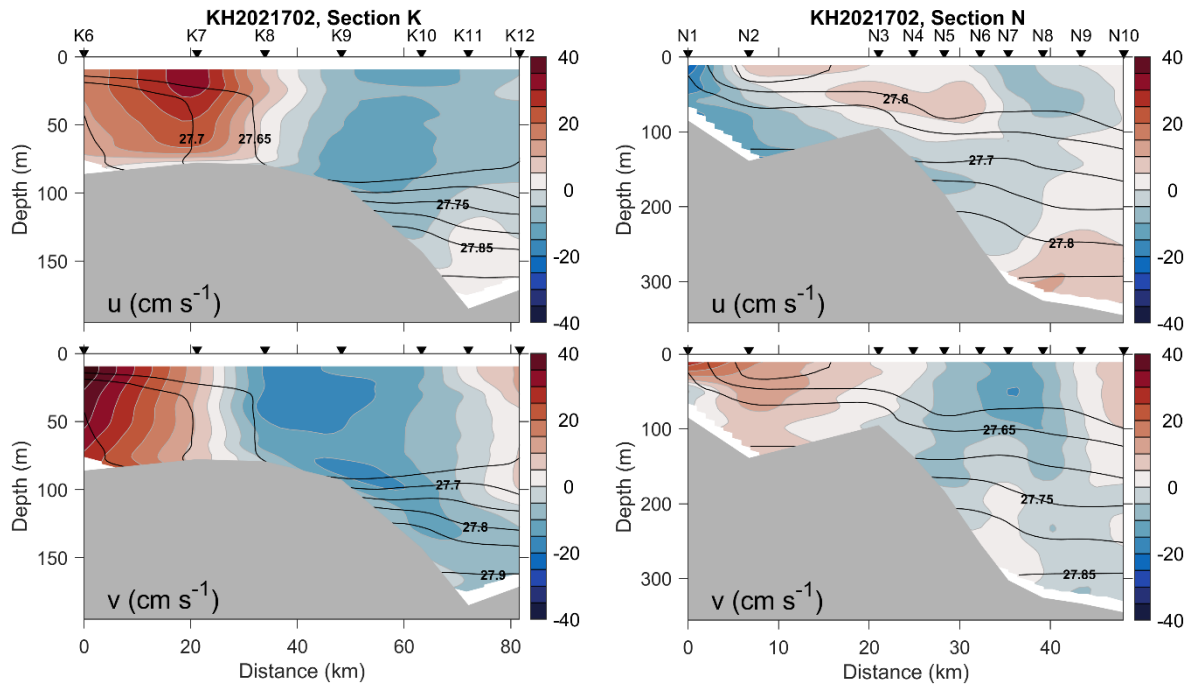


Figure 25: As in Figure 18, but for Sections K and N. Horizontal distance is referenced to the shallowest station.

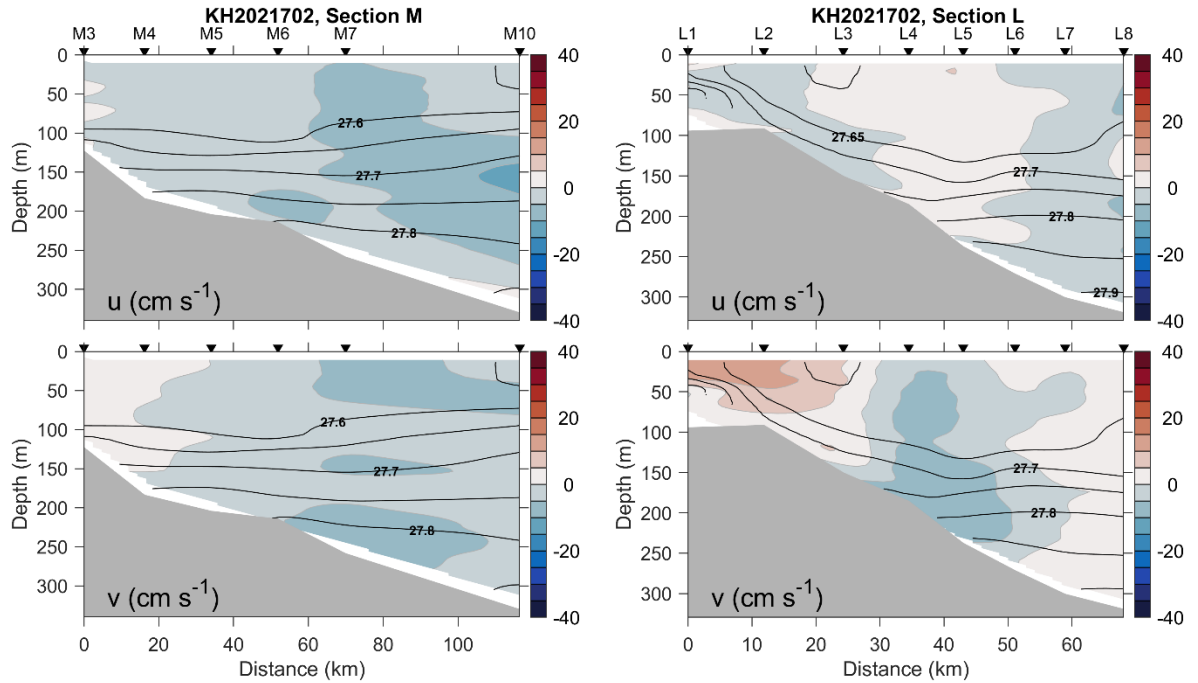


Figure 26: As in Figure 18, but for Sections M and L. Horizontal distance is referenced to the shallowest station.

Shipboard-ADCP (SADCP)

Because of their continuous operation, the vessel-mounted ADCPs are a valuable addition to our extensive dataset and may help to shed light upon the complex spatio-temporal pattern of circulation in the region and especially across our hydrographic

sections. In the following, we present preliminary processed data of the 150kHz ADCP that have been de-tided by removing the depth-independent barotropic tide obtained from the Arctic Ocean Inverse Tide Model (AOTIM) Arctic 5km 2018 model (<https://www.esr.org/research/polar-tide-models/list-of-polar-tide-models/arc5km2018/>).

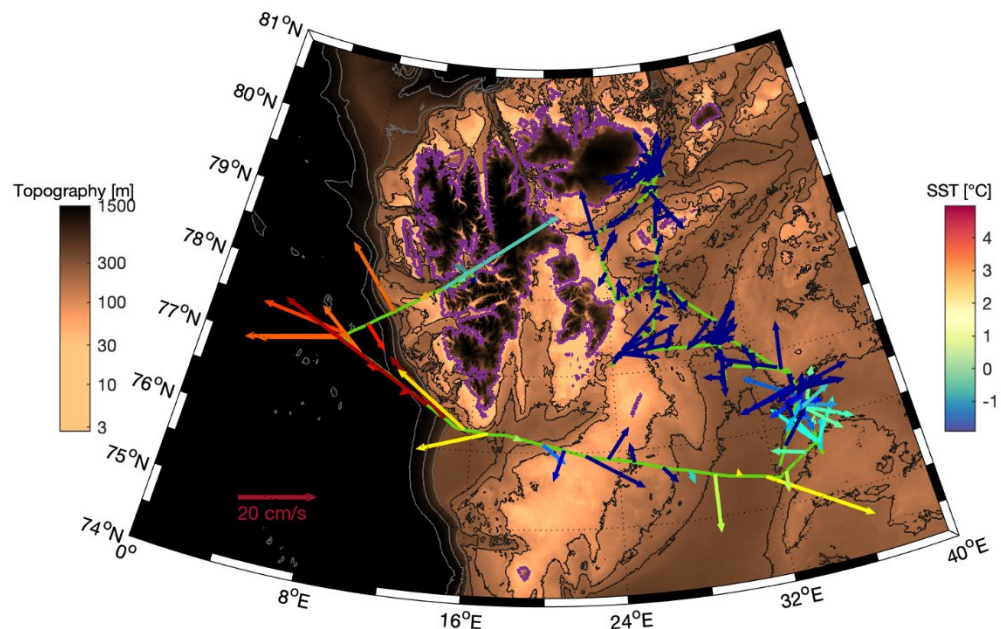


Figure 27: De-tided depth-averaged currents from the 150 kHz ADCP. Bathymetry is from IBCAO v4. Sea-surface temperature (SST) is from the thermosalinograph.

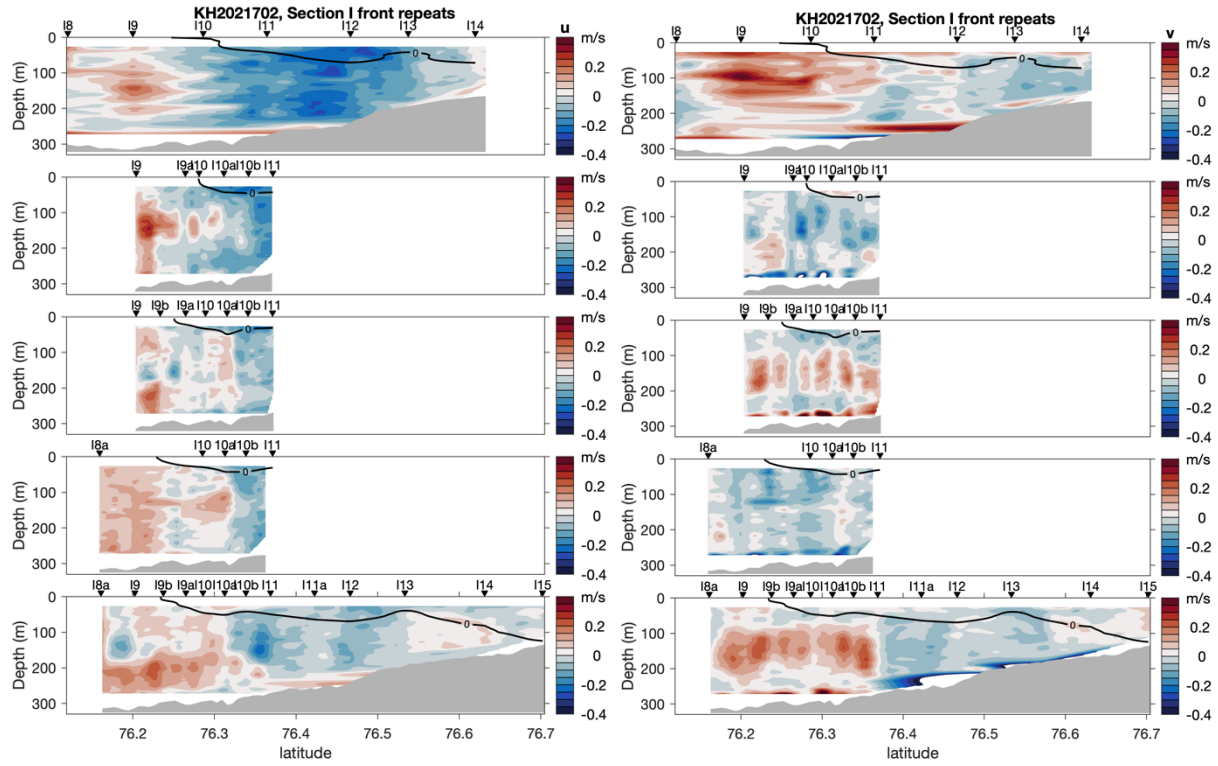


Figure 28: Repeated I-front section with de-tided currents from the 150 kHz ADCP, with zonal component u (left), meridional v (right). The 0°C contour measured by the microstructure profiler (MSS) indicating the front position is overlaid in black. Bathymetry is from IBCAO v4.

4.3 Microstructure Profiling

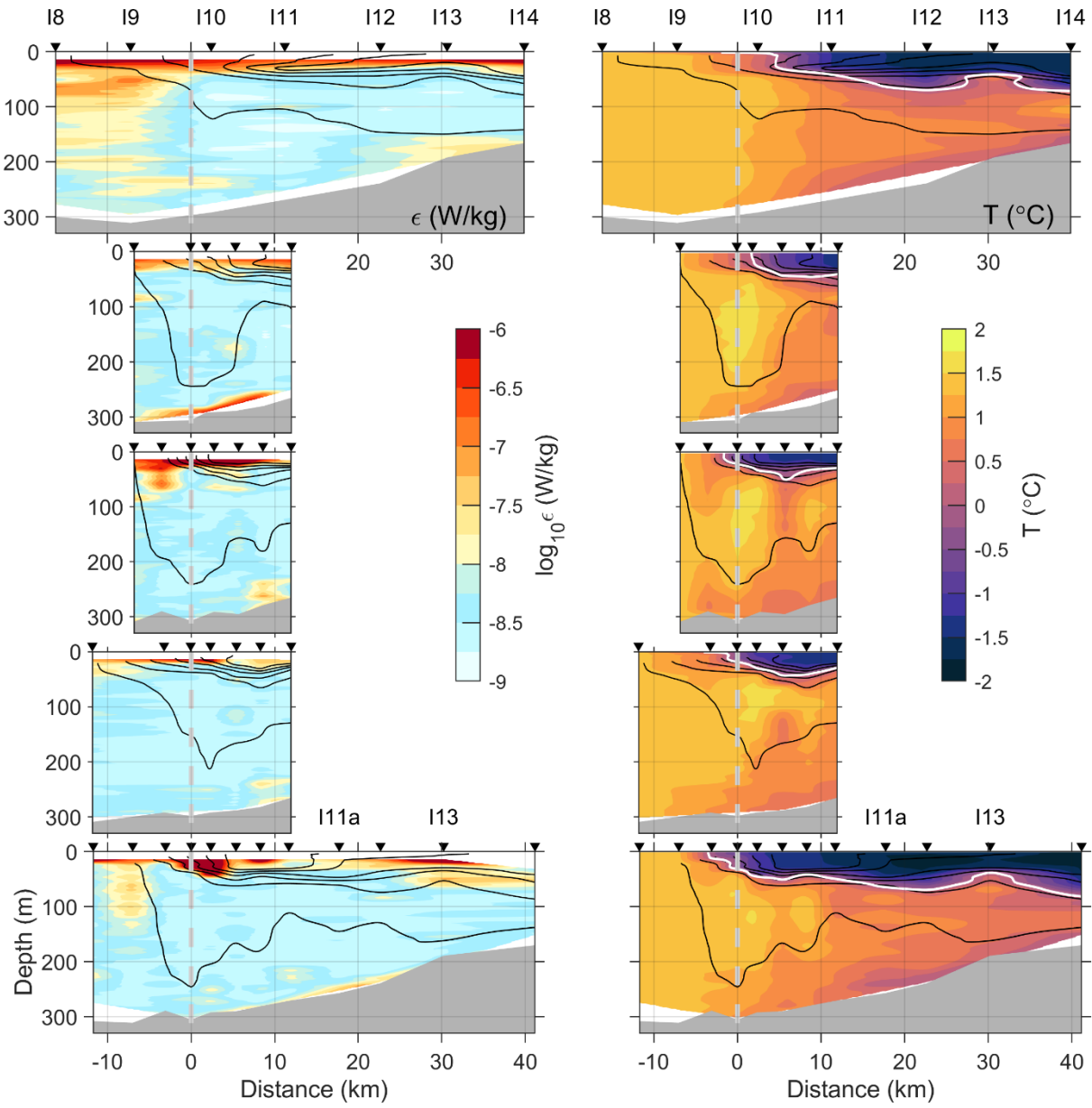


Figure 29: Repeat occupations of Section I, obtained from the microstructure profiler MSS. Left panels are the dissipation rate, ϵ , and the right panels are the temperature. Black contours are σ_0 and white contours are 0°C for reference. 1-m vertical averaged data are gridded in 150 (horizontal) x 250 (vertical) points, and smoothed over 3x5 points. Arrowheads mark station locations with station name indicated. Bottom topography is from the ship's echosounder at station location. Section I was repeated 5 times. Sections are referenced to the front location, close to the outcropping of the 0°C isotherm.

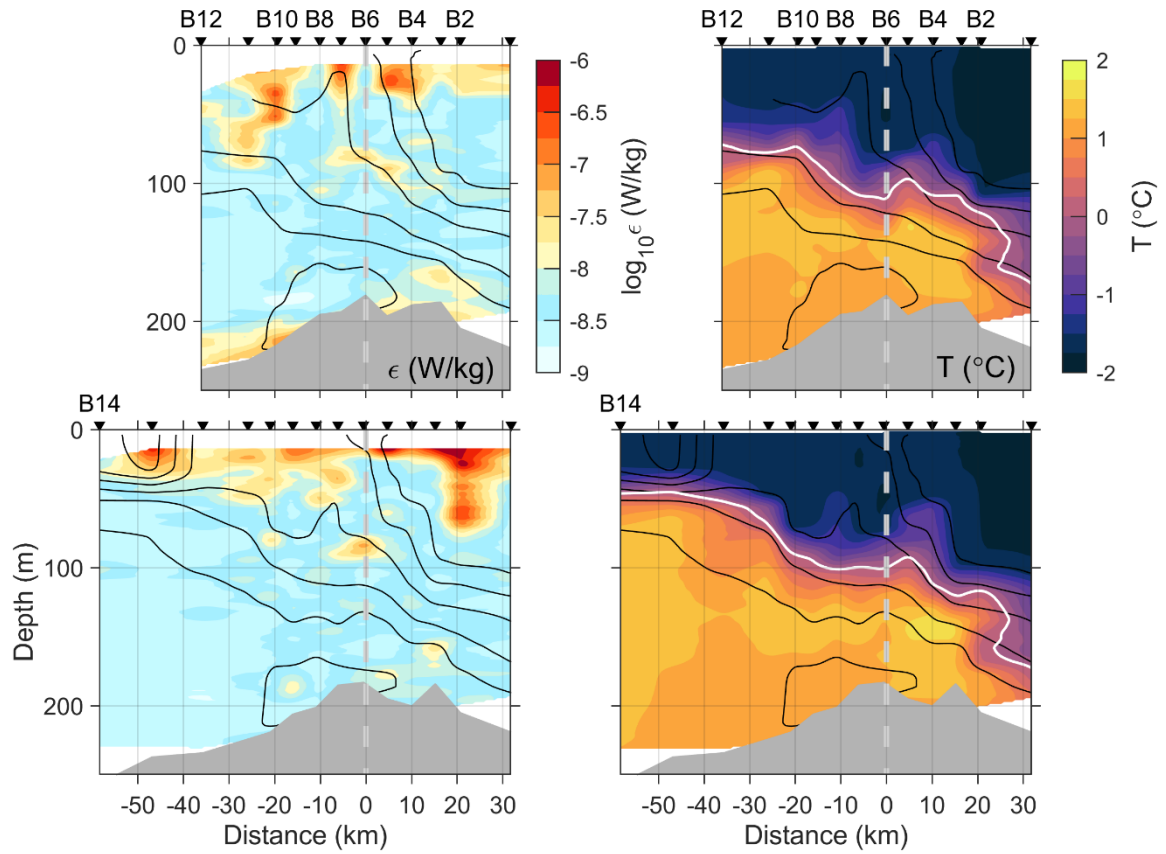


Figure 30: Same as Figure 22 but for the two repeat occupations of Section B. Horizontal distance is referenced to the front location at B6.

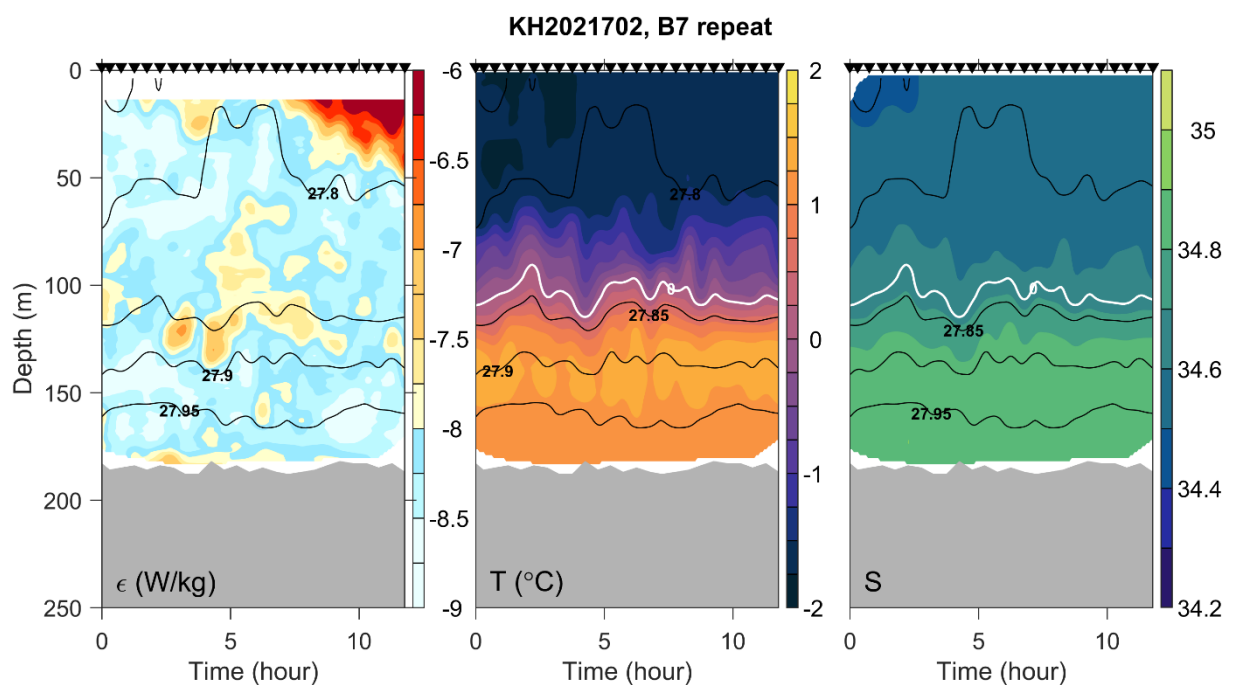


Figure 31: The front location at Section B, near B7, is occupied for 12 hours when collecting microstructure profiles every 30 min. Time series of dissipation rate, temperature and practical salinity are shown together with isopynals (black) and the 0°C isotherm (white).

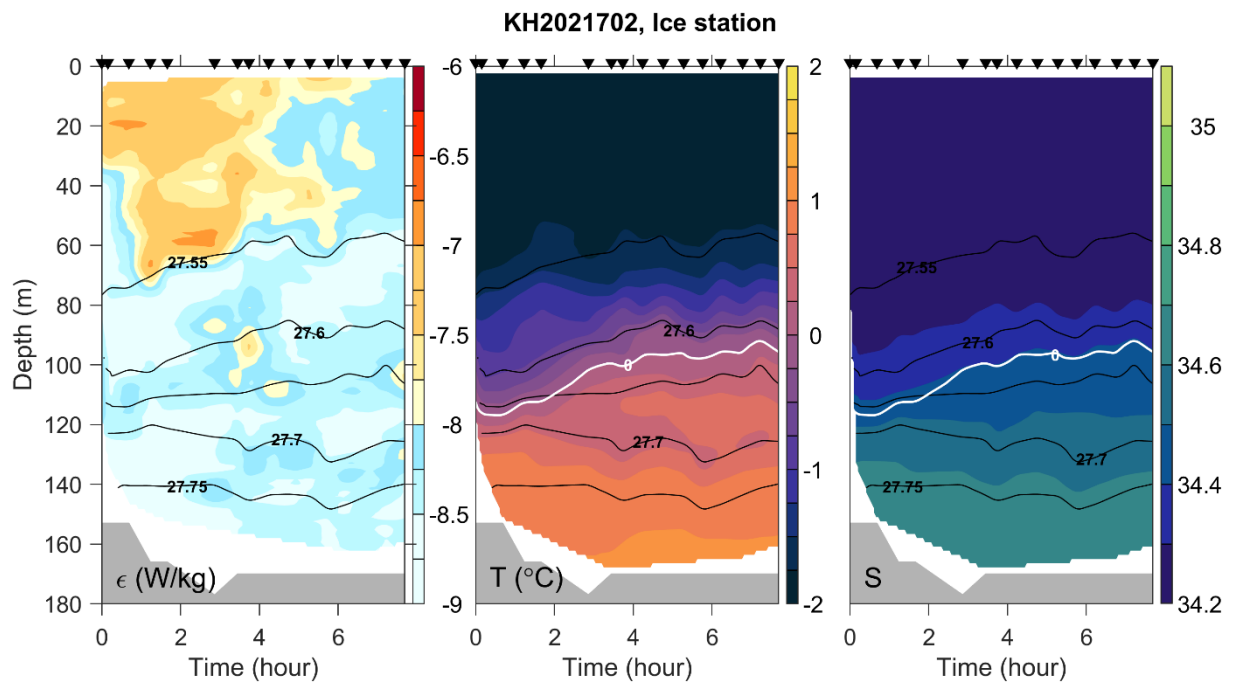


Figure 32: Microstructure measurements at the ice station.

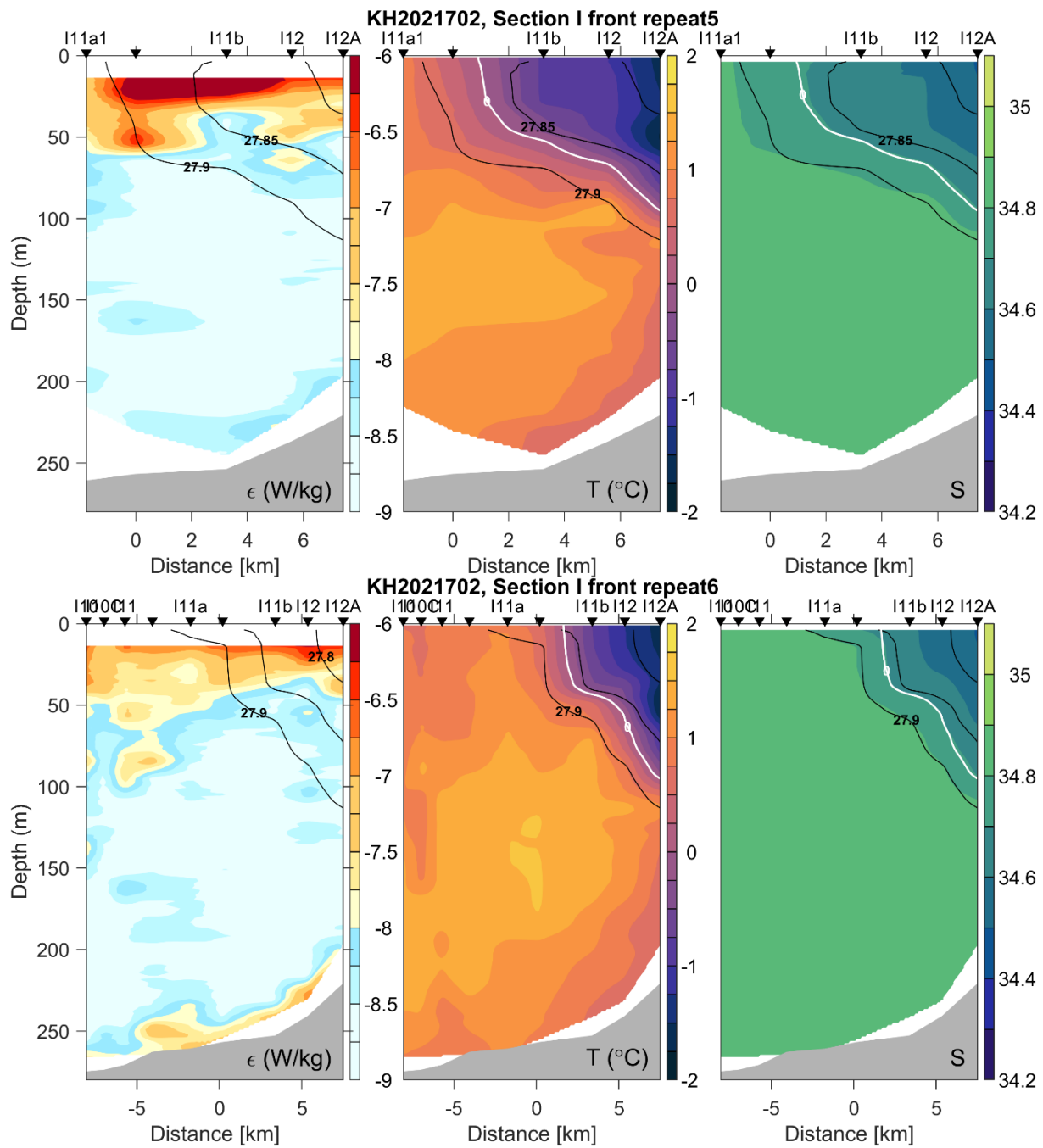


Figure 33: Repetitions 5 and 6 of the frontal region at Section I, 12 days after the end of earlier 5 occupations. The horizontal axis is referenced to the approximate location of 0 isotherm outcropping as in Figure 22.

4.4 Gliders (Eivind)

Seagliders

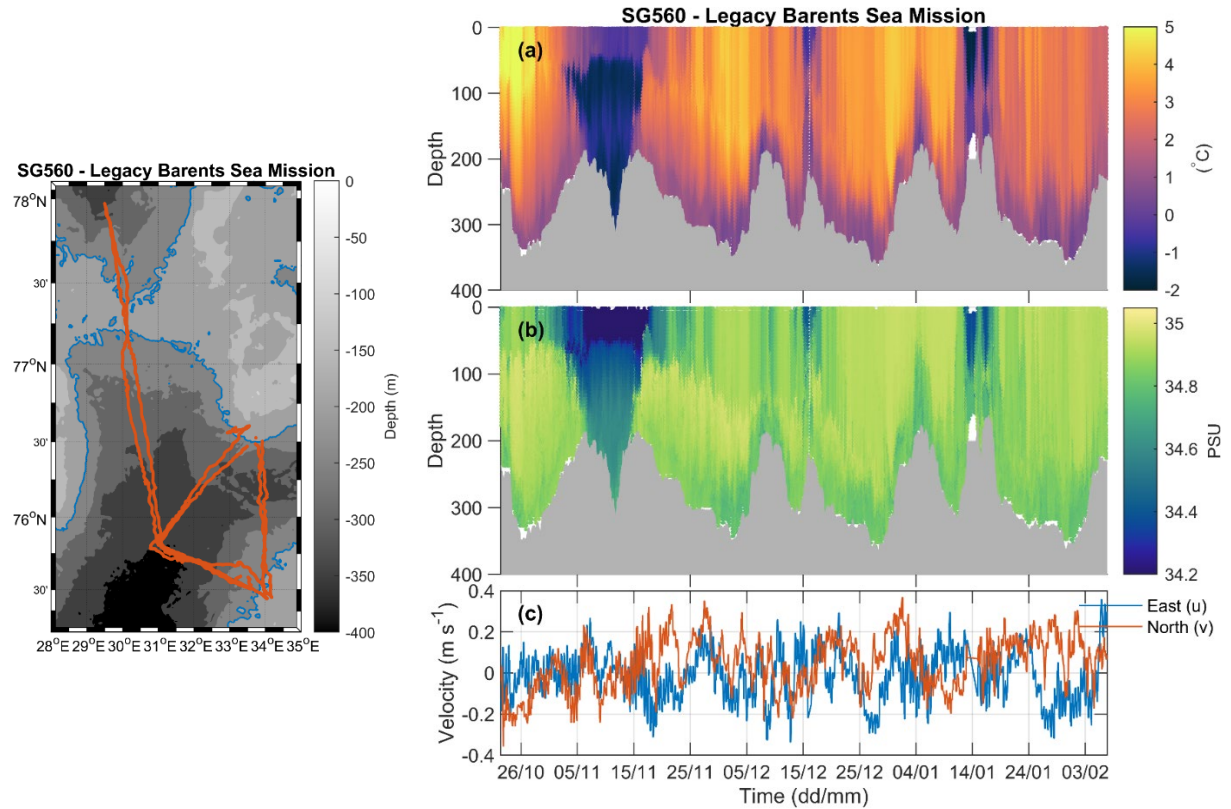


Figure 34: Red line shows glider track from the Barents Sea Mission with sg560. Blue line is the 200 m isobath. a) Temperature, b) Salinity and c) Depth average currents, measured by sg560 in the Barents Sea.

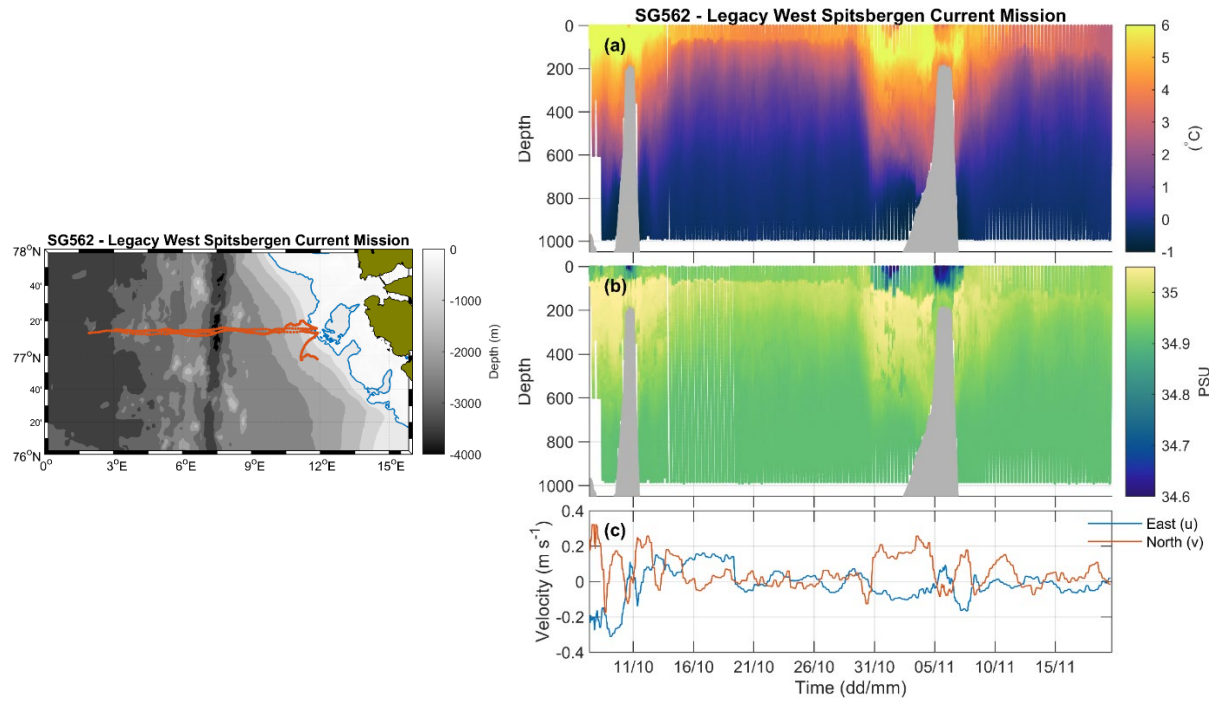


Figure 35: Red line shows parts of the glider track from the West Spitsbergen Current mission with sg562. Blue line is the 200 m isobath. a) Temperature, b) Salinity and c) Depth average currents, measured by sg562 in the West Spitsbergen Current. All data is not included.

Slocum glider

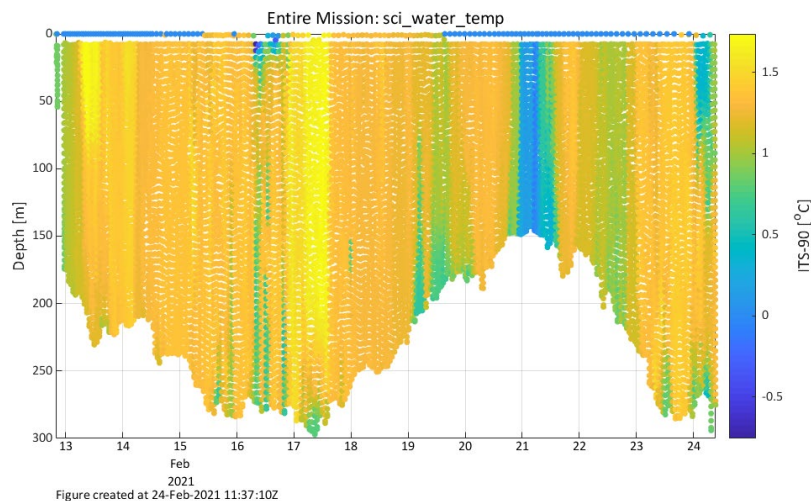


Figure 36: Temperature measured by Odin along the I section in the Barents Sea.

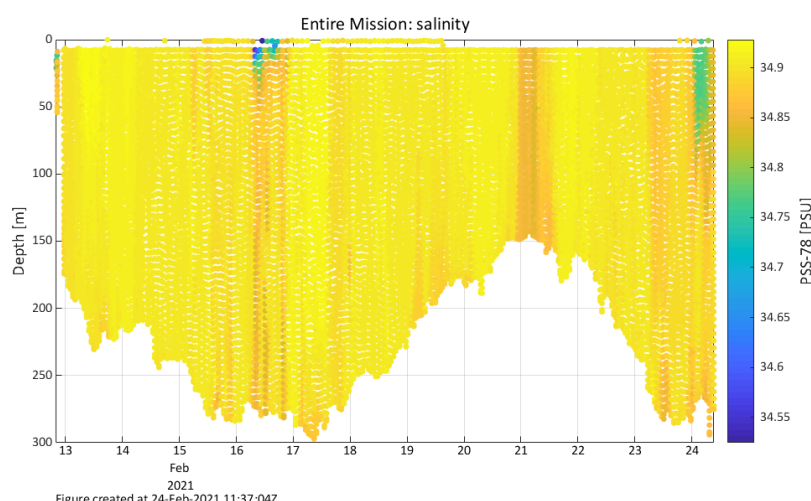


Figure 37: Salinity measured by Odin along the I section in the Barents Sea.

4.5 Autonomous Underwater Vehicle - LAUV Harald

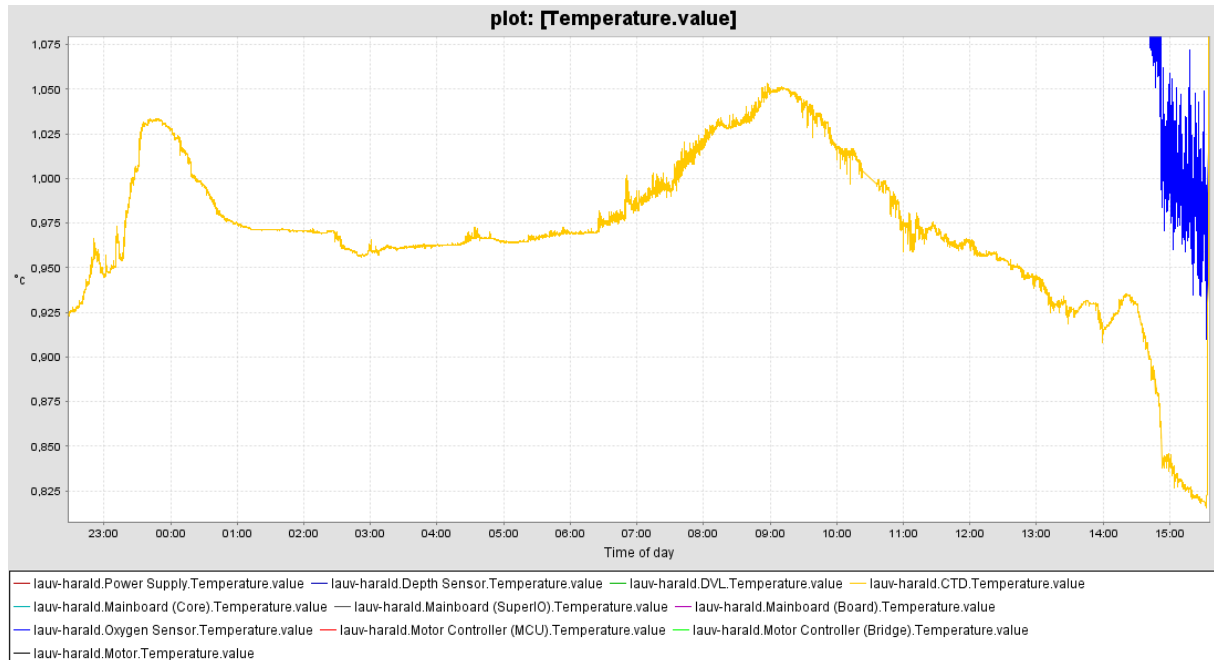


Figure 38: Temperature time series from the LAUV-Harald during the first mission.

4.6 Meteorology

Radiative Flux Measurements



Figure 39: Radiative Flux Measurements. (top) Outgoing (blue) and incoming (yellow) longwave radiation (bottom) Outgoing (blue) and incoming (yellow) shortwave radiation.

SUMO – UAV

In total 8 scientific SUMO flights (Table 5) could be carried out during the cruise, all of them consisting of one vertical profile and five with an additional horizontal survey. Figure 33 displays preliminary results in form of vertical profiles of temperature (top left), relative humidity (top right), wind speed (bottom left) and wind direction (bottom right) sampled during flight 1. The temperature profiles include data from three different air temperature sensors and in addition the downward looking IR sensor for surface temperature observations. The humidity profile also contains data from two different sensors, with the newly added HYT-271 having a much shorter response time. The two different lines in the wind speed and direction profiles correspond to two different estimation algorithms, a fast algorithm for real time estimates and a more precise post-processing algorithm, which, however, often results in smaller data availability. The displayed temperature profiles indicate a very strong surface-based inversion with temperatures of around -15 °C at 10 m and -10 °C at 50 m. The lowest observed IR temperatures even suggest a surface temperature of around -35 °C (purple line in top left panel). The humidity profile reveals values near saturation trapped in the atmospheric boundary layer (ABL) below approximately 80 m. The effect of this high humidity in combination with the strong surface-based inversion causes a strong radiation divergence of the upwelling longwave radiation component. This can be clearly seen in the IR temperature values, which show a strong increase with height in the lowermost layers. From these observations it becomes evident that accurate observations of the ice surface temperature would have to be taken at a very low flight level, however the knowledge on the mean humidity and temperature profiles may allow for corrections to be applied. The wind speed and direction profiles indicate moderate shear and an SSW direction in the Boundary Layer and more constant wind speed at about 5 m/s together with a shift to a more southerly wind direction at higher levels.

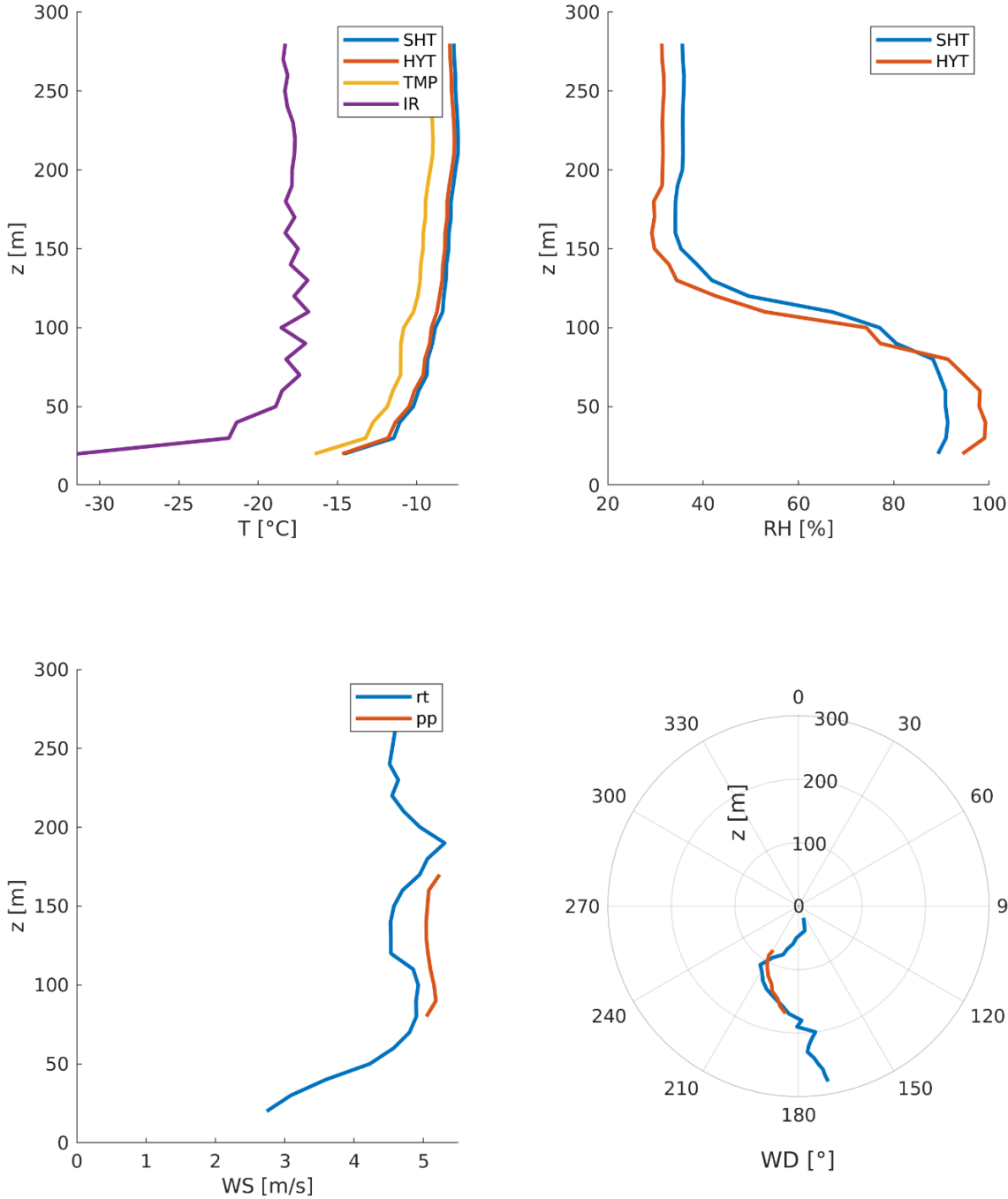


Figure 40: SUMO profile of temperature (top right), humidity (top right), wind speed (bottom left), and wind direction (bottom right).

Preliminary results from flight 4 (Figure 34) show a nearly neutral temperature profile with a lapse rate of about -9 K/km and a moderate increase of humidity with height, likely due to the decrease in temperature. These rather mixed conditions are the result of relatively strong winds of around 10 m/s at heights above 50 m from a southeasterly direction. The temperature and humidity conditions favor observations of the sea and sea-ice surface temperature. The right panel shows the observed surface temperatures along the survey flight track, which covered an area of about 1600 m in the east-west direction and about 400 m in the north-south direction. The open circles indicate the

IR surface temperatures, whereas the smaller filled circles correspond to the ambient air temperature at the flight level of approximately 60 m. The IR data reveals strong contrasts on a scale of about 100 m corresponding to areas of largely open water and, for example clearly visible in the eastern part of the survey area at about $x = 400$ m - 600 m, and almost closed sea ice to the east and west of this area. A smaller variability can also be seen at smaller horizontal scales, however, one has to consider the footprint of each IR measurement for the interpretation of these observations. The diameter of the circular footprint is related to the flight altitude depending on the opening angle of the IR sensor. In the shown case the IR sensor of SUMO-5 of 30 deg and the flight altitude of 60 m result in a footprint diameter of 30 m. Consequently, surface temperatures on length scales below 30 m cannot be resolved completely and result in smoothed IR temperature data.

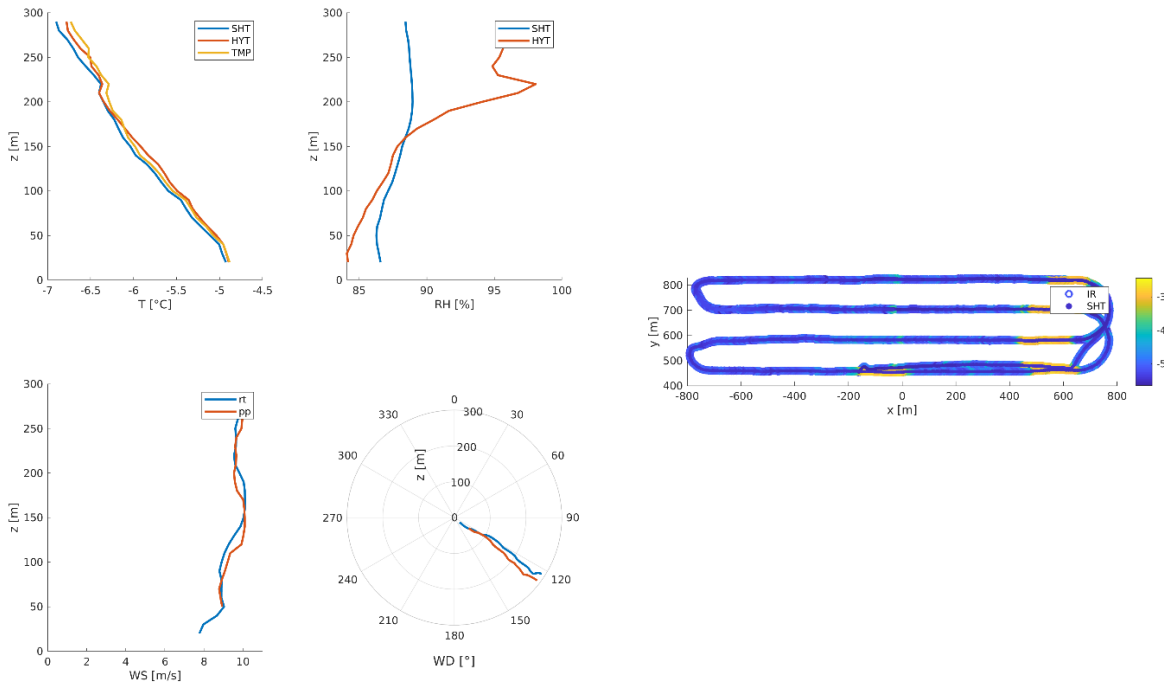


Figure 41: SUMO profiles (as in Figure 33) and survey path with infrared surface temperature (colored outer circles) and ambient air temperatures (filled circles) sampled along the survey flight path (right panel).

Ship-based remote sensing

Both wind lidars were running continuously throughout the cruise, performed very well in a harsh environment, and provided valuable data. While the Zephir lidar has a total data coverage of 86.62 %, the Windcube data coverage increased from 71.09 % to 87.34 % after the removal of the protection shield. We therefore suggest avoiding to installing the shield during future deployments, if manual checks and window cleaning can be performed in sufficiently short intervals. Figure 35 shows the respective data availability time series for both Windcube and Zephir lidar. It can be seen that the

overlap is large. This indicates a big potential for combining the measurements from both instruments in order to analyze the wind profiles from 10 to 290 m.

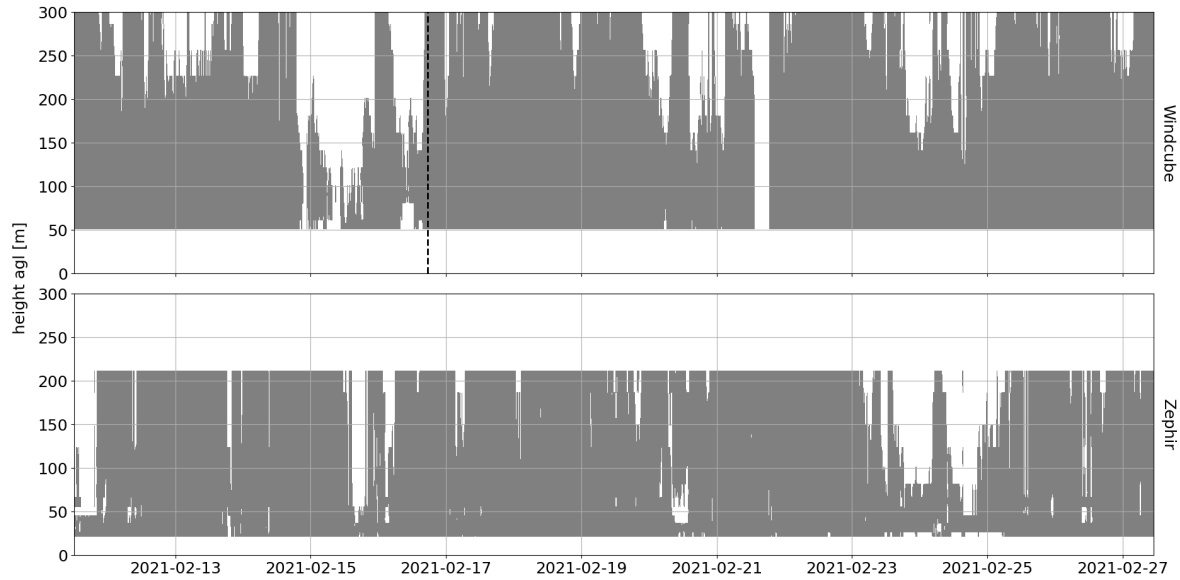


Figure 42: Data coverage timeseries for the Windcube (upper panel) and the Zephir (lower panel). The time of the removal of the protection shield is indicated with a dashed line.

An example is given in Figure 36. As the original Zephir data do not include compensation for attitude and heading of the boat, the wind direction profiles were bias-adjusted with respect to the corresponding profiles from the Windcube by matching the lowest possible height level with data available from both instruments. Afterwards, both Zephir and Windcube profiles were corrected for the lateral movement of the ship (using the GPS and gyro data set from the Windcube; the heading of the ship is indicated by the black arrow in the right panel of Figure 36). The given example shows indications of characteristic features of (ideal) atmospheric boundary layer wind fields such as the logarithmic wind speed profile or the Ekman spiral in the wind direction. It will be very interesting to use this data set in future studies to link the winds in the free atmosphere to air-ice-ocean interactions at the surface.

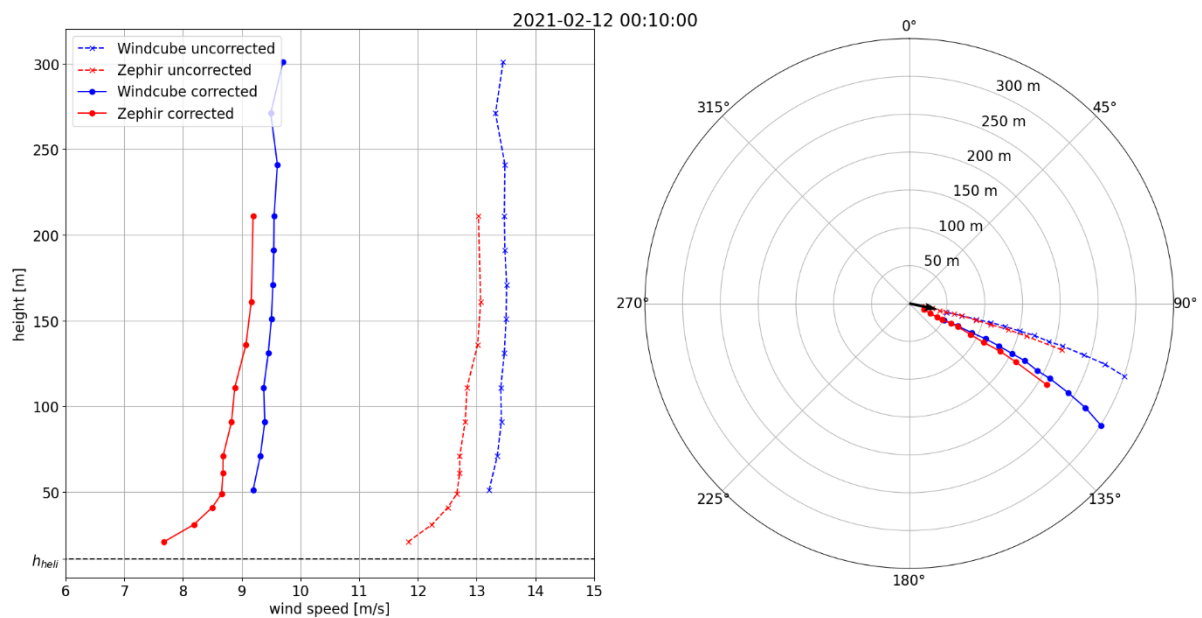


Figure 43: Example of wind speed (left panel) and direction (right panel) profiles of the Windcube and Zephir lidars from 12.02.2021, 00:10 UTC.

Radiosonde measurements

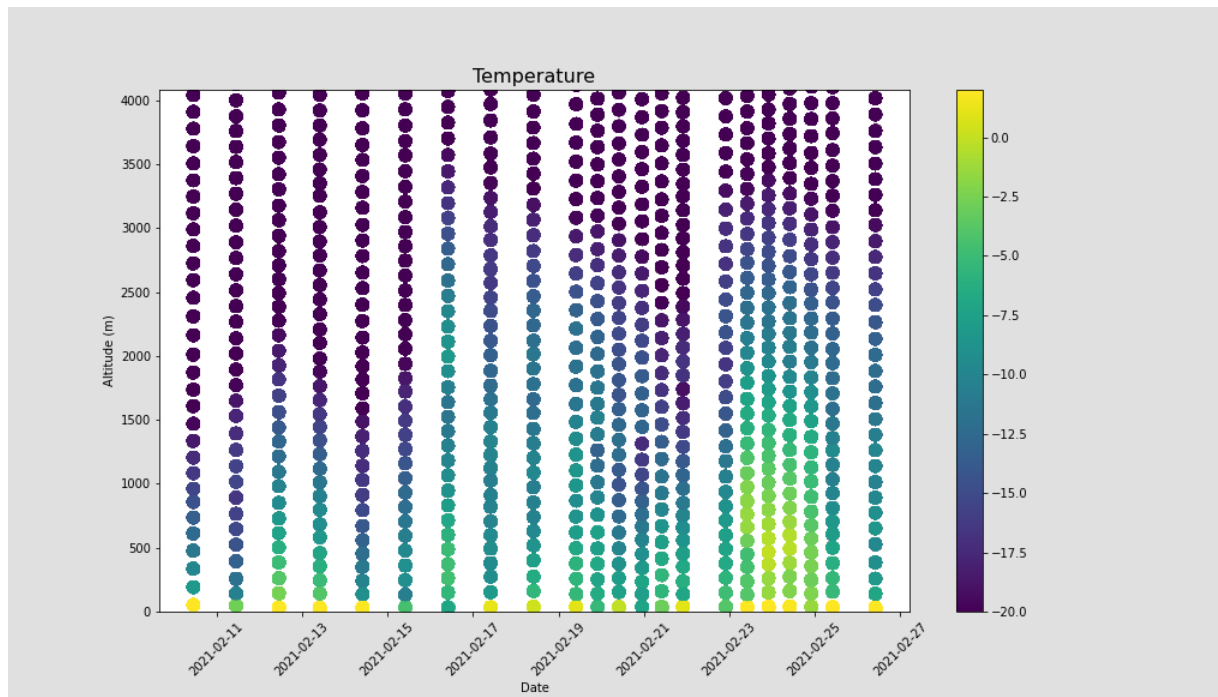


Figure 44: Radiosonde measurements of temperature.

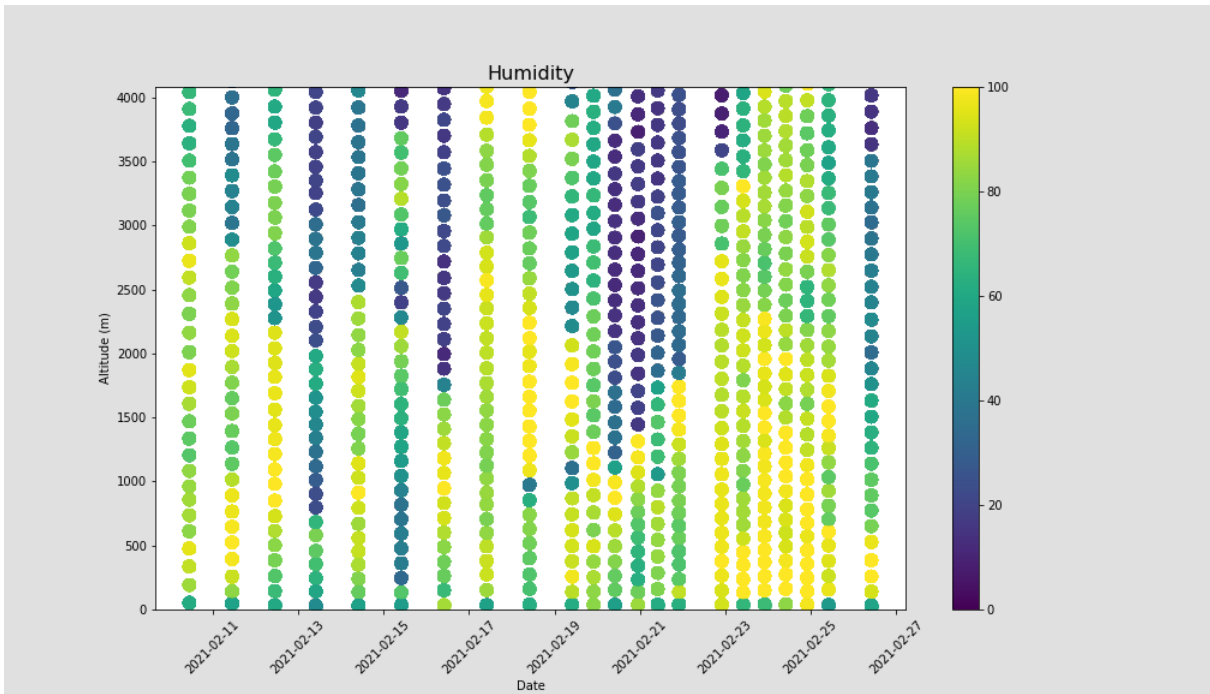


Figure 45: Radiosonde measurements of humidity.

Weather Station on sea ice

Figure 39 shows the temporal evolution of the basic meteorological and radiation parameters over the course of the entire measurement period. The period was characterized by decreasing surface pressure and gradual warming from about -10°C to -5°C, accompanied with an increase in wind speed at rather irregular small shifts in wind direction (note the wind direction in the 5th panel are not yet corrected for the orientation of the sensor). The downwelling longwave radiation reveals some relatively strong transitions as a response to changes in the cloud cover, which leads to similar but much weaker fluctuations in the upwelling longwave radiation resulting from changes in the surface temperature as a response to the forcing from the downwelling longwave radiation. The up- and downwelling shortwave radiation components are due to the short sunlight period only notable during the daylight hours, and the signal is in addition damped due to the presence of clouds during this period.

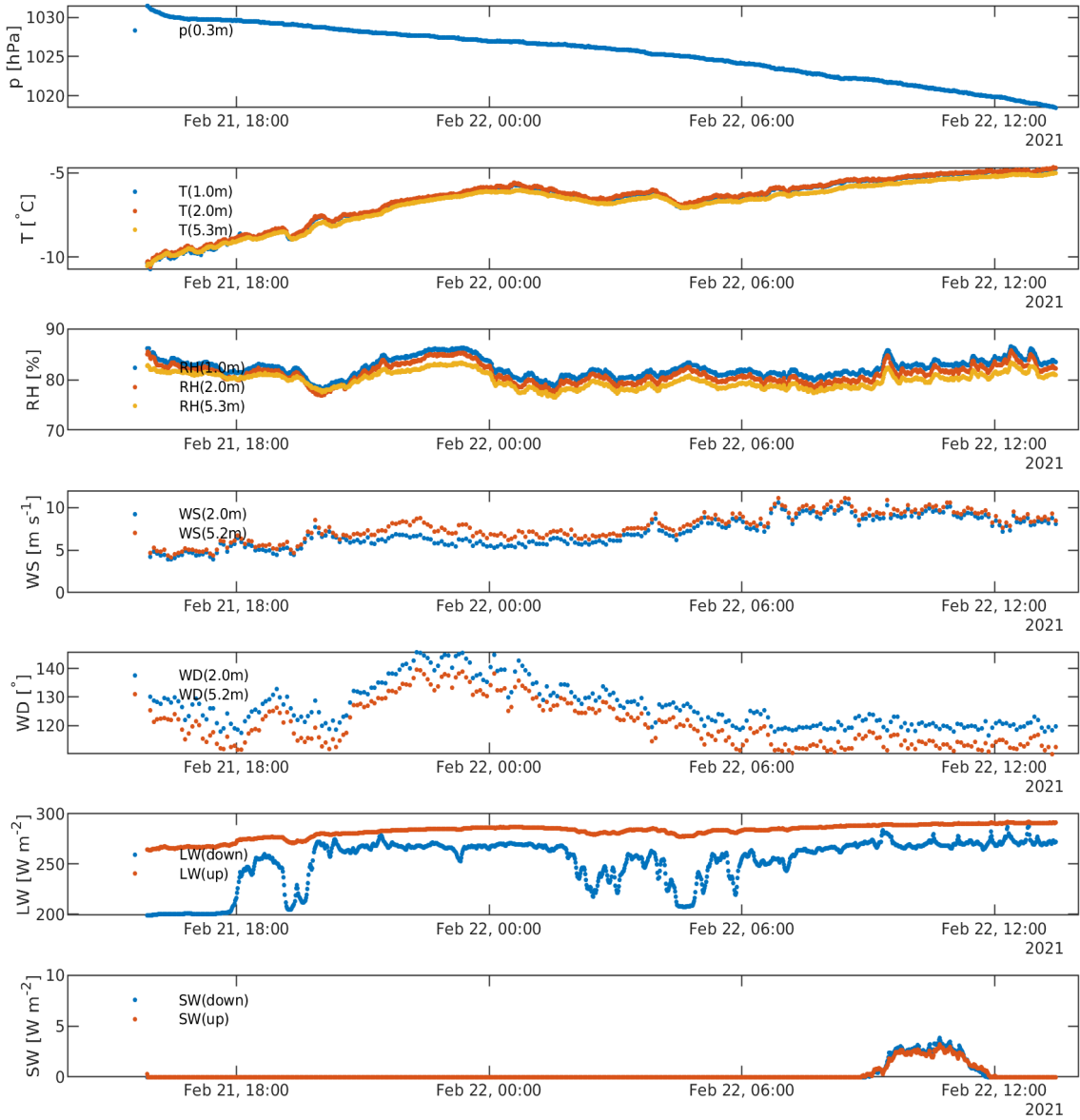


Figure 46: Timeseries of the basic meteorological parameters and the four radiation components during the sea ice observation period.

Figure 40 shows turbulent and radiative fluxes measured on the micrometeorological mast. The upper three panels display the 30-min averaged turbulent fluxes of momentum (two levels, 1st panel), sensible heat (2nd panel), and latent heat (3rd panel). The two following panels show the net longwave and shortwave components, and the last panel shows the residual of the SEB based on the measured components. All energy fluxes are displayed following the SEB convention with positive signs indicating a surface energy gain. The turbulent flux of momentum shows similar values at both levels, which are slightly increasing following the increase of wind speed. The turbulent flux of sensible heat roughly follows the inverse of the net longwave radiative flux and the corresponding resulting bulk temperature gradient between the surface and air temperature. Apart from a few larger fluctuations the latent heat flux remains at levels close to zero. The net longwave radiation is dominated by the downwelling

component and rapidly response to changes in the cloud cover, whereas the net shortwave flux plays only a minor role as described above. The resulting residual of the SEB, $R_{SEB} = SHF + LHF + LW_{net} + SW_{net}$, shows notable strong negative values, indicating an additional component contributing to a warming of the surface. One important component we did not account for in our measurement setup is the conductive ground or sea-ice flux. This SEB component is typically measured with ground heat-flux plates, but due to the long initial adjustment time in sea ice – it typically takes several days to freeze them properly – no flux plates were used in our setup. A negative residual can be explained by a positive ground flux through the ice due, i.e., heat is transported from the warm bottom, which is in contact with liquid sea water at its melting point (~ 1.9 degC), to the surface which is typically at a colder temperature. Depending on the surface temperature of the sea ice conductive heat fluxes reaching up to 40 W m^{-2} are realistic for a sea ice thickness of 50 cm, in particular under clear sky conditions. The quick response of R_{SEB} to the rapid drops in LW_{net} , which is related to shifts toward clear sky conditions, supports this explanation. Other unresolved components of the SEB like advection, or radiation divergence are very unlikely to account for a large fraction of the observed residual. Flux measurement errors may of course also contribute to a residual in the SEB, however, at first glance no obvious errors are striking.

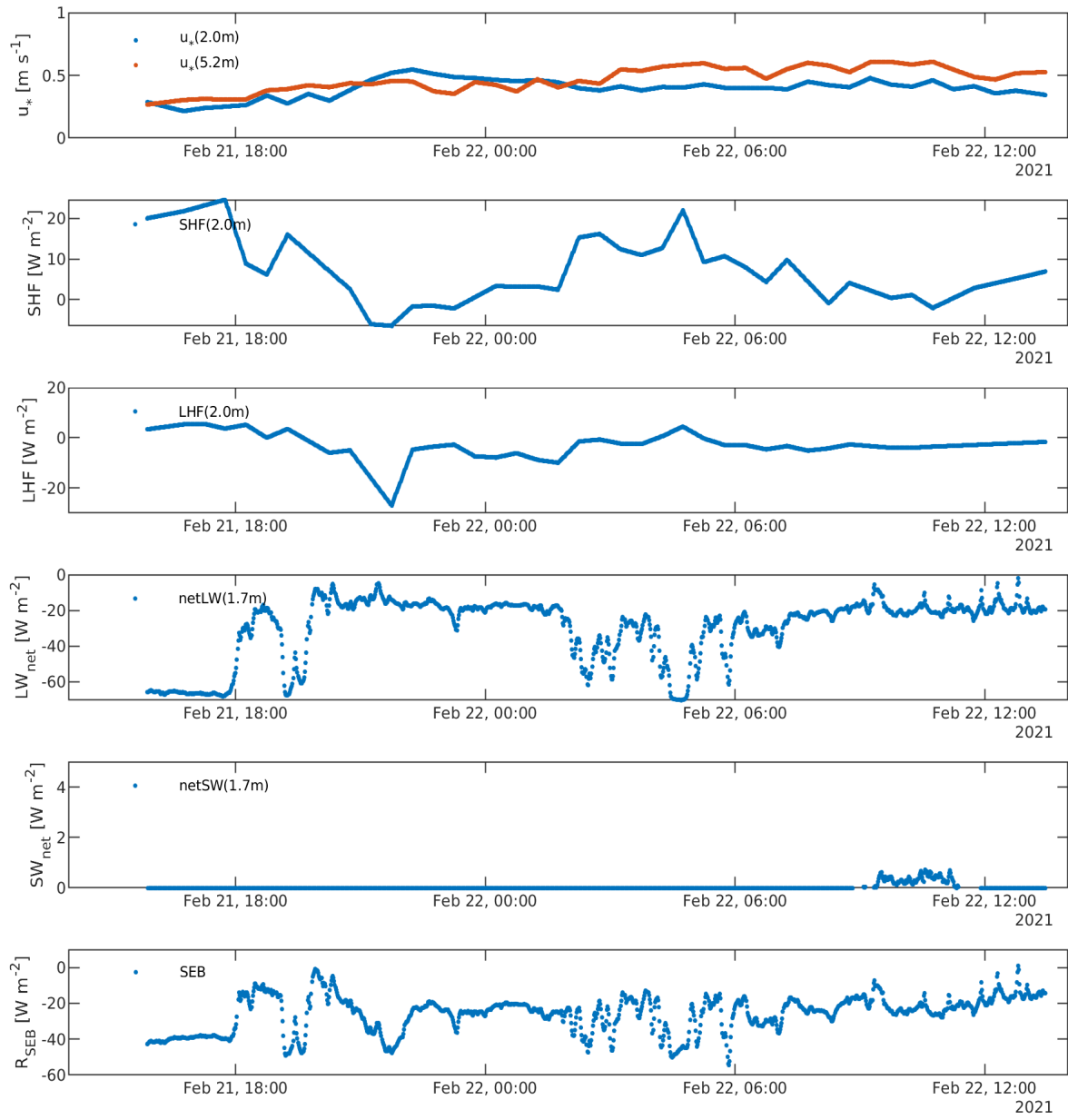


Figure 47: Turbulent fluxes of momentum, sensible heat, latent heat, radiative net long and shortwave fluxes, and the residual of the surface energy balance.

4.7 Surface Drifters

Waves in ice instruments 'v1'

Some instruments are still operational at the time of writing this report (May 2021), and data are continuously generated as more iridium transmissions are received.

The instruments v1 have been working flawlessly from a technical point of view. Some iridium transmission dropouts are observed, which is expected due to the low profile of the instruments (to avoid attracting polar bears attention) in combination with snowfalls, which reduces the quality of the satellite signals. All instruments v1 survived for around slightly over 1 month (the instrument that survived longest transmitted information for around 1.5 months). This is a good result, given the harsh dynamics

such as ice breakup and ridging that are observed in the MIZ. Based from the data transmitted, the end of transmissions for the instruments v1 were due not due to technical issues, so we believe that these were the results of ice breakup, crushing, and the physical destruction of the instruments.

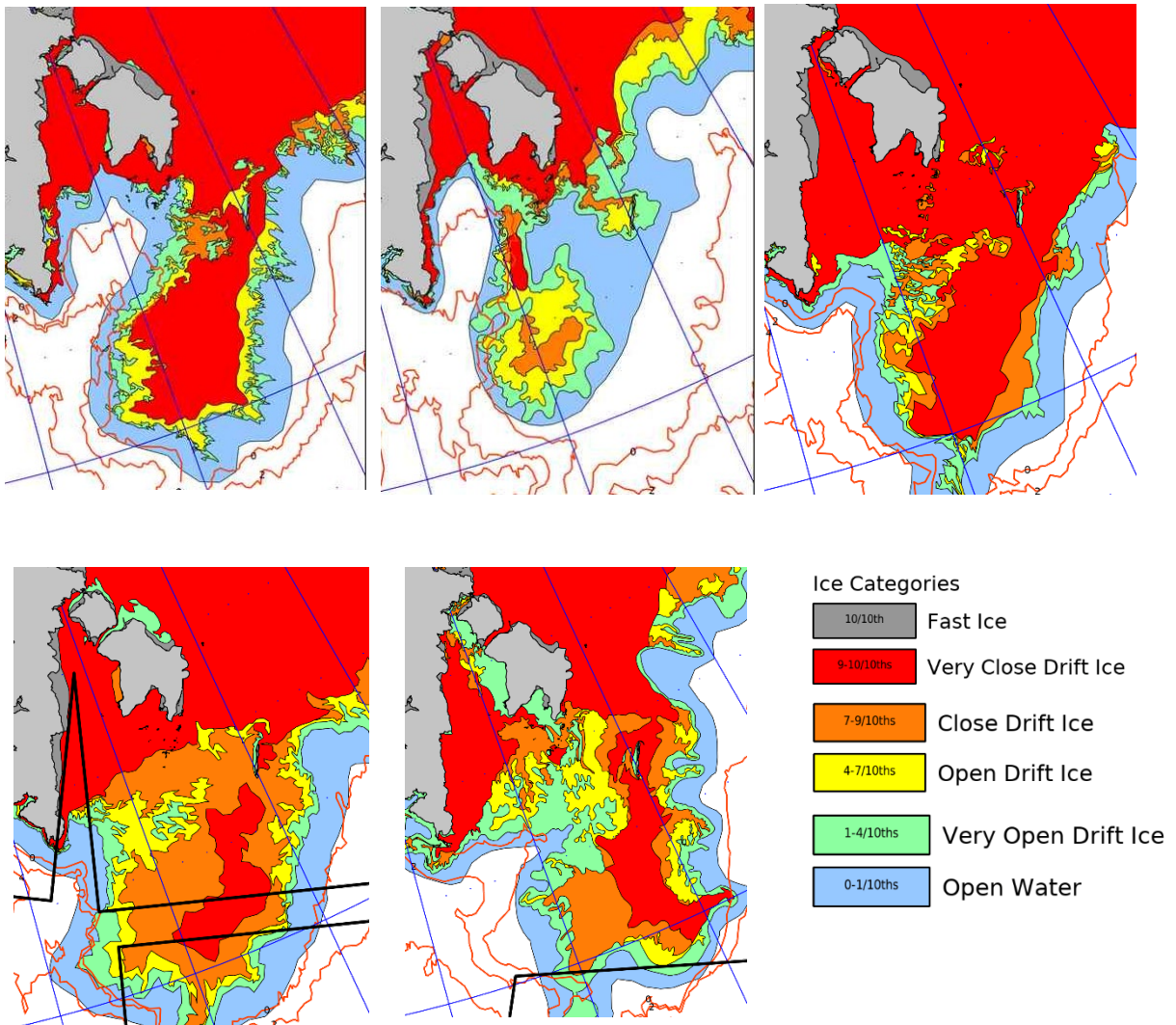


Figure 48: Evolution of the MIZ ice conditions in the area of the drifters deployment. The figures indicate the ice category, for dates (left to right, top to bottom): 2021-02-19 ,2021-02-26, 2021-03-10, 2021-03-19, 2021-03-30. These are excerpts from the ice charts available at <https://cryo.met.no/> provided by the Norwegian Meteorological Institute. The MIZ was very dynamic over period of time of the deployment, with several incoming storm and wave events, which resulted in lots of ice motion and breakup.

Results for both the drift trajectories and the spectrograms for the instruments v1 are presented below. Complex drift patterns are observed, following the passing by of several weather events. Corresponding wave systems propagating and attenuating through the marginal ice zone are also visible in the spectra of the instruments. We expect that these data will be of critical importance for calibrating wave in ice parametrizations and coupled wave-ice models.

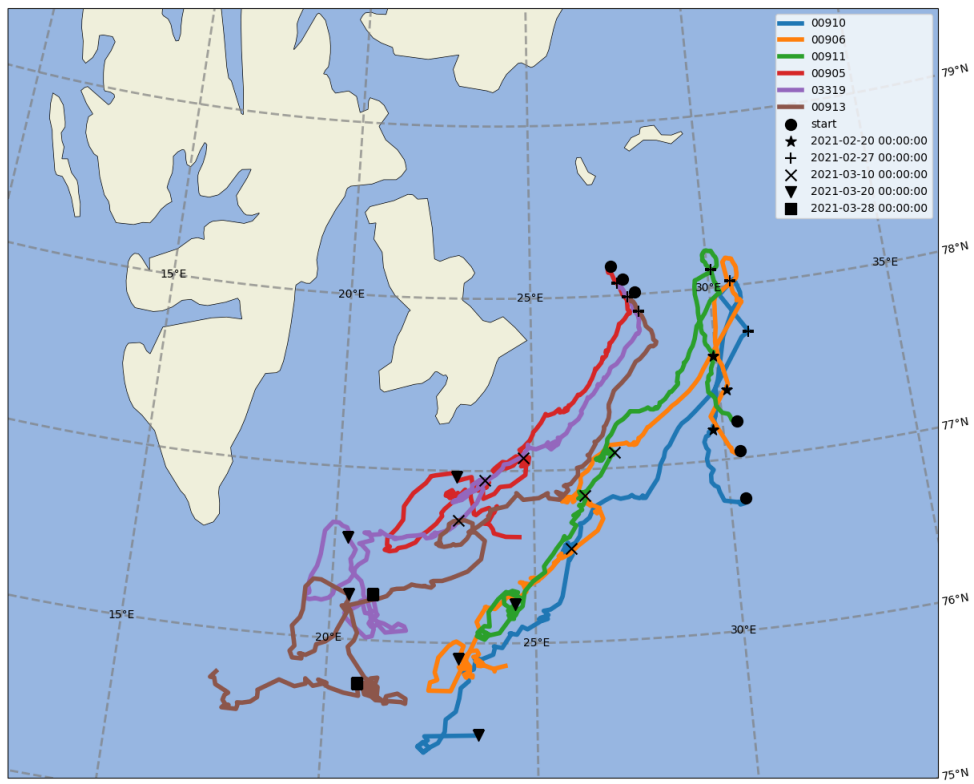


Figure 49: Drift pattern of the instruments v1 over the full duration of data transmission. Complex drift patterns are visible, which follow the forcing by both currents, winds, and waves. Several of the instruments drifted into regions with little or not ice content at the end of their trajectories (compare with the previous figure about sea ice conditions), which indicates that the ice floes they were on drifted a bit outside of the MIZ before fully melting.

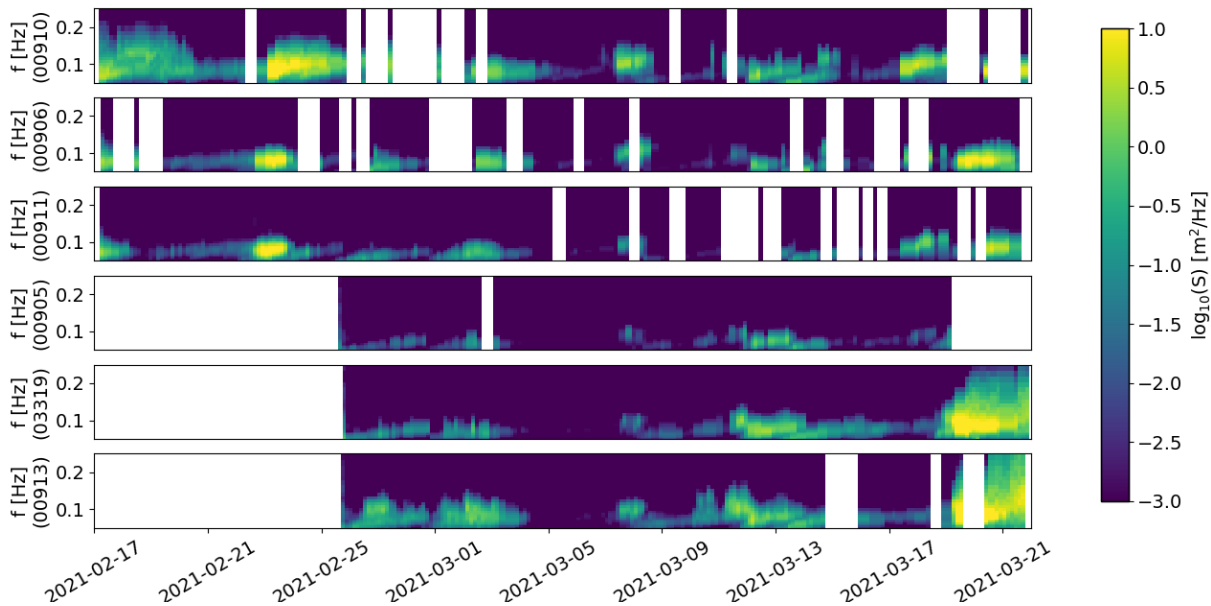


Figure 50: Spectra transmitted by the instruments v1 over the full deployment duration. Clear wave events are visible in the data. Both wave attenuation and peak frequency shift to lower frequencies as waves propagate in the ice are clearly visible in the records. The last two

instruments (00913 and 03319) ended up in the open water and probably floated on either a very small ice floe, or maybe floated a bit on their own, as visible through the very "thick" spectrogram at the end of their data transmission series.

Waves in ice instruments 'v2'

The instruments 'v2', while being an early prototype, also provided a large amount of data. All instruments 'v2' were transmitting GPS position each 30 minutes, and long drift trajectories are observed. A few of the instruments stopped to work or had some intermittently missing portions of trajectory. We believe that this is due to the very low profile of the instruments, which means that iridium messages may have difficulty being transmitted when a layer of fresh snow is present. Some instruments also stopped to transmit relatively soon, which is probably due to either technical issues, or ice breakup. However, all in all, the deployment was a success, and a large dataset of drift trajectories was collected. Some instruments were even able to survive the ice breakup and melting, and drifted all the way to the coast of Norway while floating on their own (the instruments v2 can, by contrast to the instruments v1, float).

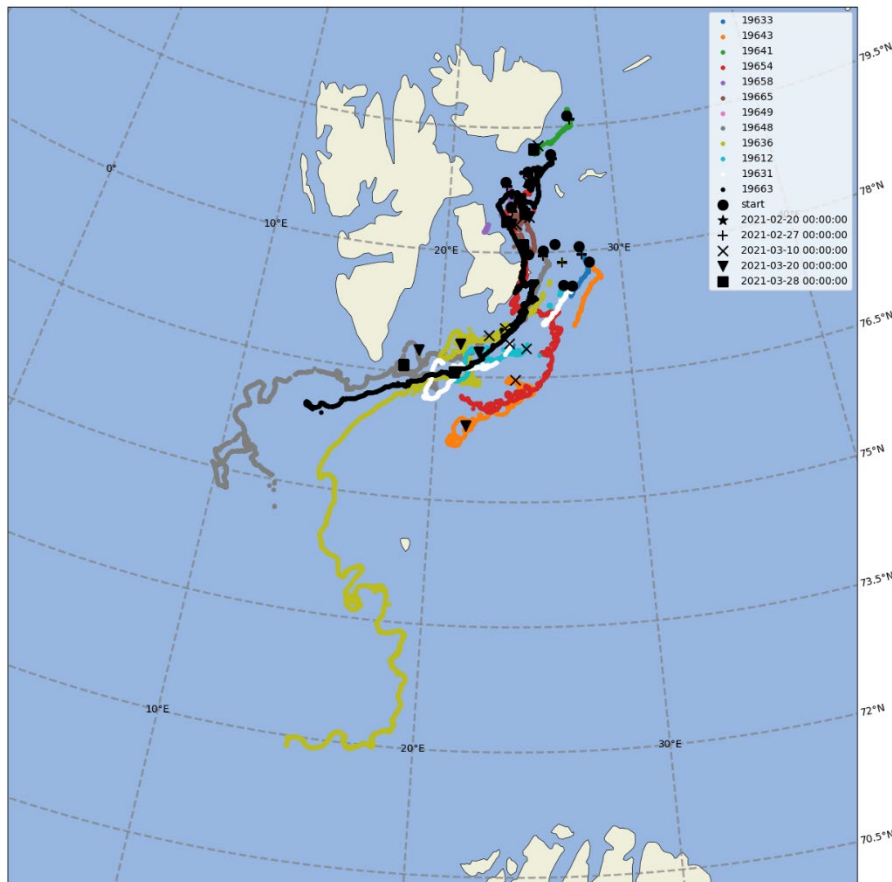


Figure 51: Drift pattern of the instruments 'v2'. A large amount of ice drift data was collected by these instruments. Some of them even survived the ice melting / breakup and drifted all the ways

to the Norwegian coast. 3 instruments are still actively transmitting at the time of writing this report.

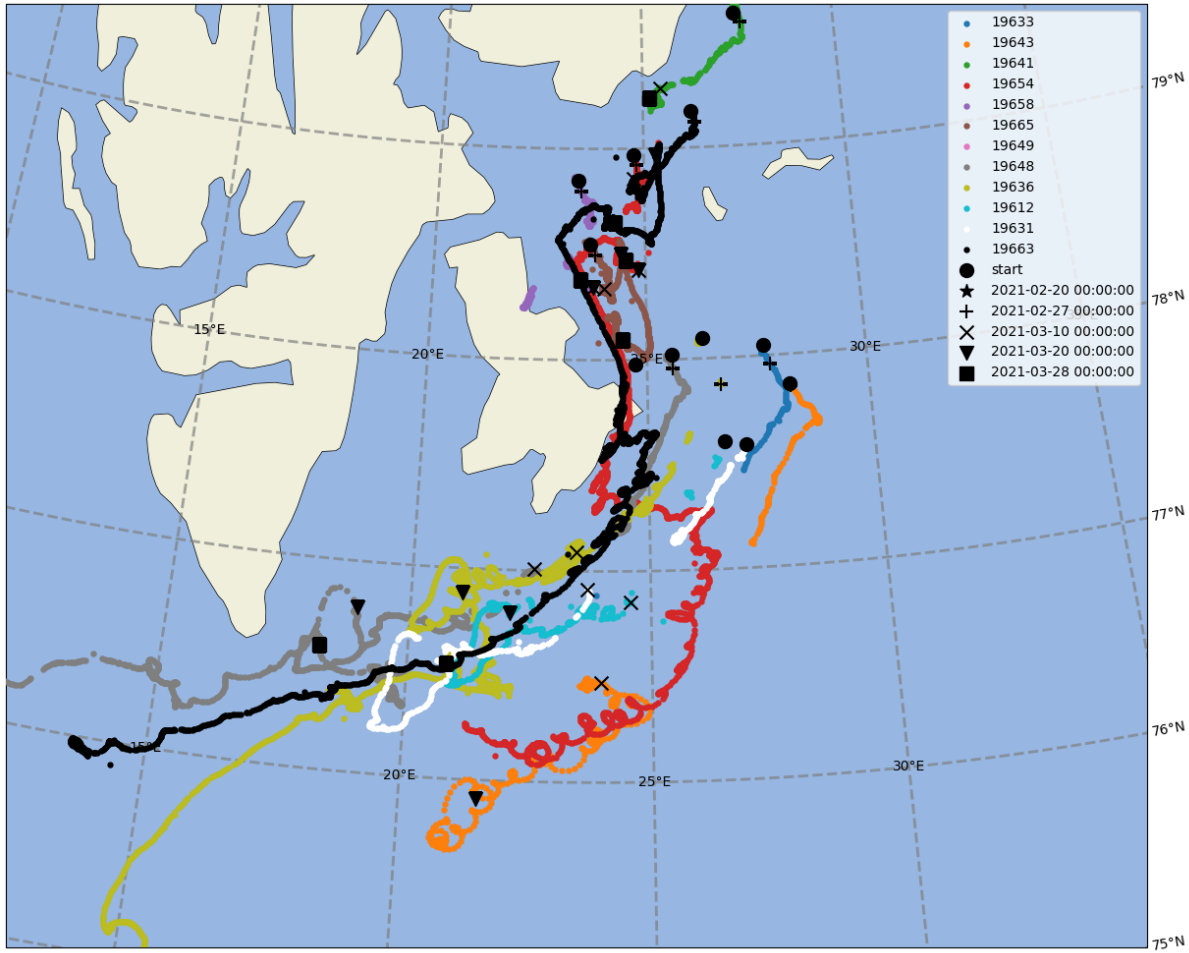


Figure 52: Drift pattern of the instruments 'v2', zooming on the area around Svalbard. Many features are visible in the drift patterns, including large scale drift to the South West, and smaller scale motion due to a combination of factors (wind, inertial oscillations, etc).

Some of the instruments 'v2' were also equipped with an IMU in order to be able to measure waves. The processing of the IMU data for computing wave characteristics has not been fully validated yet (this is a currently ongoing work), however, it is clear that some good data were taken. The spectra presented here are energy spectra for the wave elevation. There are some drops, that may come from both loss of signal due to snow cover. Interestingly, the higher sampling frequency for the wave spectra make some additional phenomena visible compared with the instruments v1. In particular, the instrument #19648 shows some wave activity with peak in activity following a 12 hours period around 2021-03-01. We think that this may be due to the ice closing and opening following tidal forcing, which may modulate wave damping by the sea ice. This will be further investigated in the months to come.

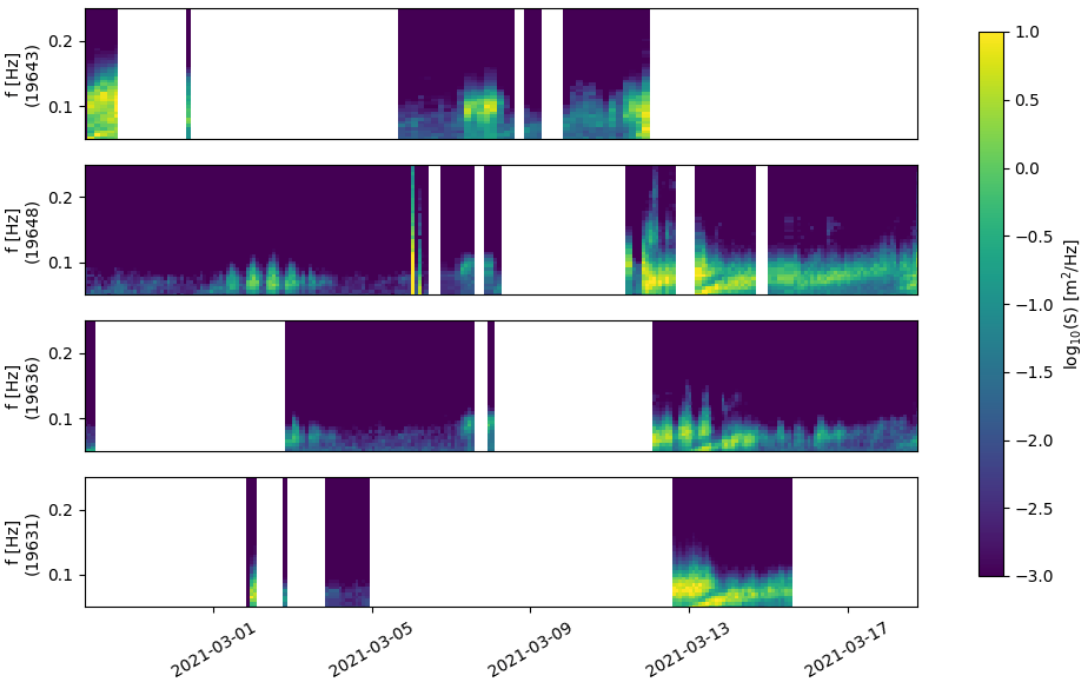


Figure 53: Spectra recorded while in the ice by the instruments 'v2' (only some of the instruments were equipped with an IMU). Wave characteristics are well visible. Some dropout are present, probably due to the ice cover. Some interesting phenomena are visible, such as the 12-hour dependence of wave activity for instrument 19648, which we believe may be related to periodic sea ice opening and closing following tidal forcing.

4.8 Measurements of waves in sea ice and open water

The ship mounted ultrasonic sensor system (IMU and ultrasonic gauge) have gathered 9GB of data. The data look promising, in particular on the transects performed in the Marginal Ice Zone at both the start and the end of the ice activities. Due to the volume of data generated, analysis is still ongoing and the present results are only preliminary. Full in-depth analysis and quality validation will require a few months. Similarly to the cruise of 2018, the main limitation of the present system is the saturation of the UG sensor. We are considering finding a new UG sensor that will provide accurate wave measurements for all sea states and significant wave heights.

The system measures the significant wave height at the location of the boat by comparing the signal from an ultrasonic probe and an IMU on the boat. Results are presented in the figure below. When outside at sea, strong icing took place, and, therefore, data are really only available for the time when the boat was inside the ice.

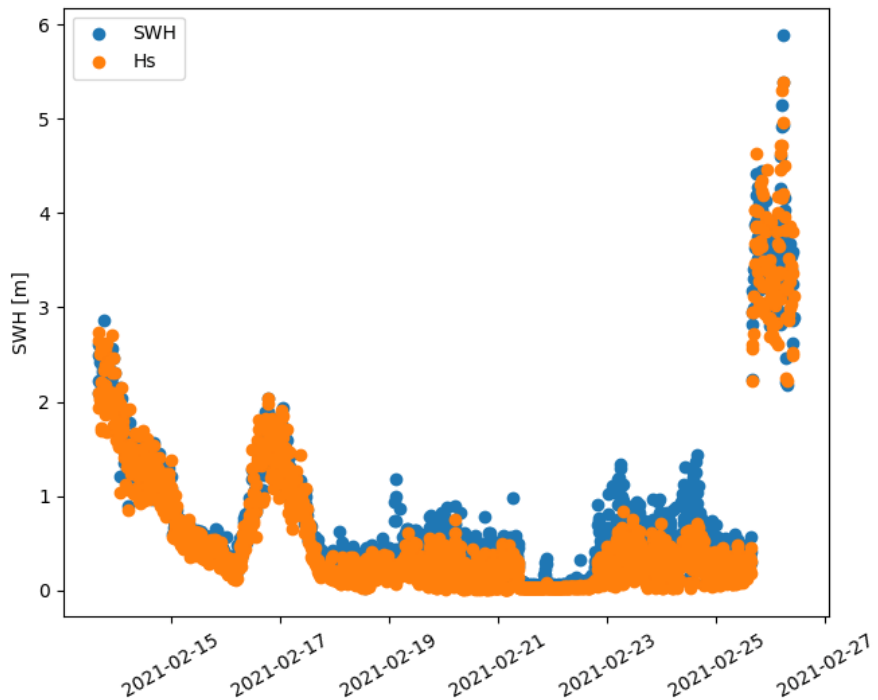


Figure 54: significant wave height computed from the ultrasound sensor. The data are relatively noisy due to saturation of the sensor and icing. However, clear wave systems are visible in the data. We are working on a new iteration of this sensor and measurement technology that will fix the limitations of the current system.

5 References

- Løken, T. K., Rabault, J., Thomas, E. E., Müller, M., Christensen, K. H., Sutherland, G., & Jensen, A. (2020). A comparison of wave observations in the Arctic marginal ice zone with spectral models, Proceedings of the 25th IAHR International Symposium on Ice.
- Løken, T. K., Rabault, J., Jensen, A., Sutherland, G., Christensen, K. H., & Müller, M. (2021). Wave measurements from ship mounted sensors in the Arctic marginal ice zone. *Cold Regions Science and Technology*, 182, 103207. <https://doi.org/10.1016/j.coldregions.2020.103207>
- Rabault, J., Sutherland, G., Gundersen, O., Jensen, A., Marchenko, A., & Breivik, Ø. (2020). An open source, versatile, affordable waves in ice instrument for scientific measurements in the Polar Regions. *Cold Regions Science and Technology*, 170, 102955. <https://doi.org/10.1016/j.coldregions.2019.102955>
- Troupin, C., J.P. Beltran, E. Heslop, M. Torner, B. Garau, J. Allen, S. Ruiz, J. Tintoré (2015) A toolbox for glider data processing and management, *Methods in Oceanography*, 13–14, 13-23, <https://doi.org/10.1016/j.mio.2016.01.001>.
- Visbeck, M. (2002), Deep velocity profiling using lowered acoustic Doppler current profilers: Bottom track and inverse solutions, *J. Atmos. Ocean. Technol.*, 19, 794-807.

Appendix I. Cruise timeline, station tables, and participant list

a. Cruise timeline (Local time and blog publications)

09.02.2021

- 14:30 Everybody aboard at after collecting the 11 participants coming from Bergen, Oslo, Trondheim and Tromsø.
15:30 Safety brief
16:30 Starting to mount the radiation, lidar, temp/humid microwave, bow wave and MSS.
20:00 Safety training with Fred SH on the rifle range. All 16 participants.
22:20 Back on the ship to finalize the instrument setups.
00:00 Leaving Longyearbyen toward IsK and stations in Isfjorden.

<https://www.unis.no/winter-darkness-revealing-the-secrets-of-the-sea/>

10.02.2021

- 01:30 IsK - CTD/LADCP in the deepest part of Isfjorden. Had to do 2 profiles since the first did not work. Finished at the station 02:22.
04:10 CTD 987 by I-SE.
05:53 CTD 991 by I-SM. Sailing to WSC glider position.
15:00 In position and searching for Seaglider sg562.
15:30 sg562 found and trying to catch with a lasso.
16:20 Deteriorating weather with increasing wind. Sq562 out of sight.
18:53 CTD/LADCP for glider calibration.
20:05 Seaglider found again.
20:15 sg562 fished up on deck with Helge's fabulous net! Sailing towards Seaglider sg560 at 31E.

<https://blogg.forskning.no/arven-etter-nansen/vintermorkets-hemmeligheter/1811964>

11.02.2021

- 11:15 Passing Sør-Kapp
19:00 Starting to cutting across the ice-tongue form Hopen to Bjørnøya.

<https://www.unis.no/women-in-science-investigating-the-barents-sea/>

12.02.2021

- 15:15 Spotted sg560
15:45 Sg560 on deck
20:30 Odin deployed

13.02.2021

- 00:00 CTD in moonpool for Odin calibration
01:58 Start of the I section at I1

- 13:15 MIZ after station I12, packed northward due to southerly wind. Swells into the ice. 16:00 I15 and the end of the I-section
- 18:40 Started the more detailed MSS section across the front that we found around I10, N76 17.1' E34 14.4'. We sail 1.2 nm south of the front I9a, collect an MSS profile and deploy the AUV Harald her to dive 5 km north and south again along E34 14.4' (5 dives).
- 23:00 AUV Harald deployed.

14.02.2021

- 00:00 AUV Harald do not send signals.
- 01:00 AUV Harald found by triangulation at 300 m depth close to the front position.
- 02:00 MSS profiling between I9 and I11 to monitor the front.
- 09:00 Signal trouble for the MSS cable, need to terminate the cable.
- 13:00 Starting up the MSS profiling again at I9 and continue to monitor the front between I9 and I11.
- 14:30 Preparing for AUV Harald rescue mission using a modified ROV Blueye with extended cable and a new remote-control system do be able to dive to 300 m depth.
- 16:45 Start to lower Blueye.
- 17:20 AUV Harald appeared with blinking light close to the position we were searching, spotted by the captain. It had been stuck in the mud after a steep descent spiraling vertically with malfunctioning rudder and active propeller, and eventually escaped the mud and popped up beside the KH!
- 19:20 Stated MSS profiling from I8a to I15.

15.02.2021

- 04:00 Sailing in sea ice to B12 and the front section B.
- 10:30 Started B-section from B12 with CTD and MSS on each station. Successful SUMO flight at station B12.
- 16:00 SUMO crashed on the sea ice at B9 but was able to recover all parts for repair.
- <https://blogg.forskning.no/arven-etter-nansen/pannekaker-med-donning-attat/1814811>

16.02.2021

- 01:30 Finale station at B1 and heading south again towards B13 (new station) with MSS on each station and CTD on every third station (B4, B7, B10, B13).
- 11:25 Three polar bears walking around the boat. One mother with two cubs (approx. 1.5 years). Very curious and made a lot of sounds.
- 18:20 Try to find the front signal at the surface and make another station B14 further south to find warm water at the surface. Did not find it and no time to sail further south at this stage, so we head to B7 for process study time series.
- 19:30 Deploy one of three wave recorders on ice floes 0.5-1 nm north of B14.

<https://blogg.forskning.no/arven-etter-nansen/den-perfekte-front/1815343>

17.02.2021

00:00 Stated process station at B7 with MSS every 30 minutes.
12:15 Stopped the process station MSS profiling at B7.
23:15 Arrived at the M4 recovery position (new estimate N77 16,145' E024 24,406').
Very close drift with drift velocities between 0.5-1 m/s driven by the tidal current.
Not possible to hold the boat for an ROV operation and decided to abort the recovery mission and deploy the new M4 mooring.

18.02.2021

02:15 M4 mooring placed at the bottom at 72 meter depth at the position: N77 16.260'
E024 24,496'.
03:00 CTD 0049 taken 200m away from the mooring position.
05:30 Start the K-section from K6.
15:00 Ended the K-section at K12.

19.02.2021

04:00 Thicker/more heavy sea ice and very low ship speed. Approaching Kong Karls Land.
07:00 Sailing between Svenskøya and Kongsøya
16:45 M1b found on the echo sounder and with the deck unit ping to the release.
17:15 CTD close to M1b.
18:15 The mooring is released, however, the mooring ended up under the crushed ice cover with large chunks of ice and grease. Difficult to communicate with the release unit due to grease ice. Pinging 110-180-370 and the lost the signal. Calculated the possible drift and new mooring position based on ice drift (25 cm/s N) and ocean current in the 50 upper meters (10-15 cm/s). Sailed to that position and found it! A lot of luck since the mooring barely made it to the surface through the layer of ice. Only the glass spheres made it to the surface.
20:30 At M1a. Found it with the echo sounder and with the deck unit ping to the release. CTD close to the M1a position. Did not manage to make a big enough hole in the ice for a release command due to more solid and more "fast ice" closer to land.
23:45 Had to give up the M1a recovery and leave it there for future cruises with less sea ice in the area.

20.02.2021

03:26 Start the N-Section at N1 with CTD and MSS.
16:45 Concluded the N-section at N10.
21:04 Deployment of M1
21:45 Deployment of M1bioac
23:47 Deployment of M1b
23:57 CTD at M1b

21.02.2021

- 09:15 Found sea ice floe to work on, N79 30,181 E027 14,894, and drifting north-east.
13:00 Starting to work on the ice floe and have established polar bear watches.
17:30 All instruments up and running.
20:30 Wind is picking up and a crack in in the ice divided the floe in two. KH was moored to the "wrong" part but we managed to release the hawsers. Weather is getting worse with more snow and poor visibility. Decided to end the work on ice and wait until next morning to continue. Ship CTD every hour.

22.02.2021

- 08:45 On the ice and continuing the ice floe work. We are drifting across Hartogbukta, the trough leading towards Austfonna.
16:35 Collected and ice core
19:30 All instruments are back aboard and we conclude the sea ice work, N79 37,502 E027 23,570.
22:05 Concluding the HTD section which is an extension of the drift in order to cross the entire trough of Hartogbukta.

<https://blogg.forskning.no/arven-etter-nansen/hvor-mange-oseanografer-trengs-for-a-baere-en-koffert/1816689>

23.02.2021

- 03:00 Stuck in heavy ice consisting of thick sea ice and glacier ice bergs.
06:30 HT7 in glacier ice and sea ice ridges.
07:15 Breaking out of the Mélange ice consisting of sea ice ridges, calved ice bergs from Austfonna and grease ice. Heading to M10.

<https://blogg.forskning.no/arven-etter-nansen/ein-uventa-reise-til-det-ukjende/1819580>

24.02.2021

- 07:30 Last station on the M-section, M3, we have time to take before heading southwards.
21:45 Start the L-section at L1.

25.02.2021

- 11:00 Concluded the L-section at L8. Tested the buoyancy of the AUV "Harald" in the moonpool. Inspected the moonpool and its closing mechanism by using Blueye.
12:15 Started to deploy surface drifters and wave loggers every 3 km towards the sea ice edge.
15:25 Last sea ice drifter put on the ice before exiting the sea ice.
15:35 Crossing the sea ice edge and out in open waters at N77 58,02 E 028 07,70.

26.02.2021

- 04:00 Recover the Slocum glider "Odin" at I14.

- 05:37 Crossing the 0-degree isotherm at the I11a station and the Polar Front is detected as surface temperature variation from -1.9 degree to 1.0 degree over 7 nm.
- 07:35 The AUV "Harlad" was deployed one nm south of I11a and we started to collect an MSS section parallel to the track of "Harlad"
- 14:15 Had to recover "Harald" and end the AUV experiment since there was an indication of a small leak in the GPS antenna.
- 19:00 Last MSS profile nr. 181 in total from the ship. Heading towards Tromsø.

<https://blogg.forskning.no/arven-etter-nansen/isflakspagaten/1821135>

28.02.2021

- 07:30 Mainland Norway at Havøysund and Hammerfest.
23:45 Tromsø.

01.03.21

- 12:00 All equipment unloaded. Leaving RV Kronprins Haakon. Very pleased with the cruise, the collaboration with the crew, all the participants and what we have achieved.

b. Station tables

Table 8: CTD Station list

St.name	CTD File	Date			UTC hh:mm	Depth m	Latitude/ N		Longitude/ E	
		year	mon	day			deg	min	deg	min
IsK	sta0025	21	2	10	00:32	279	78	19,25	15	9,76
IsK	sta0026	21	2	10	01:01	279	78	19,25	15	9,76
I-SE	sta0027	21	2	10	03:10	158	78	7,50	14	24,96
I-SM	sta0028	21	2	10	04:53	213	78	3,66	13	31,29
Glider1	sta0029	21	2	10	17:53	2280	77	16,06	8	3,72
Glider2	sta0030	21	2	12	22:59	187	75	44,06	34	33,11
Glider3	sta0031	21	2	13	11:09	240	76	28,18	34	9,20
B12	sta0032	21	2	15	09:33	234	76	57,01	30	23,48
B11	sta0033	21	2	15	11:31	228	77	2,57	30	24,05
B10	sta0034	21	2	15	12:59	218	77	5,31	30	23,65
B09	sta0035	21	2	15	14:22	204	77	8,18	30	23,99
B08	sta0036	21	2	15	16:01	200	77	10,92	30	23,95
B07	sta0037	21	2	15	17:06	188	77	13,80	30	24,21
B06	sta0038	21	2	15	18:02	182	77	0,70	30	23,90
B05	sta0039	21	2	15	19:06	196	77	19,04	30	23,62
B04	sta0040	21	2	15	20:31	189	77	22,01	30	23,65
B03	sta0041	21	2	15	21:19	186	77	24,88	30	23,52
B02	sta0042	21	2	15	22:24	205	77	27,61	30	23,74

St.name	CTD File	Date			UTC hh:mm	Depth m	Latitude/ N		Longitude/ E	
		year	mon	day			deg	min	deg	min
B01	sta0043	21	2	16	00:22	215	77	33,54	30	23,70
B04	sta0044	21	2	16	04:28	189	77	21,83	30	24,05
B07	sta0045	21	2	16	07:35	186	77	13,58	30	24,01
B10	sta0046	21	2	16	11:04	220	77	5,32	30	23,02
B13	sta0047	21	2	16	15:25	238	77	51,15	30	22,85
B14	sta0048	21	2	16	17:20	255	77	44,99	30	22,59
M4	sta0049	21	2	18	01:58	70	77	15,48	24	23,10
K6	sta0050	21	2	18	04:37	90	77	6,35	23	57,23
K7	sta0051	21	2	18	06:34	75	77	15,25	24	30,19
K8	sta0052	21	2	18	08:00	81	77	18,80	24	57,09
K9	sta0053	21	2	18	09:33	95	77	23,35	25	25,81
K10	sta0054	21	2	18	11:21	144	77	27,78	25	56,72
K11	sta0055	21	2	18	12:40	184	77	29,99	26	16,13
K12	sta0056	21	2	18	14:02	174	77	32,57	26	37,13
M1b	sta0057	21	2	19	16:10	303	79	34,27	28	9,62
M1a	sta0058	21	2	19	19:57	104	79	40,50	27	50,80
N1	sta0059	21	2	20	02:26	51	79	52,39	27	31,10
N2	sta0060	21	2	20	03:18	151	79	49,70	27	44,73
N3	sta0061	21	2	20	05:30	101	79	42,50	28	0,15
N4	sta0062	21	2	20	06:31	136	79	40,86	28	7,03
N5	sta0063	21	2	20	07:30	186	79	39,32	28	12,81
N6	sta0064	21	2	20	08:39	258	79	37,42	28	18,06
N7	sta0065	21	2	20	10:46	306	79	35,97	28	22,73
N8	sta0066	21	2	20	12:07	328	79	34,29	28	29,89
N9	sta0067	21	2	20	13:55	338	79	32,34	28	35,94
N10	sta0068	21	2	20	15:21	350	79	30,02	28	41,66
M1b	sta0069	21	2	20	22:57	295	79	34,45	28	9,17
Ice1	sta0070	21	2	21	11:34	182	79	30,68	27	16,83
Ice2	sta0071	21	2	21	15:57	167	79	31,67	27	17,72
Ice3	sta0072	21	2	21	17:58	157	79	32,26	27	18,28
Ice4	sta0073	21	2	21	19:03	157	79	32,45	27	18,56
Ice5	sta0074	21	2	21	21:19	146	79	32,95	27	19,43
Ice6	sta0075	21	2	21	22:02	140	79	33,12	27	19,60
Ice7	sta0076	21	2	21	22:58	133	79	33,32	27	19,92
Ice8	sta0077	21	2	21	23:58	131	79	33,45	27	20,30
Ice9	sta0078	21	2	22	00:57	129	79	33,59	27	20,56
Ice10	sta0079	21	2	22	01:58	125	79	33,72	27	20,60
Ice11	sta0080	21	2	22	03:01	123	79	34,05	27	20,84
Ice12	sta0081	21	2	22	04:00	115	79	34,50	27	20,94
Ice13	sta0082	21	2	22	05:01	118	79	34,97	27	21,37
Ice14	sta0083	21	2	22	05:59	118	79	35,40	27	22,10
Ice15	sta0084	21	2	22	06:59	121	79	35,85	27	22,59
Ice16	sta0085	21	2	22	08:02	137	79	36,44	27	22,93
Ice17	sta0086	21	2	22	09:01	158	79	36,86	27	23,14
Ice18	sta0087	21	2	22	10:01	171	79	37,27	27	23,32
Ice19	sta0088	21	2	22	11:01	169	79	37,46	27	23,48
Ice20	sta0089	21	2	22	12:05	170	79	37,50	27	23,55
Ice21	sta0090	21	2	22	13:00	170	79	37,50	27	23,55

St.name	CTD File	Date			UTC hh:mm	Depth m	Latitude/ N		Longitude/ E	
		year	mon	day			deg	min	deg	min
Ice22	sta0091	21	2	22	13:58	170	79	37,50	27	23,55
Ice23	sta0092	21	2	22	15:01	170	79	37,50	27	23,55
Ice24	sta0093	21	2	22	16:00	170	79	37,50	27	23,55
Ice25	sta0094	21	2	22	18:23	169	79	37,50	27	23,57
HTD1	sta0095	21	2	22	18:57	164	79	38,32	27	24,34
HTD2	sta0096	21	2	22	20:08	107	79	39,49	27	25,22
HTD3	sta0097	21	2	22	21:05	76	79	40,42	27	26,37
HT6	sta0098	21	2	23	00:13	190	79	37,78	26	39,46
HT7	sta0099	21	2	23	05:33	158	79	34,79	26	9,98
M10	sta0100	21	2	23	10:44	331	79	23,04	27	52,66
M7	sta0101	21	2	23	16:28	262	79	7,52	26	6,63
M6	sta0102	21	2	23	19:44	218	79	2,17	25	23,60
M5	sta0103	21	2	23	23:16	208	78	57,67	24	39,05
M4	sta0104	21	2	24	03:32	187	78	53,03	23	55,15
M3	sta0105	21	2	24	06:39	125	78	49,81	23	13,12
L1	sta0106	21	2	24	20:52	54	77	56,74	24	30,65
L2	sta0107	21	2	24	22:39	95	77	58,66	24	59,92
L3	sta0108	21	2	25	00:30	154	78	0,67	25	30,67
L4	sta0109	21	2	25	02:20	188	78	3,06	25	54,68
L5	sta0110	21	2	25	03:43	242	78	5,36	26	13,95
L6	sta0111	21	2	25	05:38	275	78	7,50	26	32,49
L7	sta0112	21	2	25	07:23	305	78	9,61	26	50,25
L8	sta0113	21	2	25	09:04	324	78	12,09	27	11,12

Table 9: MSS Station list

Cast	Station Name	Date-UTC	Time (UTC)	LAT	LONG	E. Depth (m)	Start (m)	End (m)
1	I1	2021-02-13	00:58	75N32,40	34E42,00	163	1	93
2	I1	2021-02-13	01:10	75N32,40	34E42,00	166	1	120
3	I2	2021-02-13	01:58	75N37,37	34E38,82	171	2	1,5
4	I2	2021-02-13	01:59	75N37,37	34E38,82	171	2	130
5	I2	2021-02-13	02:11	75N37,37	34E38,82	176	2	153
6	I3	2021-02-13	02:58	75N42,32	34E35,97	192	2	191,8
7	I4	2021-02-13	03:49	75N47,49	34E33,15	205	2	173
8	I4	2021-02-13	03:58	75N47,71	34E34,04	206	2	181
9	I5	2021-02-13	04:48	75N52,25	34E29,99	238	2	220
10	I6	2021-02-13	05:40	75N57,24	34E26,77	258	1	253
11	I7	2021-02-13	06:32	76N02,21	34E23,37	267	2	251
12	I8	2021-02-13	07:23	76N07,01	34E19,84	297	2	130
13	I8	2021-02-13	07:32	76N07,22	34E20,53	301	2	276
14	I9	2021-02-13	08:21	76N12,00	34E17,24	312	2	296
15	I10	2021-02-13	09:18	76N17,17	34E14,82	293	1	278

Cast	Station Name	Date-UTC	Time (UTC)	LAT	LON	E. Depth (m)	Start (m)	End (m)
16	I11	2021-02-13	10:05	76N21,86	34E11,41	270	2	256
17	I12	2021-02-13	11:30	76N28,00	34E08,53	240	2	297
18	I12	2021-02-13	11:45	76N28,00	34E08,53	240	2	120
19	I13	2021-02-13	12:42	76N32,25	34E05,73	193	2	170
20	I14	2021-02-13	13:42	76N37,19	34E03,13	167	2	168
21	I15	2021-02-13	14:45	76N42,06	33E59,96	137	2	136
22	I11	2021-02-13	17:38	76N22,12	34E11,98	271	2	0
23	I11	2021-02-13	17:50	76N22,29	34E12,05	266	2	254
24	I10b	2021-02-13	18:33	76N20,50	34E12,25	281	2	263
25	I10a	2021-02-13	19:13	76N18,69	34E13,62	290	2	265
26	I10	2021-02-13	19:57	76N16,86	34E15,79	293	2	293
27	I9a	2021-02-13	20:53	76N15,86	34E15,86	307	2	282
28	I9	2021-02-14	01:15	76N12,25	34E18,26	310	2	311
29	I9b	2021-02-14	01:53	76N14,01	34E16,98	291	2	286
30	I9a	2021-02-14	02:28	76N15,88	34E15,76	308	2	303
31	I10	2021-02-14	03:03	76N17,34	34E14,65	292	2	293
32	I10a	2021-02-14	03:38	76N18,92	34E13,97	296	2	296
33	I10b	2021-02-14	04:13	76N20,47	34E13,12	280	2	276
34	I11	2021-02-14	04:46	76N22,28	34E12,20	266	2	266
35	I10b	2021-02-14	05:19	76N20,40	34E12,92	282	0	0
36	I10b	2021-02-14	05:29	76N20,31	34E13,13	283	2	258
37	I10a	2021-02-14	05:56	76N18,77	34E13,86	289	2	289
38	I10	2021-02-14	06:25	76N17,12	34E15,08	293	1	274
39	I9a	2021-02-14	06:57	76N15,86	34E15,96	299	2	287
40	I9b	2021-02-14	07:29	76N14,15	34E16,63	293	2	280
41	I8a	2021-02-14	12:49	76N09,57	34E19,46	310	2	301
42	I9	2021-02-14	13:22	76N12,19	34E18,04	311	2	303
43	I8a	2021-02-14	18:20	76N09,65	34E19,96	309	2	277
44	I9	2021-02-14	19:02	76N12,15	34E17,93	312	1	287
45	I9b	2021-02-14	19:35	76N14,25	34E17,02	290	2	0
46	I9a	2021-02-14	20:04	76N15,90	34E15,96	306	2	302
47	I10	2021-02-14	20:45	76N17,16	34E15,28	293	2	274
48	I10a	2021-02-14	21:13	76N18,76	34E14,28	291	1	284
49	I10b	2021-02-14	21:39	76N20,32	34E13,36	282	2	283
50	I11	2021-02-14	22:08	76N22,12	34E11,75	272	1	254
51	I11a	2021-02-14	22:43	76N25,36	34E10,33	258	2	241
52	I12	2021-02-14	23:19	76N27,99	34E08,61	240	2	239
53	I13	2021-02-15	00:17	76N32,01	34E05,65	190	2	160
54	I14	2021-02-15	01:35	76N37,87	34E02,71	171	2	0

Cast	Station Name	Date-UTC	Time (UTC)	LAT	LON	E. Depth (m)	Start (m)	End (m)
55	I15	2021-02-15	02:58	76N42,14	34E00,21	137	3	132
56	B12	2021-02-15	10:01	76N56,98	30E23,09	235	2	215
57	B12	2021-02-15	10:12	76N56,99	30E22,52	235	2	233
58	B11	2021-02-15	12:03	77N02,59	30E23,33	228	2	218
59	B10	2021-02-15	13:28	77N06,01	30E23,41	217	2	216
60	B9	2021-02-15	14:48	77N08,19	30E23,99	207	2	0
61	B8	2021-02-15	16:22	77N11,04	30E24,26	195	2	189
62	B7	2021-02-15	17:22	77N13,58	30E24,59	193	2	183
63	B6	2021-02-15	18:22	77N16,46	30E24,15	181	2	176
64	B5	2021-02-15	19:26	77N19,00	30E23,51	196	2	184
65	B4	2021-02-15	20:37	77N22,01	30E23,36	188	2	176
66	B3	2021-02-15	21:38	77N25,36	30E23,91	186	1	180
67	B2	2021-02-15	22:42	77N27,67	30E23,37	205	1	190
68	B1	2021-02-16	00:30	77N33,58	30E23,66	219	2	194
69	B2	2021-02-16	02:37	77N27,60	30E23,00	205	2	196
70	B3	2021-02-16	03:28	77N24,57	30E23,87	185	1	160
71	B3	2021-02-16	03:39	77N24,63	30E24,36	184	1	177
72	B4	2021-02-16	04:53	77N21,87	30E25,11	195	1	183
73	B4	2021-02-16	05:03	77N21,87	30E25,68	200	2	189
74	B5	2021-02-16	05:53	77N19,03	30E23,65	195	2	171
75	B5	2021-02-16	06:01	77N19,00	30E24,27	195	2	178
76	B6	2021-02-16	06:49	77N16,27	30E23,58	183	2	182
77	B6	2021-02-16	06:57	77N16,18	30E24,12	183	1	172
78	B7	2021-02-16	08:05	77N13,27	30E24,66	182	2	172
79	B7	2021-02-16	08:12	77N13,16	30E24,95	185	2	173
80	B8	2021-02-16	08:55	77N10,70	30E23,69	199	2	188
81	B8	2021-02-16	09:03	77N10,62	30E23,82	201	2	190
82	B9	2021-02-16	09:48	77N07,96	30E23,34	205	2	197
83	B9	2021-02-16	09:56	77N07,83	30E23,24	206	2	198
84	B10	2021-02-16	11:27	77N05,17	30E22,79	219	2	219
85	B10	2021-02-16	11:35	77N05,17	30E22,79	219	2	214
86	B11	2021-02-16	12:45	77N02,54	30E22,35	224	2	221
87	B12	2021-02-16	14:04	76N57,20	30E22,94	234	1	231
88	B13	2021-02-16	15:48	76N51,16	30E23,13	236	2	222
89	B13	2021-02-16	15:57	76N51,20	30E23,65	237	2	231
90	B14	2021-02-16	17:42	76N44,99	30E22,88	256	2	231
91	B7	2021-02-16	23:14	77N13,80	30E23,42	183	1	177
92	B7	2021-02-16	23:32	77N13,64	30E22,98	186	1	178
93	B7	2021-02-17	00:00	77N13,67	30E21,86	185	1	180

Cast	Station Name	Date-UTC	Time (UTC)	LAT	LON	E. Depth (m)	Start (m)	End (m)
94	B7	2021-02-17	00:30	77N13,77	30E24,00	184	1	181
95	B7	2021-02-17	01:00	77N13,78	30E31,39	186	1	180
96	B7	2021-02-17	01:30	77N14,05	30E20,18	184	1	181
97	B7	2021-02-17	02:00	77N13,56	30E23,34	185	1	184
98	B7	2021-02-17	02:30	77N13,72	30E22,16	188	1	181
99	B7	2021-02-17	03:00	77N13,94	30E20,50	188	2	161
100	B7	2021-02-17	03:30	77N13,51	30E24,09	182	1	173
101	B7	2021-02-17	04:00	77N13,77	30E23,13	186	2	178
102	B7	2021-02-17	04:30	77N13,58	30E24,14	184	2	175
103	B7	2021-02-17	05:00	77N13,95	30E23,35	187	2	177
104	B7	2021-02-17	05:30	77N13,53	30E23,89	185	1	181
105	B7	2021-02-17	06:00	77N13,83	30E23,38	187	1	166
106	B7	2021-02-17	06:30	77N13,49	30E23,80	188	1	172
107	B7	2021-02-17	07:00	77N13,91	30E23,45	187	1	180
108	B7	2021-02-17	07:30	77N13,43	30E23,57	186	2	175
109	B7	2021-02-17	08:00	77N13,74	30E22,44	184	2	180
110	B7	2021-02-17	08:30	77N13,23	30E24,76	182	1	175
111	B7	2021-02-17	09:00	77N12,49	30E22,66	183	1	171
112	B7	2021-02-17	09:30	77N13,41	30E23,39	183	2	177
113	B7	2021-02-17	10:00	77N13,67	30E21,14	185	1	181
114	B7	2021-02-17	10:30	77N13,24	30E23,95	183	1	176
115	B7	2021-02-17	11:01	77N13,74	30E23,43	187	1	171
116	N2	2021-02-20	03:38	79N49,89	27E45,64	133	2	131
117	N3	2021-02-20	05:44	79N42,57	28E00,27	98	2	89
118	N4	2021-02-20	06:50	79N40,91	28E07,21	137	2	136
119	N5	2021-02-20	07:50	79N39,45	28E12,86	174	2	169
120	N6	2021-02-20	09:46	79N37,47	28E17,90	255	2	255
121	N7	2021-02-20	11:12	79N36,02	28E22,70	305	2	287
122	N8	2021-02-20	12:51	79N34,49	28E30,06	329	2	317
123	N9	2021-02-20	14:28	79N32,40	28E35,60	335	2	336
124	N10	2021-02-20	15:46	79N30,15	28E41,67	350	2	321
125	Ice	2021-02-21	18:15	-	-	158	2	148
126	Ice	2021-02-21	18:45	-	-	-	-	-
127	Ice	2021-02-21	18:54	-	-	-	2	149
128	Ice	2021-02-21	19:15	-	-	-	2	150
129	Ice	2021-02-22	08:30		-	153	0	0
130	Ice	2021-02-22	08:40	-	-	153	0	0
131	Ice	2021-02-22	09:12	-	-	153	2	145
132	Ice	2021-02-22	09:45	-	-	166	2	140

Cast	Station Name	Date-UTC	Time (UTC)	LAT	LON	E. Depth (m)	Start (m)	End (m)
133	Ice	2021-02-22	10:11	-	-	166	2	155
134	Ice	2021-02-22	11:22	-	-	177	2	164
135	ice	2021-02-22	11:54	-	-	170	2	168
136	ice	2021-02-22	12:15	-	-	170	2	163
137	ice	2021-02-22	12:45	-	-	170	2	166
138	ice	2021-02-22	13:15	-	-	170	0	0
139	ice	2021-02-22	13:16	-	-	170	0	163
140	ice	2021-02-22	13:45	-	-	170	2	0
141	ice	2021-02-22	13:47	-	-	170	2	165
142	ice	2021-02-22	14:15	-	-	170	2	163
143	ice	2021-02-22	14:45	-	-	170	2	163
144	ice	2021-02-22	15:15	-	-	170	0	0
145	ice	2021-02-22	15:17	-	-	170	2	164
146	ice	2021-02-22	15:45	-	-	170	2	159
147	ice	2021-02-22	16:15	-	-	170	2	162
148	HTD1	2021-02-22	19:35	79N38,32	27E24,25	164	0	161
149	HTD2	2021-02-22	20:21	79N39,50	27E25,21	106	2	0
150	HTD3	2021-02-22	21:16	79N40,42	27E26,37	76	2	69
151	HT6	2021-02-23	00:37	79N37,78	26E39,46	190	2	180
152	M10	2021-02-23	11:12	79N10,87	27E08,21	330	2	331
153	M7	2021-02-23	16:52	79N07,51	26E06,74	263	1	240
154	M6	2021-02-23	20:09	79N02,20	25E23,60	219	1	207
155	M5	2021-02-23	23:38	78N57,14	24E38,87	208	1	206
156	M4	2021-02-24	03:42	78N53,05	23E55,00	186	1	166
157	M3	2021-02-24	06:55	78N49,81	23E13,09	125	1	111
158	M3	2021-02-24	07:01	78N49,82	23E12,08	125	1	122
159	L1	2021-02-24	21:07	77N56,75	24E30,63	54	1	47
160	L2	2021-02-24	22:55	77N58,67	24E59,89	94	1	89
161	L3	2021-02-25	00:44	78N00,66	25E33,55	153	1	151
162	L4	2021-02-25	02:37	78N03,09	25E55,78	189	1	181
163	L5	2021-02-25	04:04	78N03,35	26E13,67	241	1	233
164	L6	2021-02-25	05:58	78N07,51	26E32,25	276	1	258
165	L7	2021-02-25	07:48	78N09,64	26E50,00	305	1	303
166	L8	2021-02-25	09:32	78N12,11	27E10,95	324	1	316
167	I11A1	2021-02-26	08:04	76N24,26	34E11,00	261	1	215
168	I11A0grad	2021-02-26	08:35	76N25,20	34E10,34	257	2	230
169	I11A	2021-02-26	09:09	76N26,95	34E09,81	254	1	246
170	I12	2021-02-26	10:07	76N28,19	34E08,88	237	1	222
171	I12A	2021-02-26	11:41	76N29,17	34E08,08	221	1	197

Cast	Station Name	Date-UTC	Time (UTC)	LAT	LON	E. Depth (m)	Start (m)	End (m)
172	I12	2021-02-26	12:09	76N28,05	34E09,32	241	1	232
173	I11B	2021-02-26	13:53	76N26,98	34E09,57	253	2	241
174	I11A0grad	2021-02-26	14:28	76N25,29	34E10,95	257	2	248
175	I11A	2021-02-26	14:56	76N24,24	34E11,34	261	2	264
176	I11A2	2021-02-26	15:27	76N22,99	34E11,50	263	2	253
177	I11	2021-02-26	15:51	76N22,12	34E12,37	271	2	265
178	I10C	2021-02-26	16:13	76N21,44	34E12,09	274	2	256
179	I10	2021-02-26	16:42	76N20,88	34E12,84	275	2	267
180	I10C	2021-02-26	17:14	76N21,37	34E12,33	274	1	271
181	I11	2021-02-26	17:46	76N22,10	34E12,15	271	2	271

Drawing of NLEG M1 mooring

Rigg M1-3			Dyp:	Fra bunn:	Ut:
Satt ut 20 .FEB .2021	, kl 19:00:	79 35.034 N 028 03.937 E			
Nortek S500	SNR. 812	19	233	20:00	
RBR Concerto	NR.201415	20	232		
SeaFET 2033, uCAT 22418		22	230		
2 Glasskuler i 1 m Kjetting galv.					
Sedimenteksperiment Nadjejda Espinel		24	228		
Concerto 204985 + ECO 5804		25	227		
0,5 m Kjetting galv.					
20 m Kevlar					
10 m Kevlar					
RBR SoloT	SNR. 102949	55	197		
HF36		56	196		
Svivel					
2 m Kevlar					
Aural Hvallyd	SNR. 288	60	192		
2 m Kjetting galv					
1 m Kjetting galv.					
4 Glasskuler i 2 m Kjetting galv.					
0,5 m Kjetting galv.					
20 m Kevlar					
McLane Sedim.	SNR. 14449-02	88	164		
RBR Concerto	SNR. 204982	89	163		
50 (51) m Kevlar					
RBR SOLO	SNR. 102490	149	113		
20 (21) + 10 m Kevlar					
RBR Concerto	SNR. 204979				
40 (41) m Kevlar		170	82		
RBR SOLO	SNR. 102476	209	43		
20 + 10 (11) m Kevlar					
ADCP150	SNR. 16493	240	12		
2 m Kevlar					
SeaPhox	SNR. 20172/2004	241	11	19:00	
RBR Concerto	SNR. 204986	242	10	19:05	
AR861B2S	SNR. 2632	Ping on: Release: Arm:	2B47 2B55 2BEB		
2 m Kjetting.					
2 m Kjetting galv.					
ANKER	700/(600)kg		252	0	

Drawing of M1 BioAC mooring

Institute of Marine Research
Data record book for self registering instruments detail



Ship/Platform: Kronprins Håkon Location: M1 - 3 bioAC Latitude: N 79 35,325 Longitude: E 28 05,303						0 m
#	Brand	Type	Serial No.	Depth	Comments	Material / Object
1	Nortek	Signatur 100		252	1årconfi	
2						
3						
4						
5						
6						
7						
8						
9						
10						
11						
12						
13						
14						
15						
16						

Bottom depth [m]:	259
Outgoing date:	20.02.2021
Outgoing time (UTC):	21:00
Incoming date:	Click here to enter a date.
Incoming time (UTC):	
Comments:	
Responsible(s):	
ARGOS	
Acoustic release: IXSEA AR861	
Serial no:	Battery expire:
Range code:	
Release code:	

Station name: M1 - 2-bioAC	
Color code:	
Sum weight (incl. anchor): [kg]	
Sum weight (excl. anchor): [kg]	
Sum volume: [l]	
Buoyancy (anchor on): [kg]	
Buoyancy (anchor off): [kg]	
Shackle Stainless Steel	
Shackle Galvanized Steel	
Thimble Stainless Steel	
Thimble Galvanized Steel	
Thimble Delrin	
Description	Spec No.
Shackle Stainless Steel	2.0 T
Shackle Stainless Steel	0
Shackle Galvanized Steel	2.0 T
Shackle Galvanized Steel	3.2 T
Shackle Galvanized Steel	0
Shackle Galvanized Steel	0
Shackle Galvanized Steel	0
Thimble Stainless Steel	0
ThimblesStainless Steel	0
Thimble Galvanized Steel	0
Thimble Galvanized Steel	0
Thimble Delrin	2
Bolt Stainless Steel (RCM-7)	0
	0
	0

Weight [kg]	Vol [l]	Length [m]	Material / Object
90	1,5	Signatur100	245m
			10m kevlar rope
20	0,8	Steel Duplex / Ixsea Acoustic Release	252 m
0,2		Steel / Mounting Ring 20 cm	
2m		chain 11 mm	
			Anchor 550kg
			259 m

c. Cruise participant list

Name	Affiliation	Responsibility	Task
Frank Nilsen	UNIS	Cruise leader	CTD/LADCP ++
Ilker Fer	UiB	Cruise co-leader	MSS/LADCP
Bayoumy Mohamed A. Mabrouk	UNIS	PD, phys. oceanogr.	ICEwatch/SADCP
Kjersti Kalhagen	UNIS	PhD, phys. oceanogr.	Mooring/SADCP
Lukas Frank	UNIS	PhD, met.-ocean.	RPAS/Met/SADCP
Luke Marsden	UNIS	Data Manager	ICEwatch/Data log
Till Baumann	UiB	PD, phys. oceanogr.	MSS/Glider/LADCP
Eivind Kolås	UiB	PhD, phys. oceanogr.	Glider/AUV/MSS
Stephan Kral	UiB	PD, meteorology	RPAS/Met
Helge Bryhni	UiB	Tech.	MSS/Glider/Mooring
Tore Mo-Bjørkelund	NTNU	PhD, phys. oceanogr.	AUV
Zoe Koenig	NPI	PD, phys. oceanogr.	MSS/LADCP/SADCP
Ceslav Czyz	NPI	Tech.	Mooring/MSS
Øyvind Breivik	Met	Researcher	Met
Malte Muller	Met	Researcher	Met/drifters
Jean Rabault	Met	Researcher	Met/waves
Jan Vidar Nordstrand	IMR	Instrument chief	
Sindre Nygård Larsen	IMR	Instrument	



The Nansen pose

Appendix III. Outreach

Breivik, Ø. (2021), Pannekaker med dønning attåt – En stemningsrapport fra Vintertoktet til Arven etter Nansen, <https://blogg.forskning.no/arven-etter-nansen/pannekaker-med-donning-attat/1814811>

Breivik, Ø. (2021), Hvor mange oseanografer trengs for å bære en koffert? <https://blogg.forskning.no/arven-etter-nansen/hvor-mange-oseanografer-trengs-for-a-baere-en-koffert/1816689>

Breivik, Ø. (2021), Isflakspagaten, <https://blogg.forskning.no/arven-etter-nansen/isflakspagaten/182113>

Kalhagen, K. (2021), Women in Science: Investigating the Barents Sea, <https://www.unis.no/women-in-science-investigating-the-barents-sea/>

Mo-Bjørkelund, T. (2021), Ei uventet reise til det ukjende,
<https://blogg.forskning.no/arven-etter-nansen/ei-uventet-reise-til-det-ukjende/1819580>

Nilsen, F. (2021), Winter darkness: Revealing the secrets of the sea,
<https://www.unis.no/winter-darkness-revealing-the-secrets-of-the-sea/>

Nilsen, F., (2021), Vintermørkets hemmeligheter, forskning.no, 10. februar 2021,
<https://blogg.forskning.no/arven-etter-nansen/vintermorkets-hemmeligheter/1811964>

Nilsen, F., (2021), Den perfekte front, forskning.no, 16. februar 2021,
<https://blogg.forskning.no/arven-etter-nansen/den-perfekte-front/1815343>

The Nansen Legacy in numbers

6 years

The Nansen Legacy is a six-year project, running from 2018 to 2023.

1 400 000 km² of sea

The Nansen Legacy investigates the physical and biological environment of the northern Barents Sea and adjacent Arctic Ocean.



>10 fields

The Nansen Legacy includes scientists from the fields of biology, chemistry, climate research, ecosystem modelling, ecotoxicology, geology, ice physics, meteorology, observational technology, and physical oceanography.

>350 days at sea

The Nansen Legacy will conduct 15 scientific cruises and spend more than 350 days in the northern Barents Sea and adjacent Arctic Ocean between 2018 and 2022. Most of these cruises are conducted on the new Norwegian research icebreaker RV *Kronprins Haakon*.

280 people

There are about 230 researchers working with the Nansen Legacy, of which 73 are early career scientists. In addition, 50 persons are involved as technicians, project coordinators, communication advisers and board members.

10 institutions

The Nansen Legacy unites the complimentary scientific expertise of ten Norwegian institutions dedicated to Arctic research.



50/50 financing

The Nansen Legacy has a total budget of 740 million NOK. Half the budget comes from the consortiums' own funding, while the other half is provided by the Research Council of Norway and the Ministry of Education and Research.



Norwegian Ministry
of Education and Research



With funding from
The Research
Council of Norway

nansenlegacy.org

[nansenlegacy](#)

nansenlegacy@uit.no